

Solar Charging Electric Vehicles

Analysing the charging efficacy of an off-grid, solar powered electric vehicle charging system in long stay carpark applications

Edward Heath



Solar Charging Electric Vehicles

Analysing the charging efficacy of an off-grid,
solar powered electric vehicle charging
system in long stay carpark applications

by

Edward Heath

to obtain the degree of Master of Science
at the Delft University of Technology,
to be defended publicly on Wednesday 26th, August at 9:30 AM.

This work contributed to the paper published in EU PVSEC 2020 proceedings.

Student number: 4727142
Project duration: July, 2019 – August, 2020
Thesis committee: Prof. dr. A. J. M. van Wijk, TU Delft, supervisor
Prof. dr. A. H. M. Smets, TU Delft
Dr. ir. G. R. C. Mouli, TU Delft

Preface

*Edward Heath
Delft, August 2020*

This thesis marks the conclusion of my studies at TU Delft; a challenging and highly rewarding accomplishment to be added to my arsenal of experiences. I am proud of my work and relieved to have completed it, to overcome a mountain that, one year ago, had a summit that was out of sight. I acknowledge my own weaknesses and have learned a lot about myself in completing this project, I feel I have grown as an engineer and as a person.

When looking back to the beginning, before starting this project I had big ideas! I was to make a far more complicated model and consider all sorts of variables. Essentially I wanted to reinvent the wheel. I overestimated my ability and believed I could complete a more complex study than that which is presented in only 9 months, whilst juggling a part-time job.

Without the valuable guidance of Rishabh I think I would long since have strayed on this journey. His words of wisdom and ability to contain my, in hindsight, unrealistic ideas and proposals proved to keep me on track and level headed. In October 2019, what now seems like a lifetime ago, Rishabh told me that the goal of any research is to:

“Bring simplicity out of something complex.”

When stated like this it seems so simple, so achievable. In juggling the pressures of a demanding job and master’s graduation project I often lost sight of my goal. I forgot how to make the complex, simple.

The cherry on top of completing this project, and the culmination of my studies, is being accepted to present a poster at EU PVSEC 2020 and having a short paper published in the EU PVSEC 2020 proceedings based on the findings of this research. I am overjoyed to have been granted this opportunity and, quite frankly, surprised. However, it is something I relish and will never forget.

I would also like to thank Ad van Wijk for his insights during this project and for chairing my defence committee. Arno Smets and Gautham Ram Chandra Mouli, I too thank you for taking the time to sit on my defence committee. Finally, to Max and Lars, I thank you for your patience and tolerance during the lockdown.

Together we will turn this world upside down.

Michael Heath

Contents

List of Figures	vii
List of Tables	ix
1 Introduction	1
1.1 Problem Definition & Motivation	1
1.2 Report Structure	3
2 Solar Charging of Electric Vehicles: the Current Status	5
2.1 Electric Vehicles and Charging Technology	5
2.1.1 Electric Vehicles	5
2.1.2 Charging Infrastructure	6
2.1.3 Transport Sector Targets	7
2.2 Solar Power	9
2.2.1 Share in the Energy Mix	9
2.3 Carport Design and Suitable System Placement	11
2.3.1 Designing the System	11
2.3.2 Suitable Parking Spaces	14
2.3.3 PowerParking Project	15
2.4 Why Not Grid Connected?	15
2.4.1 Grid Effects from EV Load Connections	15
2.4.2 High Grid Connection Costs	16
2.4.3 Limited Airport Grid Capacity and Demand	16
2.4.4 Power Quality of Large Scale PV Systems	18
2.4.5 Potential Drawbacks	19
2.5 Technology Required for an Off-Grid System	19
2.5.1 PV Panels	19
2.5.2 Inverter	20
3 Model Development	23
3.1 System Topology	23
3.2 Carpark Model	25
3.2.1 Occupying the Carpark	26
3.2.2 EV Model Selection	29
3.2.3 Initial State of Charge	29
3.3 Solar PV System Model	32
3.3.1 Irradiance Model	32
3.3.2 PV Module Model	33
3.3.3 Cell Temperature Model	33
3.3.4 Inverter model	33
3.4 Battery Model	34
3.5 Charging Strategy	35
4 Results & Discussion	39
4.1 Charging Efficacy of an Off-Grid EVSC for Long Stay Carparks	39
4.2 Sensitivity Analysis	42
4.2.1 Increased Average Carpark Occupancy - <i>Occ</i>	42
4.2.2 Altering the Allowable Parking Duration - <i>Dur-X</i>	44
4.2.3 Lowered Average Initial SOC - <i>SOC</i>	46
4.2.4 Improved Modules - <i>Mods</i>	47
4.2.5 Array Tilt Angle - <i>Tilt X</i>	49

4.3	Conclusive Remarks	50
4.4	Worst Month Analysis - December	52
5	Business Case Analysis	57
5.1	Component Costs	57
5.1.1	AC Charger	57
5.1.2	Carport Structure	57
5.1.3	PV System	57
5.1.4	Total System	58
5.2	Revenue and Savings	59
5.3	Net Present Value	60
5.4	Levelised Cost of Electricity	60
5.5	Discounted Payback Period	61
5.6	Results	61
6	Conclusions & Recommendations	63
6.1	Conclusion	63
6.1.1	Off-grid EVSC System	64
6.1.2	Profitability of the System	65
6.1.3	Potential for Improvement	65
6.2	Future System Designs and Research: Recommendations	66
6.3	Limitations of the System and Approach Used: Reflections	67
	Glossary	69
	Bibliography	73

List of Figures

1.1	Example of a grid-connected solar carport used for EV charging [1]	2
2.1	Charge points in EU nations [2]	8
2.2	Charge points in the Netherlands [3]	9
2.3	Predicted EV penetration in 2030 [4]	9
2.4	Charts presenting the global and Dutch energy mixes [5]	10
2.5	Example of installed solar carport [6]	11
2.6	Common support structures for carports [7]	12
2.7	FastNed system installation [4]	13
2.8	Azimuth dependence of monopitch and duopitch carports [7]	14
2.9	Seve Ballesteros-Santander Airport energy usage	18
2.10	Common inverter topologies [8]	21
3.1	Diagram showing the topology of a single carport. The red square represents the AC chargers. The blue area represents the canopy area on which the PV modules are placed. The 4 small rectangles between this carport and the adjacent two are the concrete mounts on which the V-frame sits, as visible in 2.6	24
3.2	Simulated parking patterns of Lelystad Airport	28
3.3	Distributions used in calculating the initial SOC upon connection to the EVSC	30
3.4	Distribution of the initial SOC upon connection to the EVSC	31
3.5	Simulated data for EVs occupying the EVSC system from the previous year	31
3.6	Energy produced throughout the year. Simulated power data produced by NREL's SAM software was interpolated and	34
3.7	Flowchart explaining the iterative logic used through the time series	37
4.1	Representative data of the EVs using the EVSC	39
4.2	Bar chart displaying the charging efficacy of the EVSC system, split into final SOC ranges	41
4.3	Plot showing how final SOC and energy curtailment varies over the year with generation. Each red dot represents a single EV departure event.	41
4.4	Final SOC distribution profile during the worst performing month, December	42
4.5	Plot showing how the number of active occupant EVs varied relative to the increased average number of occupants	43
4.6	Bar chart displaying the charging efficacy in the case of an increased average number of occupants	44
4.7	Bar chart displaying the charging efficacy in the case of increased minimum allowable parking duration	45
4.8	Bar chart displaying the charging efficacy in the case of decreased maximum allowable parking duration	46
4.9	Shifted distribution of the initial SOC upon connection to the EVSC	47
4.10	Bar chart displaying the charging efficacy in the case of decreased average initial SOC	47
4.11	Bar chart displaying the charging efficacy in the case of increased PV module efficiency	48
4.12	Sun chart showing the sun's position throughout the year	49
4.13	Bar chart displaying the charging efficacy in the case of increased module tilt angles	50
4.14	Bar chart displaying the annual energy profiles of the <i>SOC</i> , <i>Occ</i> , and <i>Mods</i> cases. "Consumed" represents the energy delivered to EV batteries.	51
4.15	Bar chart displaying the annual energy profiles of altered allowable parking durations. "Consumed" represents the energy delivered to EV batteries.	51
4.16	Bar chart displaying the annual energy profiles of various module tilt angles. "Consumed" represents the energy delivered to EV batteries.	52

4.17	Bar chart displaying the monthly variance in charging efficacy for the base case	53
4.18	Bar chart displaying the monthly variance in charging efficacy, clipped for the lower final SOCs	53
4.19	Bar chart displaying the changes in December charging efficacy with sensitivity analysis cases	54
6.1	The performance of the EVSC system in the base case	64

List of Tables

2.1	AC Charger Standard in Europe [9]	7
2.2	One-off costs and annual costs for an EV charger installation [10]	17
2.3	Comparison of conversion efficiency performance for technologies [11]. Representative table and does not claim to be all-encompassing. (mc-Si is p-type emitter, Czochralski method, PERX)	20
2.4	Comparison of common inverter topologies [8]	21
3.1	LONGi LR6-60PB-315M module specifications [12]	25
3.2	SMA Sunny Highpower100-20 inverter specifications [13]	25
3.3	Top 14 planes at Schiphol based on share of total flight movements [14]	27
3.4	Passenger arrival profile	28
3.5	Passenger grouping profile	28
3.6	EV models and their associated battery parameters. The usable battery capacity in kWh and energy consumption were retrieved from [15]	35
4.1	EV usage of the EVSC	40
4.2	Energy values in the EVSC simulation	40
4.3	Abbreviations used to refer to each sensitivity analysis case, whereby the addition of X represents a sub-case	42
4.4	Theoretical module used	48
4.5	Charging efficacy of the tilt angle sensitivity analysis case during December	55
5.1	Summary of the all costs, first components and then for the entire system	59
5.2	Summary of the all revenue streams	60
5.3	Summary of the economic assessment, the subscript <i>Grid</i> indicates the purely grid-dependent alternative	62
6.1	Summary of the economic assessment, the subscript <i>Grid</i> indicates the purely grid-dependent alternative, whilst the subscript <i>PV+Grid</i> refers to the grid inclusive case.	65

Introduction

The climate crisis humanity is currently facing has had many effects on society and technology, not least the acceleration in developing sustainable options for power generation. The now prevalent solar panel and wind turbine have seen great success in this time, as well as the electrification of lifestyles, both in the household and on the roads. With global interest in both solar photovoltaic (PV) systems and electric vehicles (EVs) experiencing sustained growth over the past decades, many studies have been conducted exploring the potential for combining these two technologies.

It has now become widely accepted that, whilst it may not be the sole saviour for global energy systems, PV technologies and their associated applications are likely to account for a large proportion of power generation during and after the energy transition. This energy transition away from a fossil fuel dependent society is a part of the larger action to tackle climate change, a movement that has seen international ratification in such treaties as the Kyoto Protocol [16] in 1992 and the Paris Agreement [17] in 2015. The *Future of Solar PV* report published by IRENA [18] expects solar PV to account for 13% of global power generation by 2030, and up to 25% by 2050, driven in part by the falling prices of modules and the balance of systems (BOS).

In conjunction with the intention to transition towards a sustainable energy mix, many governments aim to electrify the transport sector in a bid to meet their climate directives. As of 2017 the transport sector in the EU-28 accounted for 27% of greenhouse gas emissions [19] with road transport responsible for 71.7% of the total transport sector. Hybrid EVs offer the advantage of reduced tailpipe emissions relative to their internal combustion engine counterparts, whilst battery EVs emit no pollutants from the tailpipe. In light of this, many governments have implemented policies and incentives to accelerate the adoption of EVs. It is now estimated that anywhere from 2% to 20% of the global passenger vehicle fleet will have an electric motor by 2030 [20], although the figure around 6% seems realistic and feasible. The EV30@30 campaign set the goal for all member countries to achieve a 30% market share of vehicle sales by 2030 (excluding two-wheelers) [21].

With such ambitious expectations being endorsed, large scale and widespread adoption of both PVs and EVs must be realised across many industries and at all system levels. This study will add to the collective knowledge on combining the two technologies and develop a system model for the niche application of an off-grid solar powered electric vehicle charging carport for long stay car parks.

1.1. Problem Definition & Motivation

The application of solar charging EVs is not new and various studies into different aspects of the system have been performed already, such as: the percentage of demand PV can cover [22], minimising grid exchange [23], the use of a secondary battery energy storage system (BESS) [24], vehicle-to-grid (V2G) potential [25–27], inclusion of electrolyser [28, 29] and more. Summaries of previous work has been presented in studies [30] and [31].

For simplicity, the application of solar charging EVs is considered to be limited to EV solar carports (EVSC), here defined as a sheltered parking space suitable for cars and light commercial vehicles (small vans) with an array of solar PV modules on the roof, as depicted in figure 1.1. No additional PV array situated nearby, for example on an adjacent building roof, is included and the electricity generation

is limited to that which is from the EVSC canopy array. Thus, the PV capacity per parking space is that which can be installed on the canopy directly above that space with some margin for overhanging edges. These systems allow for dual use of the land: sustainably generated electricity with up to 100% self-consumption to charge the EVs parked within the sheltered space. Indirect impacts of these systems include the increased incentive to own an EV, thus reducing toxic tailpipe emissions, and the reduced greenhouse gas emissions from electricity generation in fossil fuelled plants used to power the utility grid.



Figure 1.1: Example of a grid-connected solar carport used for EV charging [1]

Airports provide parking for their customers as a part of their service, parking which ranges from the 10-minutes required to drop-off a passenger, up to the several-day long stay parking. As it stands, many passengers prefer to drive to airports if they intend to be gone for an extended period since luggage can easily be transported, especially if there are multiple passengers involved such as for a family. This results in large numbers of cars being parked for long durations at airports.

With the global push towards an electrification of the transport sector EVs are set to undergo an increased uptake in coming years. This will lead to an increased share of EVs arriving at airports for long stay parking use. These EVs, whilst remaining parked for long durations, require charging since the drive to an airport from their home would likely leave the EV with a SOC too low to complete the return journey in one leg. Current options for EV owners using long stay parking at airports include:

- Charge just before entering the carpark at either a public fast charging service if available and for a relatively expensive price or slow charge for a highly inconvenient length of time and risk missing the flight
- Park in a designated EV parking space at the airport and wait while the EV battery charges before parking elsewhere for the duration of stay. Currently, Schiphol does not allow the reservation of these charging spaces.
- Charge before driving home at either a public fast charging service if available and for a relatively expensive price or slow charge for a highly inconvenient length of time which is undesirable after a long day of travelling

None of the currently offered options present a desirable solution to the issue. A returning EV owner using long stay parking at an airport wants their EV to be adequately charged upon return so

as to complete the next leg of their journey without further delay. This requires charging at the airport that does not present inconvenience to oneself and to other passengers. An airport itself has a limited grid capacity and the added load from multiple EVs is likely going to be large, especially in decades to come. Furthermore, the option of installing a large array of DC fast chargers is unfeasible due to the extreme power demand imposed.

With respect to the global transition towards sustainability, where possible, systems must be installed that provide a service whilst limiting the negative effects. Therefore, if EV charging demands in this situation can be met without relying on polluting power generation from the grid then this alternative method must be utilised.

As such, this study investigates the charging efficacy of an off-grid, solar powered EV charging solution for long stay parking at airports. Charging efficacy is here defined as the effectiveness of EV charging achieved by the system and is gauged through the final SOC distribution. It has not been quantifiably defined, rather it is a loose term to describe the charging performance.

The case of Lelystad Airport in The Netherlands is considered as a location for such a pilot project due to the current developmental goals of the airport and association with the PowerParking project. The system was simulated for a year and the overall adequacy of EV charging was analysed. A sensitivity analysis was conducted to gauge the limitations of the system and offer recommendations to improve charging efficacy with a consideration of the worst performing month. To this end, the research question is presented as:

What is the charging efficacy of an off-grid, solar powered electric vehicle charging system in long stay parking applications?

With the following subquestions:

1. To what extent do the defining system variables alter the charging efficacy of the system?
2. How does the business case of such a system compare to a conventional grid-dependent system?

1.2. Report Structure

Chapter 2 provides the EVSC system with some context, presenting the current trend in PV and EV adoption and provides further argumentation for the development of an off-grid system. Some previous work is reviewed and the foundations for this work are laid.

This knowledge is then applied in chapter 3 where the system topology is detailed and the chosen components are specified. This chapter goes on to describe the models that were developed throughout this study and used to perform the system simulations.

Chapter 4 then presents the results of the base simulation that used the models as developed in chapter 3. The findings are discussed before the results of a sensitivity analysis are presented, in which 14 more simulations were performed. Having identified the worst performing month in the initial simulation, this month was then analysed for the other simulated cases and compared.

An economic assessment is performed in chapter 5, identifying the proposed EVSC system's profitability as an investment. This is completed using the levelised cost of electricity, net present value, and discounted payback period indicators and approximate values found through the research performed.

Finally, chapter 6 summarises the findings of this study and includes the key take-aways and some recommendations for EVSC system design based on the sensitivity analysis. A discussion on the limitations of the methods and challenges faced are discussed before some suggestions for future research are proposed.

2

Solar Charging of Electric Vehicles: the Current Status

Electric vehicles and the infrastructure required to support them, whilst rapidly growing, are far from mature. Currently in a breakthrough phase, the technology is experiencing rapid progress in socio-cultural, economic, ecological, and institutional changes [32], all of which add to the collective learning of the industry and aid advancement. When considered alongside a movement towards global digitalisation, the advent of autonomous driving, and the push for shared mobility, EVs are in the driver's seat.

The European Parliament has recognised the importance of electric mobility in achieving the EU's ambitions of reducing greenhouse gases and slowing climate change. So much so that the CO₂ standards of 2020/21 require all carmakers to reach an average EV sales share of 5% by 2020 and 10% by 2021 under threat of fines [33]. As it stands in 2020, only 0.5% of the total passenger car fleet in the EU are EVs [34], a bleak figure. However, new registrations of EVs account for 7% of total passenger vehicle registrations in the EU during 2020 so far [34], more than double that in 2019.

By 2021 over 200 EV models will become available to the European market and by 2025 it is expected that European EV production will reach 4 million vehicles per annum. This results in a total of 33 million EVs on European roads by 2030 under the current policy scenario, with this number rising to 44 million in the climate neutral scenario proposed by The European Federation for Transport & Environment [33].

This chapter will provide context for EVSCs and further motivation for their deployment in off-grid long stay parking applications.

2.1. Electric Vehicles and Charging Technology

2.1.1. Electric Vehicles

EVs are rapidly growing in popularity and falling in price. Encouraged by authoritative bodies and the market, consumers are buying more EVs, original equipment manufacturers (OEMs) are providing more and better products, and automotive manufacturers are developing and producing more EV models [35, 36] giving the consumer a wider range of options whether they are interested in a battery electric vehicle (BEV) or plug-in hybrid electric vehicle (PHEV).

A battery electric vehicle is defined as an electrically driven vehicle using one or more electric motors as a means of propulsion. There are many classifications of vehicles that fall under the umbrella term of EV, ranging from moped to train. In this paper EV refers specifically to passenger cars. Furthermore, since the charging system in this study deals only with BEVs, the term EV will henceforth only refer to BEVs. BEVs are powered solely by electric motors with the electricity stored in a large rechargeable battery pack, charged through the same channels as with PHEVs. Aside from the clear potential for mitigated tailpipe emissions, BEVs offer other advantages over their ICE counterparts, including higher low end torque [37] and higher efficiencies [38].

The controversial discourse surrounding EVs is the lifetime emissions, the total emissions resulting from vehicle use. ICE engines of course burn fuel, whether petrol or diesel, which accounts for ap-

proximately 80% of the vehicle's lifetime emissions [39]. Other sources include manufacturing of the vehicle itself. It was concluded that Tesla Gigafactory 1 could result in 50% reduced emissions for battery cell production when compared to South Korean, Japanese, and Chinese battery cells [39]. When considering the traction battery is responsible for about 40% emissions associated with manufacturing of BEVs [39], there is a large potential for improvement still.

It has been shown that EVs can offer up to 85% reduced lifetime emissions [40], with even the worst case scenario in the EU achieving a 25% decrease. Here, the primary contributing factor is the electricity generation used to charge the EV batteries; a nation that is heavily dependent on fossil fuels results in higher EV lifetime emissions. Additionally, the region of battery production has an impact with Swedish manufactured batteries having a reduced footprint than Chinese batteries [40].

All modern day EVs, whether BEV or PHEV, use Li-ion battery technologies as the battery energy storage system due to the wide array of advantages over now outdated technologies such as lead-acid and nickel-metal hydride. These include: higher energy density, higher power density, higher Coulombic efficiency (over 99%), higher energy efficiency (up to 95%), and wide operating temperature range [41–43]. Furthermore, the lithium based technologies still have potential for development and improvement. Lithium ion technologies have undergone a fall in price of over 70% between 2010 – 2016 [44] and are projected to fall further.

Whilst the technology is maturing and the infrastructure to support a high penetration of EVs is developing, EVs and the required infrastructure are already sweeping the market, driven by the early adopters and progressive nations. An absolute count of new EV registrations and the share of total vehicle registrations is indicative of the year-on-year growth of the EV market. 2010 saw a mere 1400 new EV registrations in Europe, of which all but 2 were BEVs, whilst 2017 brought around 300,000 new EV registrations in Europe, of which 135,000 were BEV [2]. Global EV sales reached close to 2 million in 2018, and a year-on-year growth of 68% (2017 to 2018) [36]. Europe, the second largest EV market, saw the sale of 385,000 new units. The increase in sales in 2018 is 31% relative to 2017, a decreased growth rate with respect to 2017's 41% growth relative to 2016. However, Europe boasts the nations with highest market share of EVs. Norway was near on 50% in 2018 with Iceland, having the world's second highest penetration of EVs, at 17.2%, and Sweden at 7.9% [36].

In 2019 3.3% of the total newly registered passenger cars in the EU were electric, 2.1% being BEV and 1.2% PHEV. This resulted in the BEV and PHEV total market share of 0.26% and 0.22% by the end of 2019 [45]. Considering Europe is touted as being an EV hub, these figures are still extremely low considering the EU GHG emissions targets of 60% below 1990 levels by 2050, a reduction in conventional combustion engine vehicles of 50% by 2030 and being completely phased out by 2050. This would require an EV market share of at least 20% by 2030 [46].

The Netherlands saw 15.2% of new passenger car registrations belong to BEVs in 2019, whilst 1.3% were for PHEVs, compared to 5.4% and 0.6% respectively in 2018 and 1.9% and 0.3% respectively in 2017. However, whilst BEVs have seen a continuous and sustained annual growth in new registrations over the past 9 years, PHEVs have experienced turbulent market shares of new registrations, ranging from 0.9% in 2012 to 9.2% in 2015 back to 0.3% in 2017 [47]. This is due to the changing subsidy programmes in place in the Netherlands during this time. Similarly, the total fleet share of BEVs has seen continuous growth up to 1.26% in 2019, whilst PHEVs market share peaked in 2016 at 1.2% before falling to 1.13% in 2019. Combined market share has experienced continuous growth and currently sits at 2.39% in 2019 [45].

2.1.2. Charging Infrastructure

Charging of the EV's batteries can take place conductively or inductively. AC conductive EV chargers are currently the common choice of charging infrastructure and are used in this system design. They are relatively inexpensive and simple to manufacture and install. In Europe the Type 2 connector is used which can deliver up to 7.4 kW in single phase or up to 43 kW in a three phase configuration, however these higher power AC chargers are often installed at work places or specially considered public charge points, whilst 3.6 kW or 7.4 kW chargers will suffice for home installations. It takes a relatively long time to charge an EV with these lower power chargers, however, they are cheap and highly efficient with a low grid impact. The specifics of this charging standard are presented in table 2.1. It should be noted that the on-board charger within every EV converts the AC power supplied via the AC charger to DC and boosts the voltage to appropriately charge the EV battery. EV batteries are in the range 200 V - 800 V [48] and as described later in section 3, assumed 345.6 V in this case.

DC chargers are a less mature charging method and offer a much higher charging power, up to 350 kW, able to charge an EV from 20% to 100% in under 15 minutes in some cases. Although now the limiting factor is the ability of the battery to accept that high charging power. Since now the rectification is being performed in the charger itself the power can be delivered directly to the EV battery, this means less on-board charger equipment is required (if the EV were to only be charged using DC chargers), however the increased power electronics and higher operational power levels in the DC charger results in a larger and much more expensive product. The high powers these chargers deliver mean a higher load power drawn from the grid and places higher stresses on the grid when operating.

Table 2.1: AC Charger Standard in Europe [9]

Plug	Pins	Charging Level	Voltage, Current, Power
Type 2 (Mennekes)	4 power pins, 2 control pins	AC Level 1	1 ϕ 230 V, \leq 32 A, 7.4 kW
		AC Level 2	3 ϕ 400 V, \leq 63 A, 43 kW

There were around 33,000 charging points in the Netherlands in 2017, the highest number in Europe, followed by about 25,000 in Germany and around 15,000 in both France and the UK, as can be seen in figure 2.1. Considering the drastic difference in size between the Netherlands and the Big Four members, in both population and land area, it shows how the Netherlands is pioneering EV uptake in Europe through charging infrastructure [2]. Furthermore, the Netherlands has one of the lowest numbers of EVs per charge point across Europe and the lowest among nations with more than 1000 charge points, at 4 EVs per. Germany, France, and the UK have 6, 9, and 9 EVs per charge point respectively. However, this large number of charge points in the Netherlands is predominantly 'normal' power points (in this study considered to be <22kW), with Germany, France, and the UK having more high-power charge points.

By May 2020 the Netherlands had installed around 32,000 public charge points and 24,500 semi-public, totalling over 56,000 regular AC charge points. Additionally, the total number of fast-charging points, both public and semi-public, was 1308 as illustrated in the comparative figure 2.2. Semi-public charge points are here defined as those installed at shopping centres, workplaces, parking garages etc [3].

The EU adopted the Alternative Fuels Infrastructure Directive in 2014, which recommends a required level of infrastructure for charging of 1 charge point per every 10 EVs. Currently, there is around 1 for every 5 in the EU as a whole, however it is expected that the fleet-share of EVs will increase substantially, resulting in around 2 million charge points by 2025 [35]. The 2018 Energy Performance of Buildings Directive requires that at least one charge point is to be installed for every newly built non-residential building, as well as any existing building undergoing renovation that has over 10 parking spaces (ranging from health centres, shopping malls, local supermarkets, schools etc).

When a consumer purchases an EV it becomes the largest consumer of electricity in that person's private household, excluding extreme consumption cases. If, by 2030, 15% of all cars on European roads are EVs, a realistic and achievable number as shown in several scenarios [49–51], 95 TWh will be added to the annual electricity demand, roughly 3% of the total EU electricity consumption [52], and potentially an additional 20 GW to peak power (about 3% of expected 2030 peak load) [2]. This figure assumes an unspecified percentage of chargers being used at peak times and an unspecified average charger power for both standard and fast charging options. This would require around 5 million charge points, of which 500,000 would be fast charging. With necessary smart charging measures coupled with such innovative peak reduction applications as an off-grid EVSC, this large demand increase could be successfully managed and the threat of a congested power network can be mitigated.

2.1.3. Transport Sector Targets

Currently the transport sector is responsible for around 25% of all European GHG emissions. Since 1990 GHG emissions in other sectors have been falling, whilst the transport sector observed a decrease only in 2007 before increasing again in 2013, still above 1990 levels. Within the transport sector, road traffic is by far the largest emitter accounting for over 80% of all EU vehicular GHG emissions [35].

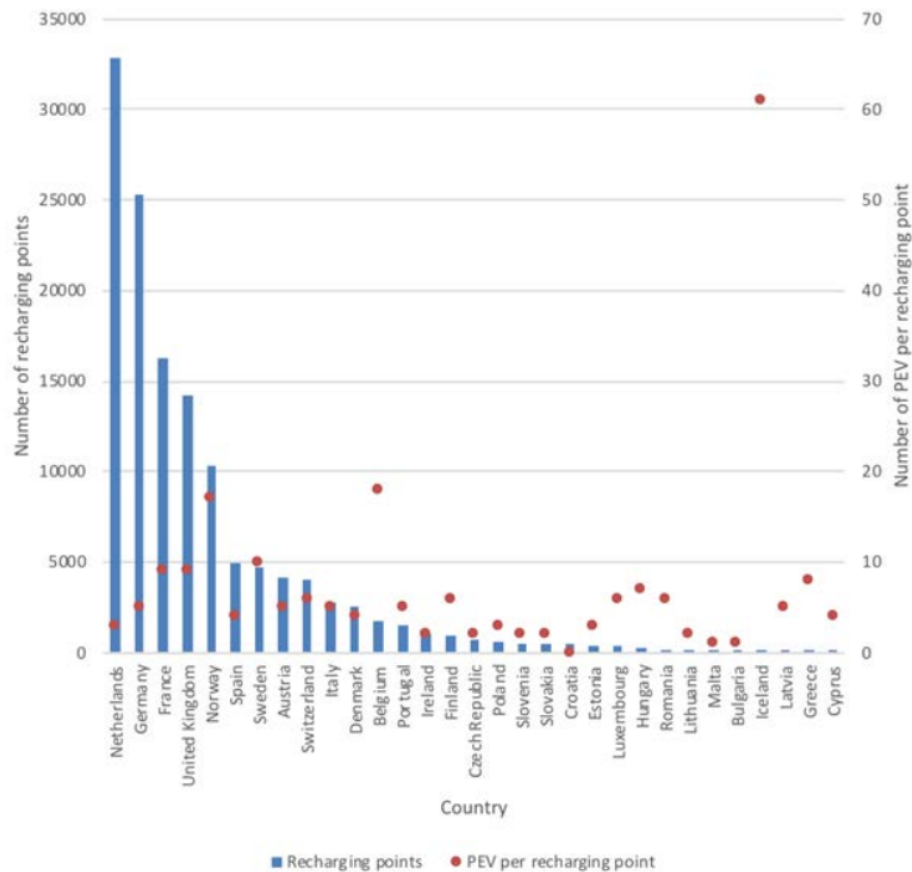


Figure 2.1: Charge points in EU nations [2]

Although no explicit targets for total fleet share of EVs have been defined, 2030 could see between 20%-70% of both BEV and PHEV combined, as illustrated by the two curves in figure 2.3. The lower considers scenarios based on just achieving emission targets whilst the upper curve includes expected technological developments for EVs, such as improved battery technology resulting in segment-A EVs becoming competitive with their ICE counterparts [53]. This is in an attempt to meet the EU-wide GHG emission targets:

- Cut overall GHG emissions to at least 40% below 1990 levels before 2030
- Cut transport sector GHG emissions to at least 60% below 1990 levels before 2050
- From January 1st 2020, an EU fleet-wide target of 95 g CO₂/km for the average emissions of new passenger cars. This is to be updated every 5 years [54]

In the Netherlands specifically the targets are more clearly defined [55]:

- By 2020 10% of all new passenger cars sold are to have electric power chain and plug
- By 2025 50% of newly sold cars are to be EVs, 30% of which are fully electric (15% total)
- By 2050 100% of newly sold cars are to be zero emission vehicles

Since 8.4% of newly registered cars in the Netherlands are BEVs with a total combined figure for BEVs, PHEVs, and FCEVs of 11.5% the 2020 target has been met.

There is no clearly defined number of charge points that is required to sustain the EV fleet, however, the Netherlands has adopted the strategy of installing more than currently demanded such that any future growth, which may be rapid when it comes, is not hindered by the lack of charging infrastructure.

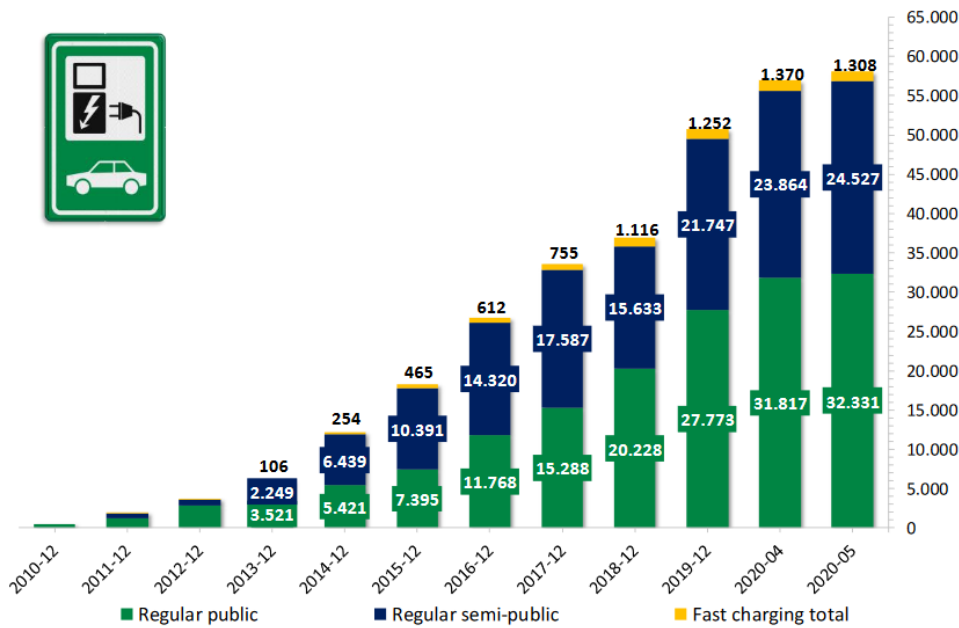


Figure 2.2: Charge points in the Netherlands [3]

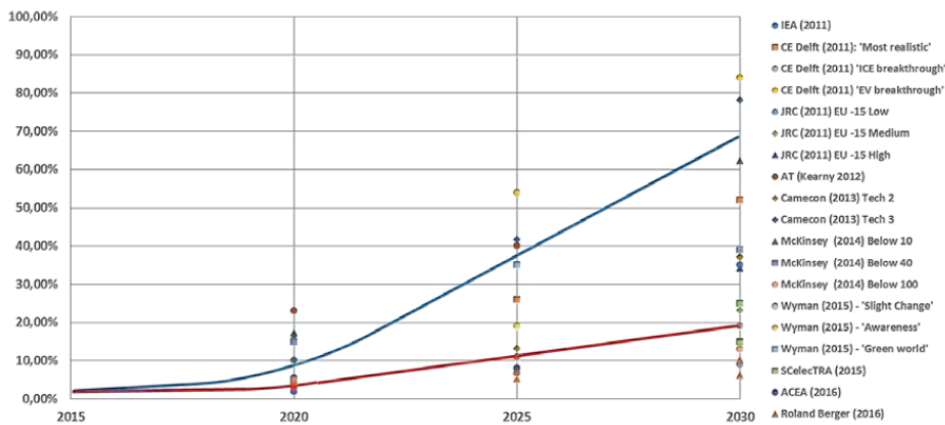


Figure 2.3: Predicted EV penetration in 2030 [4]

Furthermore, the emphasis is on public and semi-public chargers since private charge points are a personal choice to the user and will be installed at their home if space is available. Fast-charging points are much fewer in number and only located along motorways and other key hotspots for fast charging demands.

2.2. Solar Power

So far this chapter has discussed EVs and the conventional grid-connected charging infrastructure, however, a key component of EVSCs is the PV array and accompanying balance of system (BOS). This section presents the current state of affairs with regards to solar systems and their penetration within the EU and specifically the Netherlands.

2.2.1. Share in the Energy Mix

Across the EU the installation of PV systems had been gradually gaining traction before China claimed top position in large-scale manufacturing of PVs, driving module prices down and opening the door to the next stage in solar system installations, whether distributed rooftop systems or utility-scale dedicated PV farms. The European Commission’s (EC’s) 2019 progress report on renewable energies

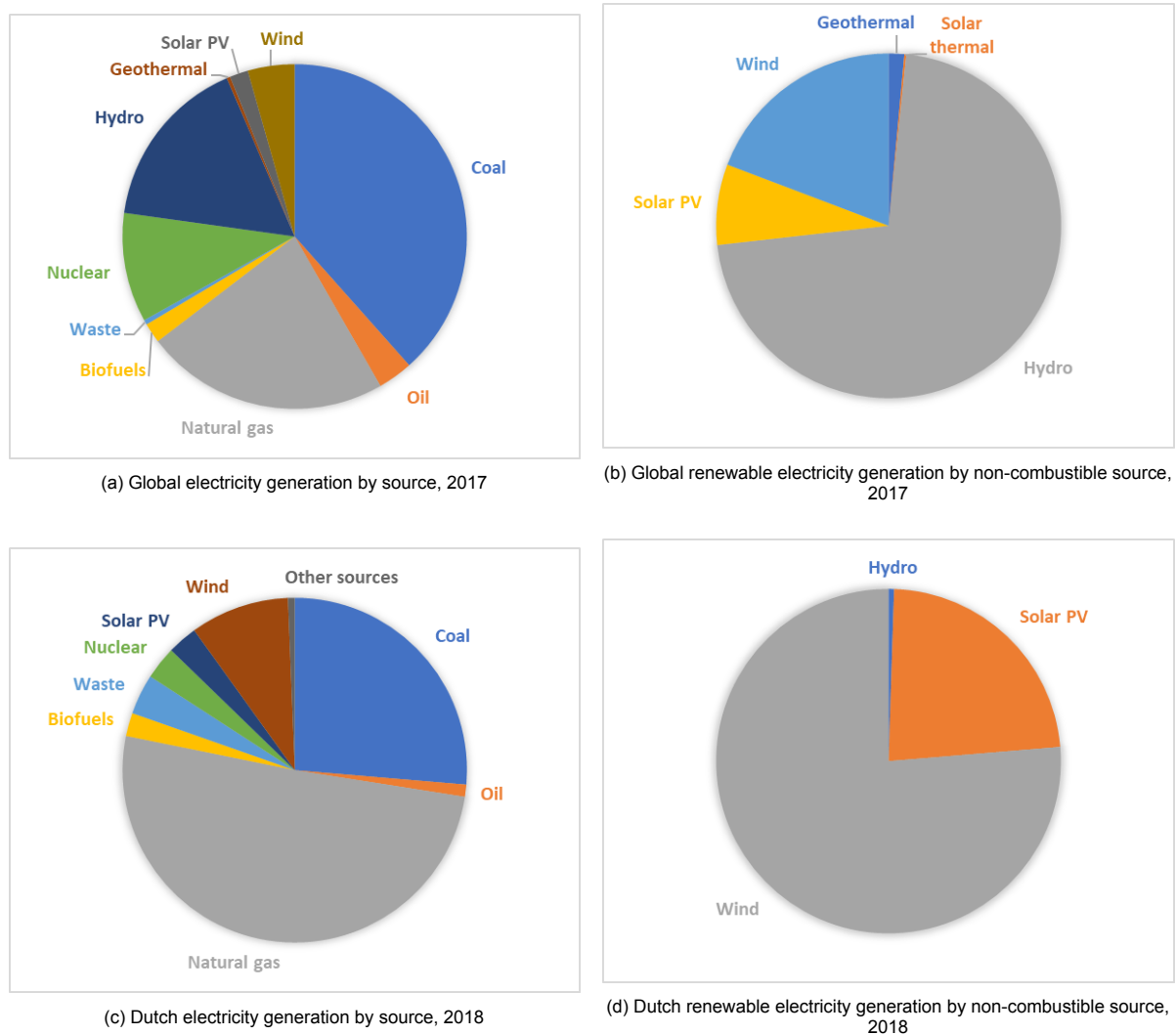


Figure 2.4: Charts presenting the global and Dutch energy mixes [5]

[56] concluded that the EU was on track to exceed the 2020 renewable energy target of 20% share of renewables, set in 2009's legally binding European Renewable Energy Directive. An increase in grid-connected systems from 11.3 GW at the end of 2008 to 117 GW by the end of 2018 was observed, with 2018 boasting 95.4% of all newly installed power generation capacity being from RES. Of that, 42% was solar PV [56]. In order to reach a GHG emission reduction of 65% by 2050, the cumulative installed PV capacity across the EU would need to reach 441 GW by 2030. Whilst for a 57% GHG emission reduction by 2035, 825 GW of PV capacity would need to be installed by 2030 [56].

The Netherlands Environmental Agency (PBL) is expecting the nation's installed PV capacity to have grown fivefold over the next decade, 2020 – 2030 [57]. This means that by 2023 the Dutch installed PV capacity will exceed 15 GW and amount to approximately 27 GW by 2030, of which 30% is thought to be distributed rooftop systems. Assuming the national electricity generation would rise to 140 TWh in 2030 from 120 TWh in 2020 [58], this would correlate to about 11.4% from solar PV assuming the sector goal of 16 TWh PV generation by 2030 is achieved.

In 2017 solar PV was responsible for 443 TWh of electricity production globally whilst solar PV accounted for 3201 GWh of electricity generation in Netherlands in 2018, or 2.31% [5], as can be seen in figures 2.4b and 2.4d, respectively. Global electricity generation by solar PV as a share of total generation has grown by 2.7% between 2015 - 2017, and 6.8% between 2010 - 2017. Electricity produced by solar PV in the Netherlands has grown by 10.5% between 2015 – 2018, and 21.8% since 2010 [5].

2.3. Carport Design and Suitable System Placement

Charging EV batteries using the power generated by a PV array is not a new innovation; in fact many studies, pilot projects and system installations have been completed. This section aims to give an introduction to carport design as well as give a brief insight into some of these previous studies. From there, the suitable locations for this system design are described and the PowerParking project is introduced.

2.3.1. Designing the System

A solar carport is a structure that shelters cars underneath with PV modules on the canopy roof, as can be seen in figure 2.5. Such structures are popular in hot and sunny climates since the shade provides protection to the vehicles, preventing sun damage like faded or cracked paintwork and even damage to the interior. Alternatively, shelter from rain and snow is provided for the not so hot and sunny climates. A large advantage of these structures is the dual use of land they can provide; the parking space itself retains the initial value with the now additional benefit of having on-site renewable electricity generation. This improves the business case since the owner can gain additional revenue if the power generated is sold to the grid or being used to charge customers' EVs, or reduce electricity bills if it is fed directly into the building's electricity supply.



Figure 2.5: Example of installed solar carport [6]

There are many designs of support structure that can be used for the carports, as summarised in [7]. Figure 2.6 provides an overview. Typically the T-frame is 10% more expensive than the V-frame option since the added strength supplied by a second strut in the V-frame design reduces the foundation requirements needed to resist wind loads. There are a number of foundation options available, from up to 6m long steel helical screws driven into the ground, to large 8m² concrete pads. Finding pricing for such foundations proved difficult and is largely dependent on ground quality.

This idea of a solar carport can be taken further to incorporate EVSCs, and can result in a large increase in grid-independence for grid connected systems due to the self-consumption of solar generated power on-site. This benefit can also be passed onto the user who may experience reduced electricity charging prices. The implementation of these EVSCs can be both public and private, for example at the shopping centre or workplace. However, for an individual EV to experience the benefit of PV charging it must be parked for a considerable amount of time.

Fast-Ned, a company that supplies fast charging services of up to 350 kW on Dutch and German motorways have such structures as shown in figure 2.7. However, it is important to note that in this









Frame Type	Bays	Monopitch	Duopitch
T-frame	1		N. A.
	2		
V-frame/ Gull wing	1		N. A.
	2		
Portal frame	1		N. A.
	>2		N. A.

Figure 2.6: Common support structures for carports [7]

case the PV panels offer very little benefit since the charging power levels are considerably higher than the PV panels on-site can provide. Assuming around 42 modules are on the structure pictured and that these are high efficiency modern modules at around 350 Wp. The rated power of such an array is only 14.7 kW and even this will rarely be achieved in northern Europe. Therefore, even when operating at its rated power this array could contribute around 10% of the required charging capacity of one of the four charging ports installed, assuming the chargers used are 150 kW, and this would be for a short time only given the intermittent nature of solar power. It is then clear that such an application is entirely dependent on the electricity grid and that the PV array only serves to improve public opinion and to aid the company's perceived alignment with the energy system transition. For PV panels to have any meaningful impact on the energy delivered to EV batteries the parking duration must be long.

In 2011 the Oak Ridge National Laboratory (ORNL) installed a solar assisted EV charging system for 25 vehicles, the first of its kind in the region [59]. Consisting of 47 kW PV array, grid connection, and an 84 kWh reserve battery bank this system uses the utility grid to charge the EVs, offering both AC charger and DC charger options. The reserve battery bank is also charged from the grid and offers supplementary energy in times of peak demand. The solar generated electricity is fed to the ORNL grid which in turn serves the EVs. The intention of this system is to use the PV and battery bank combination



Figure 2.7: FastNed system installation [4]

to shave peak load demands [60].

Mouli et al. investigated the design of a 10 kW PV array used for charging EVs during business hours in Dutch workplaces [23]. As is the common theme among such designs, a grid connection was pivotal in ensuring security of supply year-round due to the large seasonal variation in irradiation experienced in the Netherlands. The study goes on to analyse the potential for including a battery bank of up to 75 kWh alongside the grid connection, here the battery bank only interacts with the PV or EV and never the grid directly. It was shown that even with a battery bank of 75 kWh the system could never be completely independent of the grid. Additionally, the benefits from increasing reserve battery storage capacity experienced diminishing returns and underutilisation of the storage. Ultimately, through dynamic charging and reserve battery daily grid exchange can be limited but not negated.

Novoa et al. [22] installed a pilot nano-grid at the University of California, in which 48 kW PV array is deployed, 20 Level-2 (USA) EV chargers, and a 100 kW/ 100 kWh reserve BESS are integrated. The nano grid is also connected to the university 12 kV microgrid. A range of EV models (over 20) are used by staff offering representative workplace charging which is extended to weekend charging too. Whilst the charging efficacy was not their main research goal they showed that 100% self-consumption was achievable but even in the most promising solar EV charging scenario (maximising self-consumption, zero curtailment) only 80% of EV charging load was met; a grid connection was necessary to account for the remaining 20% of load.

Some interesting studies into off-grid solar powered charging stations for EVs and fuel cell cars have been completed [28, 29]. Here the inclusion of a water electrolyser and hydrogen storage tank allows for fuel cell vehicle refuelling as well as the energy storage of excess solar generation. However, both systems included a diesel generator for times of energy shortage and are committed to different research goals than this study.

The common approach to designing EVSCs is to have a bi-directional grid-connection. This offers the necessary security of supply for periods when the PV generation cannot deliver the required power and allows for dumping when PV generation surpasses the energy demand from EVs. Alternatively, stand-alone systems require a reserve battery bank and even an alternative power source such as a diesel generator. However, the use of a reserve battery introduces some disadvantages such as a reduced system efficiency and increased installation and maintenance costs whilst a diesel generator is contrasting the clean energy motivation.

Another important consideration is the power distribution mode, AC or DC. Since PVs and batteries operate in DC it is logical to use a DC bus as has been shown in previous research [23]; higher system efficiencies can be achieved through fewer conversions and a future proof design is realised. However, when one considers the pricing for DC chargers with respect to AC chargers [61], their relative immaturity compared to AC chargers, and the focus of OEMs on providing high power DC chargers,

for now at least, an AC link is more advantageous in this low power application.

Of course, the orientation of the PV modules is also an influential factor in EVSC design. As with conventional PV installations the same general ideas apply; have an optimal tilt angle and orientation relative to the sun, whether that be the annual average or a seasonal preference, and situate with as little shade as possible. However, one large constraint on EVSCs that conventional ground mounted arrays don't experience is the high wind load due to their elevated and exposed design. The foundations for EVSCs are a large part of the installation costs [7] and these can grow rapidly with wind load which is highly dependent on the roof tilt angle and whether it is mono- or duo-pitched. As discussed earlier, the V-frame design offers greater frame strength without the need for extensive foundation works. That being said, the foundations required are very site specific and largely depend on the ground conditions.

When considering the system azimuth, figure 2.8 illustrates the dependence for northern-hemisphere systems; duo-pitch rooves exhibit little dependence on the orientation of their tilt whilst mono-pitched rooves obviously do. The limiting factor, if retrofitting a pre-existing carpark, is simply the carpark layout and the feasibility of optimal roof orientation. If designing and constructing a carpark from scratch with the idea of implementing EVSCs then the decision of a south facing tilt is obvious for monopitch carports in northern hemisphere locations.

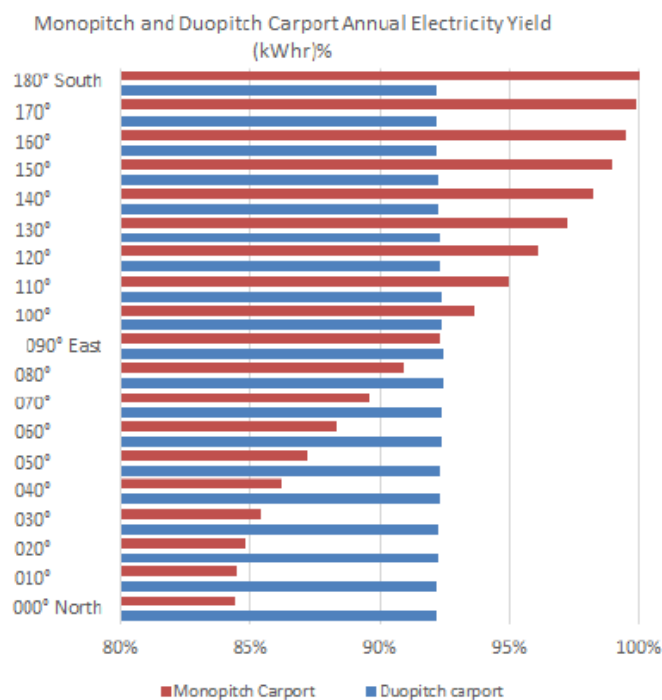


Figure 2.8: Azimuth dependence of monopitch and duopitch carports [7]

2.3.2. Suitable Parking Spaces

When considering the charging of EVs, more power is of course desirable for the consumer in regular public charging situations since the time spent charging is often an important property. However, there are charging scenarios where power level is not of importance; overnight charging at the user's home and long stay carparking being two prominent examples. Neither have a large requirement for fast charging times since time is not a confining property – an overnight charging event typically takes 3.1 hours [62] and is often at a constant 3.7 kW or 7.4 kW.

This study investigates the potential of utilising an off-grid EVSC system for long-stay carports at airports. The design decision to not include a grid connection or secondary battery bank is justified by the long duration of stay and charging times. This application is, to the author's best knowledge, only being investigated by this research group.

Long-stay carports at airports see occupants stay from 48 hours upwards and as such the need for urgent charging of the vehicle between the 9am – 5pm working hours is annulled. For example,

this study found the average long-stay duration to be 121.7 hours, corroborated by data retrieved from Boston Logan International Airport (BLIA) which had a mean of 110 hours. It was found in this study that the average daily irradiance in the Netherlands is 2.85 kWh/m². The usable installation area for modules is approximately 16.5 m² per parking space, given that parking spaces are generally 5m x 2.5m [63] in the Netherlands and allowing for some amount of overhanging canopy. For standard 60 cell mono-silicon modules the area is 1.6m² and their conversion efficiency is around 18% [12], meaning 10 PV modules per parking space. Assuming an EV battery efficiency of 95% [64], an on-board charger efficiency of 93% [65], and an AC charger efficiency of 99.5% [64], one can expect about 7.4 kWh per EV per day. Considering the average duration of stay, this suggests the charging efficacy of this system will be effective.

The majority of long stay car parks are situated at airports, however, other locations where this application could be feasible are at harbours for offshore workers, international logistics companies, car sharing hubs, car rental services, festivals, camping and caravanning parks and more.

2.3.3. PowerParking Project

PowerParking is a consortium of actors working towards developing a scalable and reproducible framework for solar powered electric vehicle charging stations for long-term, large-area parking. It gained the support of the European Regional Development Fund early on and has since been conducting research into the system design, potential for V2G power feeding, optimal component usage, user acceptance and more. The chosen site of the pilot was the long-term parking for Lelystad Airport and the regular parking dedicated to the neighbouring Lelystad Airport Business Park, however, recent developments have indicated this pilot project may not be realised. More information can be found at [66]. The consortium members are:

- Province of Flevoland
- Lelystad Airport
- Schiphol Nederland B.V.
- Ontwikkeling Maatschappij Airport Lelystad Almere (OMALA)
- TUDelft & The Green Village
- Pontis Engineering
- Eneco
- Alfen

The research hereby performed contributes to their work and, as described earlier, is solely concerned with determining and analysing the charging efficacy of the off-grid application whilst investigating the system performance sensitivity to certain parameters. It is intended to serve as a design aid for similar applications.

2.4. Why Not Grid Connected?

In not having a grid connection this system realises certain benefits and seeks to mitigate some problems, from reducing the initial investment and maintenance costs to mitigating grid imbalances from variable solar generation and EV load connections. This section explains the reasoning behind an off-grid EVSC system.

2.4.1. Grid Effects from EV Load Connections

Fuelled by the need to be range competitive with combustion engine vehicles, EV battery capacities are increasing and with it so too does the demand for an increased charging capacity [36]. Currently, the largest EV battery on the market is used by Tesla in the Model S, X and 3 at 100 kWh (95 kWh usable) but the Roadster and Cybertruck are rumoured to have up to 200 kWh [15]. The average battery capacity, including PHEVs, is now 44 kWh up from 37 kWh in 2018, whilst in most countries BEV batteries are around 50-70 kWh on average [21]. Such large battery capacities place a large

and lengthy electricity demand on the utility grid, especially when multiple in a neighbourhood are connected. With EV penetration in Netherlands potentially reaching 40% by 2030 [62], these high demands will burden the power grid with unprecedented stresses potentially causing wide spread grid congestion.

Current charging infrastructure and EV charging user battery interaction [67] has prompted owners to predominantly charge EVs overnight at their residence [68] or charging at the workplace during working hours. Plugging in EVs when arriving home after work in the evening is synchronous with an increase in evening household electricity demand and the setting of the sun. This large increase in household electricity demand during an already high demand period that coincides with the fall in PV generated power is an issue and will inevitably lead to distribution system congestion and possibly even shortages.

The increase in load demand can overload transformers leading to overheating and a degradation in transformer lifetime and an increase in system losses [68]. If the increase in evening demand pushes the peak over the transformer's rated capacity its aging could be drastically increased and potentially result in damage. Wu et al. [69] revealed in a simulation that for a 10 kV MV grid in Ronne (Bornholm, Denmark), consisting of 31 10/0.4 kV transformers, up to 15 transformers will be overloaded and one line will be overloaded with a 50% penetration of EVs, although no voltage drops above 5% were observed. Chargers were 16A, 3-phase in the worst-case scenario of 50% EV penetration.

Inevitably, EV charging will result in power quality issues within the distribution level, such as; voltage and current harmonics, under voltage conditions and power imbalances. As stated in [70], an EV charged at Level-2 can almost double a household's peak electricity demand leading to increased voltage drop in the secondary service voltage. Additionally, it was concluded that the distance between an EV load and the local substation transformer plays a large role, with a greater distance resulting in a larger additional voltage drop. Furthermore, doubling the power capacity of an EV charger or adding an additional EV load to an existing EV load will double any additional voltage drop. Increasing the penetration of EVs will inevitably lead to increased voltage drop in the secondary wires [68].

With these advances in EV battery capacity and increased penetration of EVs the utility grid and its associated hardware will come under increased stress. As such, innovative solutions should be implemented where possible to limit these inevitable future stresses.

2.4.2. High Grid Connection Costs

The Nationaal Kennisplatform Laadinfrastructuur's (NKL, Netherlands Knowledge Platform) benchmark for 2018 [10] put the costs of connecting an EV charging station to the grid at 23% of the total system installation cost, whilst in 2013 it was only 14%, summarised in table 2.2. This reflects the falling costs of hardware relative to grid connection cost. The absolute cost of which has been increasing, seeing a 14.5% increase from 2013-2018. Furthermore, the periodic maintenance of the grid connection was given to be 37% of total periodic costs. This is a significant proportion of a system's costs and in designing the charging system to be stand-alone the business case becomes a lot more appealing due to the dramatic reduction in both initial and recurring costs.

The NKL benchmark goes on to state that $\pm 15\%$ can be expected for all given costs depending on the level of EV adoption in the location in question. More specifically, urban areas which typically see a higher level of EV adoption, hence charging demand, will see higher costs due to this demand. Additionally, these average costs were determined for a 3 x 25 A charging station with 2 sockets; the 25 A grid connection is to service a 16 A charge point. In future it is expected that public EV charge points will provide 32 A chargers and more, thus requiring a larger grid connection, increased safety measures, and increased costs. However, for the application presented in this study a 16 A charge point is suitable and the cost percentages given earlier remain representative.

2.4.3. Limited Airport Grid Capacity and Demand

Being likened to small cities, airports are thriving hubs of transport and trade, serving regional, national and international purposes. An airport can be split into two main areas of operation; the landside and the airside. Landside operation concerns the movement and processing of passengers and their luggage within the terminal buildings. This includes parking, entertainment, restaurants and bars etc. The airside deals with aircraft and all related activities, namely, organization and control of take offs and landings, refuelling, loading and unloading of luggage, lighting and consists of airfield lighting, navigation and communication systems, the control tower itself, firefighter buildings and hangars [71].

Table 2.2: One-off costs and annual costs for an EV charger installation [10]

Component	Benchmark 2013 [€]	Benchmark 2018 [€]
One-off costs		
AC Charger (3x25 A, 2 sockets)	2000	1330
Location determination	700	350
Layout of the parking space	700	450
Grid connection	655	750
Installation	600	390
Annual costs		
Grid connection (3x25 A)	210	190
Communication	125	70
Insurance premium	25	25
Maintenance & repair	450	190
User issues	25	35

Total energy consumption, defined as production plus imports minus exports (or total primary energy supply) of Schiphol in 2018 was 1901 TJ (528 GWh) [72]. By far the most important energy source in airport terminal buildings is electricity; in 2014 93% of energy usage in Spanish airports was electrical [73]. Energy consumption at Seve Ballesteros-Santander airport is presented in figure 2.9a. Clearly landside consumption is dominant with the terminal building being the largest contributor. Of this, the heating, ventilation and air conditioning (HVAC) services present the largest consumption in energy, with Seve Ballesteros-Santander airport seeing 30.58% of 2015 energy consumption stemming from HVAC use. Of course, Spanish airports require vastly more air conditioning and cooling than Dutch airports, however Dutch airports require more air heating than their Spanish counterparts. So whilst this figure is not an accurate representation of Schiphol or Lelystad airport it presents the themes of electricity usage common among all airports.

Such large electrical demands require a huge capacity to distribute the electricity in the form of transformers and cabling, which, along with the grid connection itself, will incur large expenses. Furthermore, daily electricity demand experiences peaks relative to the flow of passengers, as seen in figure 2.9b. Again, it is HVAC that accounts for the majority of this consumption which aims to bring the terminal buildings to a comfortable temperature for the passengers and staff. The minimum requirement of the electricity capacity is dependent on these peaks, which are highest in the months of July, August, January and February, plus a margin for security of supply.

Since the arrival of passengers at the beginning of the day is a cause for the largest peak in demand, the addition of large EV charging loads to the airport's grid at these times could result in power loss throughout the network and catastrophic interruptions for an airport. By implementing this EV charging solution the threat of power shortage or electrical capacity overload during demand peaks can be reduced without the need for expensive utility grid connection capacity increases.

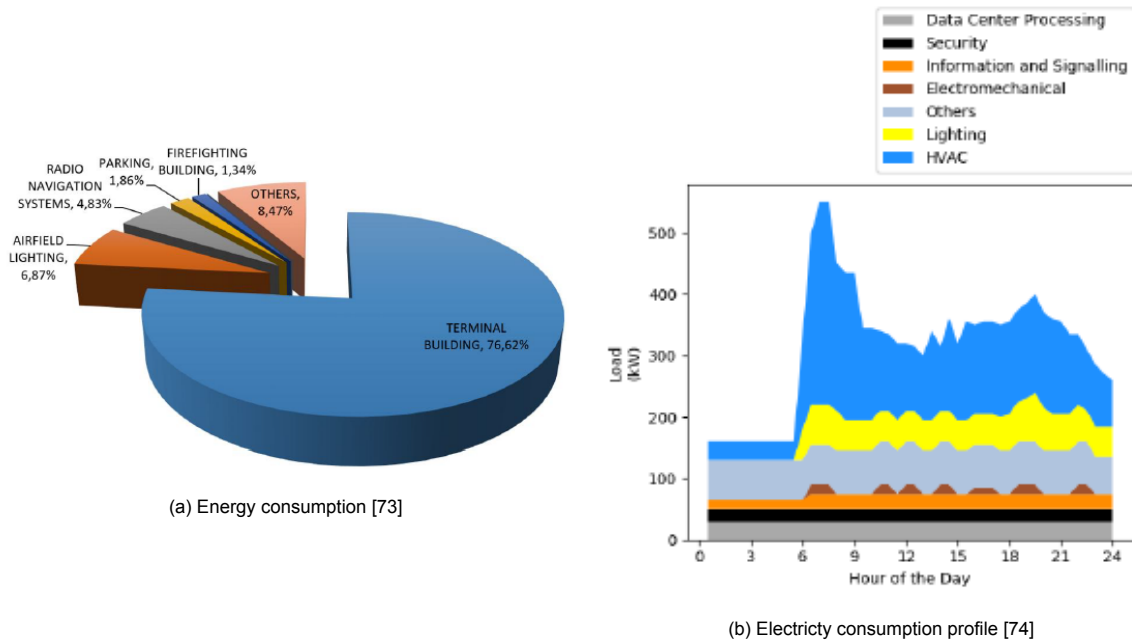


Figure 2.9: Seve Ballesteros-Santander Airport energy usage

2.4.4. Power Quality of Large Scale PV Systems

Whilst the introduction of decentralised generators at the distribution network level is both necessary and beneficial, it comes with its negative impacts, mostly in the form of grid effects. The severity of these grid effects is enhanced for large systems; according to the IEEE standard 929-2000, the installed capacity of small, intermediate and large systems is defined as being below 10 kW, 10 kW – 500 kW, and above 500 kW respectively. Hence, the system presented in this study is of an intermediate size, but the modularity of the design allows for much larger systems to be installed.

Solar power generation is inherently intermittent and unpredictable due to the meteorological variables upon which it depends. Therefore, power generation can fluctuate greatly over the course of a day due to cloud coverage with shading effects adding further detriment. This constant and often fast variation has large impacts within the utility grid. Large seasonal variations further add to the imbalance experienced between summer and winter months.

Firstly, for a large penetration of PV which could consist of many utility scale PV systems, this inconsistency of supply, or lack of security of supply, requires a fast-ramping spinning reserve able to provide for the grid demands in cases of widespread cloud coverage. If a 1 MW utility scale PV system were to undergo a transition from direct sun to complete cloud coverage within a minute, spinning reserves must be able to ramp up to 1 MW within that same time period to cover the loss of generation. It has been found that this is highly polluting and can partially negate the positive effects of utilising renewable generators [75]. Essentially, the higher the penetration of PV, the more spinning reserve is required to counteract the potential loss of generated power and is often expressed as a certain percentage of maximum dispatch load [75]. Furthermore, conventional generators using large turbines inherently possess inertia and the ability to better dampen frequency oscillations. In replacing these with PV arrays the grid is left unable to adequately counteract sudden active power imbalances.

Another adverse effect of high PV penetration is the power quality. Power inverters connecting PV arrays to the grid can produce current harmonics, leading to higher voltage and current total harmonic distortion at the point of common coupling (PCC) [76]. High order current harmonics caused by high pulse inverters, although often low in magnitude [77], can resonate with the system when at high frequencies causing voltage fluctuations and a reduction in power quality. Varying the active power fed to the grid will cause harmful frequency fluctuations, whereas reactive power fluctuations result in voltage disturbances.

For small and intermediate scale PV systems, usually situated in the low-voltage distribution level (ie. household rooftop systems), instances at which production is greater than demand result in reverse power flow from the low-voltage side to the mid-voltage. This results in overloading of distribution feed-

ers and power loss [76]. Furthermore, overvoltages across distribution feeders as a result of reverse power flow will also become more common with increasing small-scale PV penetration and likely exceed the accepted levels; operational voltages $\pm 10\%$ of nominal value are allowed [78].

One might then ask, why then the need for solar panels at all? Why not disregard them entirely and have a grid connection to charge the EVs? This will likely be an option and for some scenarios it may be the best option, although it is likely to come at a high cost as mentioned in section 2.4.2 or perhaps won't be possible due to the reasons presented in section 2.4.3. The key idea with this system is the self-consumption arising from being a stand-alone system. By directly charging EVs from the PV array one bypasses these grid-feeding effects of PV power and reduces dependence on fossil fuel power sources. Again, for the sake of future energy systems, society should implement such innovative solutions where possible.

2.4.5. Potential Drawbacks

So far in this section only the benefits of going off-grid have been presented, yet with these benefits come challenges. The most impactful is of course the potential for insufficient charging. As mentioned previously, the intermittent nature of solar PV introduces an element of uncertainty for such an application and the drastic seasonal variation, which sees winter irradiance at a level 5 times lower than that of summer months in the Netherlands [23], is expected to cause the majority of inadequate charging events. To overcome this without a grid connection is complicated, even with a large BESS as shown by Mouli et al. [23]. However, that is indeed the intention of this study; to determine the charging efficacy of such a system and to investigate the system's sensitivity to various parameters.

Another shortcoming in this design approach is the inevitable energy curtailment during summer months. The system is not sized in a typical manner, rather it is based on the usable PV installation area per parking space. Given the rated power of modern high efficiency PV modules this leads to $10 \times 315 \text{ Wp}$, or 3.15 kWp per parking space and about 15 kWh per space per day in June, the best performing month in terms of electricity production. This will lead to a high proportion of EVs standing idle in the carpark and as a result a high amount of energy curtailment. This curtailment in production is obviously an underutilisation of the installed capacity and should be avoided if possible, suggesting the need for an alternative solution in place of curtailment.

2.5. Technology Required for an Off-Grid System

Two clear distinctions can hereby be made in system design: grid-connected systems and stand-alone systems. As the names imply, the defining factor of these two are whether or not they are connected to the local/national electricity grid. As discussed in the previous section, 2.4, there are a number of consequences that result from large-scale PV connections to the grid, hence, this section will be concerned with the equipment and technology required for off-grid systems and more specifically the system modelled in this study.

2.5.1. PV Panels

Obviously, the most fundamental component in the system is the PV module. There are a variety of power generating technologies used in modules, the details of which are outside the scope of this study, but a brief introduction to some of the options is here made.

By far the dominant technology in the market is crystalline silicon (c-Si), accounting for 95% worldwide PV module production in 2017 [11], with mono-crystalline silicon (mc-Si) accounting for 34.6% and multi-crystalline silicon (pc-Si) accounting for 65.4% of the crystalline silicon production. Further categorisations can be made within crystalline silicon technologies, such as: the number of busbars used, with 9 bus bar variants now being the preferred number in high efficiency modules in 2020, the introduction of PERC technologies which are dominating new designs for high efficiency, and half-cut cell technologies becoming the new norm.

The remaining 5% of global module production is taken up by the thin-film technologies, namely; copper-indium-gallium-selenide (CIGS), cadmium-telluride (CdTe), and amorphous silicon technologies. These accounted for 1900 MWp , 2300 MWp , and 300 MWp respectively, or 42.2%, 51.1%, and 6% respectively.

Benefits of using c-Si include:

- Relative maturity of the technology

- Higher conversion efficiencies
- Higher power generated per m²
- Lower module prices due to large-scale and well developed manufacturing lines and a competitive market

Benefits of thin film technologies include:

- Lower material costs resulting from vastly thinner semiconductor region (3 μm as opposed to 180 μm)
- Higher potential conversion efficiency, yet to be realised

Table 2.3: Comparison of conversion efficiency performance for technologies [11]. Representative table and does not claim to be all-encompassing. (mc-Si is p-type emitter, Czochralski method, PERX)

Technology [%]	Lab Cell [%]	Lab Module [%]	Market Module[%]
mono-crystalline silicon (mc-Si)	26.7	24.4	20.5 (Solaria)
multi-crystalline silicon (pc-Si)	22.3	19.9	17.5 (Canadian Solar)
CIGS	23.4	19.2	17.5 (SOLIBRO)
CdTe	21.0	18.6	18.5 (First Solar)

As it stands c-Si is by far the most common choice for the majority of applications, including rooftop and solar carport system designs. Even then, the choice of module size must be made. The option of 60 cell or 72 cell modules are available, although more recently 120 half-cut cells and 144 half-cut cells are dominant. Their sizes are roughly 1.6 m² and 2 m² respectively, although current trends indicate cell size, and as a result module sizes, are increasing and some manufactures now even produce 78 cell modules. The decision is usually driven by modules costs, system installation costs which consider standards for module handling, system voltages, and the usable area for installation.

2.5.2. Inverter

PV modules output power in DC whilst the utility grid as well as many common loads require AC. Hence, switch-mode power electronic inverters are employed to enable PVs to connect to the grid or to other AC loads. For this application a uni-directional inverter is required. It is important to distinguish the difference between grid-connected and stand-alone inverters, although the details of the grid-connected inverter is outside the scope of this study.

Grid-connected inverters, being connected to the utility grid, must produce AC power that is in-phase with the grid and operating at the same voltage and frequency [8]. Furthermore, they often come with an integrated MPPT device to ensure optimal PV array operation whereby any excess generation can be fed to the grid if not consumed by the immediate loads, for example a rooftop home system. In times of grid disruption and brown/black out they are turned off to prevent islanding.

Stand-alone inverters are not connected to the utility grid and as such need to be able to control the AC voltage and frequency independently [8]. Often connected to a BESS the need for an integrated MPPT is mitigated since the PV array is connected to the battery via a charge controller which would house the MPPT. Of course, this is just a common design feature and other topologies are available. Additionally, since these inverters are designed for use with batteries they incorporate the necessary protection methods to prevent over discharge. Again, since inverter and system efficiencies are not the concern of this design no BESS is included and the PV array output power is fed directly to the inverter.

A brief summary of the potential topologies is presented in table 3.2 and visualised in figure 2.10. In this design, as discussed in section 3.1, three string inverters were implemented each accounting for a large string of modules.

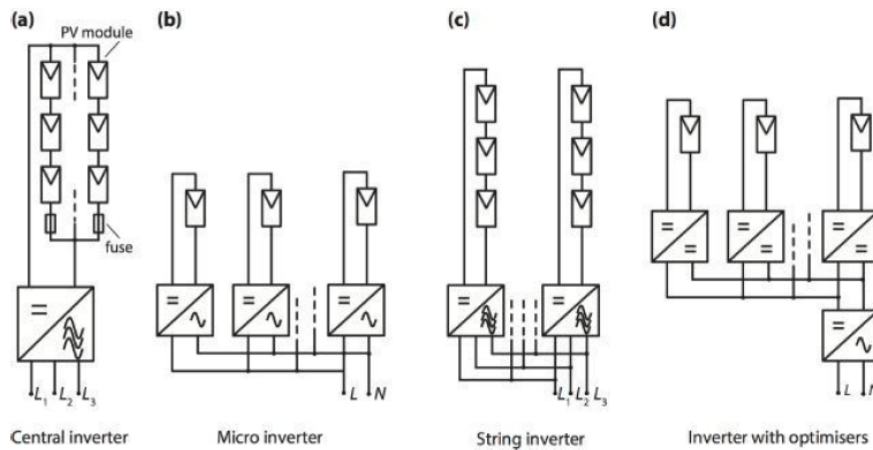


Figure 2.10: Common inverter topologies [8]

Table 2.4: Comparison of common inverter topologies [8]

Topology	Features
Central inverter	Entire array of PV modules is connected to this single (or stacked) central inverter(s). Any MPPT estimation would be applied to all modules within the array. High power rating. Pros: simple and cost effective Cons: mismatch losses (increased by age and shade), little flexibility/expandability, power losses in string diodes
Micro inverter	Operate on a module (or multiple module) level. Low power rating. Often requires a DC/DC boost step prior to signal inversion. Pros: minimal mismatch losses, high system flexibility Cons: often operate at inefficient levels, expensive
String inverters	Operates on a string of modules, the power of which can vary depending on the application. Pros: partial shading affects only one string and not the whole array meaning reduced mismatch losses relative to central inverter. Cons: High string voltages require special consideration since these are often installed in household rooftop systems.
Central & optimizers	A blend of central and micro inverter concepts. The optimizer consist of an MPPT unit and DC/DC converter and is installed on a module basis. This then all feeds into one central inverter which can dictate the accepted input voltage by means of current manipulation, altering DC/DC converter output setpoint. Pros: each module has optimal operating conditions, high DC/DC converter and inverter efficiencies, relatively little power consumption Cons: More equipment resulting in a greater expense and higher chance of malfunction of failure.

3

Model Development

This chapter is concerned with the EVSC system, both physical design and computational model as used for the simulations. A description of the physical system topology is presented first. Then each constituent model of the greater system model is detailed, namely: the formulation of arrival and departure times of EVs using the system, the calculation of their initial SOC, the solar power generation, and the battery model used in the charging process. Finally, the charging logic is detailed.

3.1. System Topology

A total parking capacity of 108 spaces was used. This was chosen so as to better configure the system to an inverter and be able to evenly split the chargers across the 3-phases. Each parking space is 2.5 m x 5 m, as per Dutch parking guidelines [63]. The carports, of which there were 27 structures, were positioned in one long row. Each structure housed 4 parking spaces with two AC chargers placed in the centre, as presented in figure 3.1, each capable of providing 2 simultaneously operable charging connections rated at 16 A, 3.7 kW. Assuming a 0.5 m gap between the spaces, allowing for a 0.5 m² area in the middle for the charger, a 0.5 m roof overhang on each side (front & back), and a 15° roof tilt, there was a total usable canopy area of 69 m². This accommodated 40 PV modules, each of 1.6 m², in a 4 x 5 configuration.

The canopy roof, and hence the PV array, was tilted 15° due south. As explained in section 2.3, the tilt angle of such structures are typically in the range 10° - 15° so as to keep the wind load exerted on the structure minimal and installation costs relatively low, whilst improving daily yield with respect to the horizontal plane array. Having said that, the design of the support structure was chosen to be the V-frame option since this typically reduces costs by 10% due to the added strength supplied by a second strut, allowing for the higher tilt of 15° [7].

At this tilt angle the north side of the canopy is 3.08 m higher than the south side. Therefore, if two rows of carports were installed and assuming a 6 m wide thoroughfare [63], hence a 4.5 m separation between canopy edges, row shading would occur below a sun altitude of 34.4°. If the tilt of the canopy was reduced to 10°, shading effects would occur below a sun altitude of 25.2°. With an annual average maximum sun altitude of 39.6° at this location, and winter average maximum sun altitude of 20.5°, as found in the meteorological data file, shading would be a common and highly detrimental occurrence. Therefore, one row of EVSCs was decided upon. With the dimensions and spacings as presented and the inverter placement in the middle of the row, the average AC cable length is 39 m.

The LONGi LR6-60PB-315M modules used in this application were selected from the module database in the National Renewable Energy Laboratory's (NREL's) System Advisor Model (SAM) software and are 60-cell mono-silicon PERC modules. Some module specifications can be found in table 3.1. Since the version of SAM used for this study was the 2018 release, the modules in the database were already fairly out dated. As such these modules have now been discontinued, but their replacement which boasts 360 Wp and half-cut cell technology costs around €140 per module [79], or 0.38 €/Wp. If one were to purchase in large orders this price would surely fall. Similar modules have been seen to cost less than 0.2 €/Wp [80]. Whilst in today's terms a mono-silicon PERC module rated at 315 W is relatively low, considering the typical range of 340 W - 370 W [11], it serves as a good generalisation

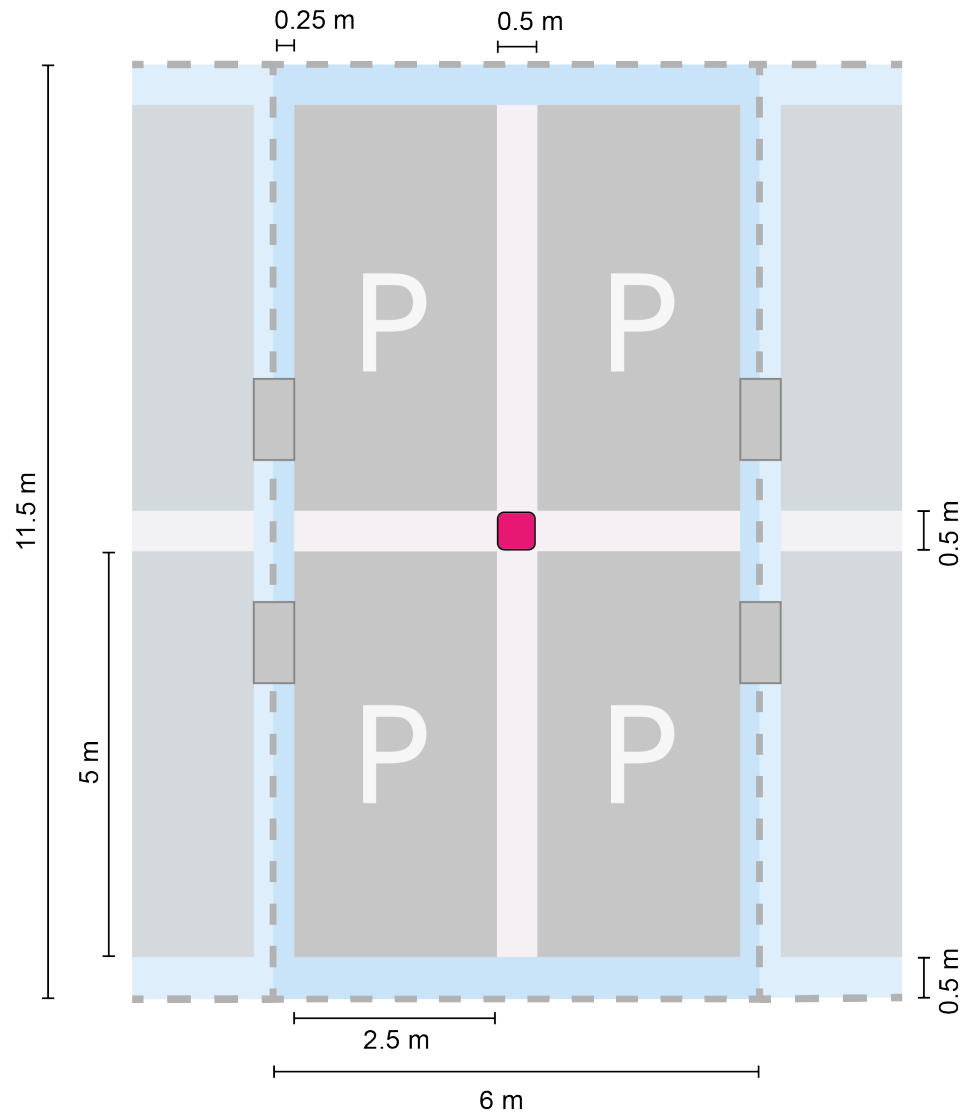


Figure 3.1: Diagram showing the topology of a single carport. The red square represents the AC chargers. The blue area represents the canopy area on which the PV modules are placed. The 4 small rectangles between this carport and the adjacent two are the concrete mounts on which the V-frame sits, as visible in 2.6

Table 3.1: LONGi LR6-60PB-315M module specifications [12]

Parameter	Value
P_{\max}	315 W
V_{OC}	40.8 V
I_{SC}	10.05 A
V_{MP}	33.5 V
I_{MP}	9.41 A
η	19.3%
Temperature coefficient P	-0.370 %/°C
Temperature coefficient V	-0.286 %/°C
Temperature coefficient I	0.057 %/°C
Dimensions	1650 x 991 x 40 mm

to the modules installed currently.

The inverter chosen for this system is the off-grid capable SMA Sunny Highpower PEAK3, some details of which can be found in table 3.2. The AC chargers used in this design are standard European Type-2 rated at 3.7 kW, 230 V, and 16 A.

Table 3.2: SMA Sunny Highpower100-20 inverter specifications [13]

Parameter	Value
Max. PV array power	150 kWp
Max. input voltage	1000 V
Mpp Voltage range / rated input voltage	590 V to 1000 V / 590 V
Max. input current / max. short-circuit current	180 A / 325 A
Output type	3-phase AC
European weighted efficiency	98.6%

The rated power per canopy is $40 \times 315 \text{ W} = 12.6 \text{ kWp}$, and a total system rated generating power of 340.2 kWp from 1080 modules. Since the system was off-grid and the modules did not need to constantly operate at MPP, instead operating at the required level as demanded by the loads, no power optimizers or MPPTs were included in the system design. Inverter sizing, partially dependant on module configuration, was completed using summer I_{SC} and winter V_{OC} values. Using the temperature coefficients presented in 3.1, these were found to be 10.30 A and 42.24 V respectively, assuming summer module operating temperature of 60°C and winter module operating temperature of 0°C. The modules were arranged in strings of 20 with 18 strings in parallel forming a subarray, meaning each subarray consisted of 9 canopies. Each subarray was then connected to an inverter, meaning a total of three inverters and a DC to AC ratio of 1.13. This is a fairly low DC to AC ratio for such high latitudes; an oversized system performs better in low light conditions and the annual energy yield would increase regardless of the power clipping implemented in summer months when irradiance is high. However, finding a suitable inverter for such an application proved difficult so the decision was made to continue with this setup.

The chosen inverters output power in 3-phase, meaning the loads had to be split between the phases. Although this introduced phase imbalances into the system there is no alternative practical solution.

3.2. Carpark Model

Before charging of EVs using the EVSC could take place the knowledge of the number of EVs present within the carpark at that specific timestep was required. To deduce this, one must determine the arrival and departure times of each individual EV. Due to the lack of usable parking data for long-stay car parks in European airports, the arrival and departure times of electric vehicles using the solar charging carpark

were simulated. A methodology for modelling carpark usage in airports was found in the literature [81], in which Li identified the four influencing factors to be airline information, passenger arrival profile, passenger driving profile, and parking profile. This section details the generation of arrival events, the duration of stay associated to each booking, the choice of EV per booking and the arrival SOC of that EV. The approach used for this is briefly described here before a detailed approach is given below.

- Using the flight departure times of Schiphol a passenger arrival profile was produced
- Using Schiphol data and passenger vehicle fleet statistics this was reduced to EV arrival events
- Data from another airport was used to form a distribution of parking duration
- Data on the Dutch EV fleet was used to assign an EV model to each arrival event
- EV specifications and literature were used to simulate the initial SOC upon arrival

3.2.1. Occupying the Carpark

The most fundamental driver of carpark use is the number of passengers arriving at the airport. Passengers' arrival time is related to the scheduled departure of their flight, with the daily departure times accurately broadcast on all airport websites and actively updated. The departure times of all flights leaving Schiphol for the month of November 2019 were collected and extrapolated to the full year using monthly variation values for both Schiphol and Lelystad. Furthermore, since Lelystad Airport is much smaller than Schiphol and is intended to service European destinations the number of flights each month was scaled to match 2019 values. On average, 63% of monthly Schiphol traffic was determined to be European bound and O&A (origin and arrival) [14].

The method of extrapolation was to copy the schedule of November to every other month whilst applying monthly scaling values from Schiphol's 2019 flight records [14] and the Lelystad PowerParking working group assumptions [82]. The data set described the number of flights departing Schiphol at each time step throughout the year, however, each month was simply a scaled copy of the November schedule rounded to integer values. This was not a very realistic representation and so some variance was introduced. Firstly, a function to add random noise to the series was implemented by multiplying each value by a value drawn from a normal distribution with mean value of 1, and standard deviation of 0.1. This function was applied to all months excluding November. If 5 flights departed at 11:05 on 02/11/2020, it could then be that 5.6 flights would depart at 11:05 on 02/06/2020, rounding up to 6.

Additionally, a random selection of flight departures were shifted 5, 10, or 15 minutes. The proportion of shifted flights was chosen to be 5%, 3%, and 1% respectively, and could shift either forwards or backwards. The times by which a departure time could shift were chosen to introduce 'local' and slight variance whilst the proportion of flights that were shifted kept fairly low. The order of operation was to shift 5% of all flights 5 minutes forward, shift 5% of all flights 5 minutes backward, shift 3% of all flights 10 minutes forward, and so on. A flight could be shifted more than once. This method was applied after the random noise function and included November flights.

The result of both these methods on the data set was an added level of variance such that the number of flights departing at each time step were not direct replicas of the November schedule. Although the outcome of this method was small and likely would not have serious implications for passenger arrival times later on, it was deemed to be more realistic and a worthwhile inclusion. Schiphol has a 5-minute interval time for flight departures. Multiple flights can be scheduled to take off in the same 5-minute interval due to the use of multiple runways and throughput of aircraft.

$$PD_t = \sum_{f=1}^F PD_{f,t} \quad (3.1)$$

PD_t is the total number of passengers departing in time step t . $PD_{f,t}$ is the number of passengers departing on flight f in time step t . In order to generate PD_t it was necessary to determine the occupancy of each departing flight. A short list of the top 14 aircraft departing from Schiphol, accounting for 90.8% of total movements, was created [14] and their respective number of seats and share of total movements listed. Table 3.3 shows the maximum occupancy of these aircraft. A truncated normal distribution was then generated so as to draw a number of passengers per flight. The limits of this distribution were 45

and 294 with respect to table 3.3, the lower limit being 60% of the smallest plane. The mean value of this distribution was then equal to the average passengers per flight per month.

Table 3.3: Top 14 planes at Schiphol based on share of total flight movements [14]

Plane	Share of total movements [%]	Number of seats
Boeing 737-800	22.6	175
Embraer 190/195	15.0	106
Airbus A320	11.3	150
Embraer 170/175	9.4	75
Boeing 737-700	9.0	143
Airbus A319	6.7	138
Airbus A330-300	3.0	250
Airbus A321	2.9	200
Boeing 777-300	2.4	381
Boeing 777-200	2.3	280
Boeing 737-900	2.0	178
Boeing 787-9	1.9	294
Dash 8-400	1.6	78
Boeing 767-300	1.5	214
Airbus A330-200	1.4	243

The next step was to determine the number of passengers arriving in time step t , PA_t . This is dependent on the number of passengers departing in future time steps and how early each passenger arrives. For each passenger departing in time step t , so for each $p_{t(D)}$ in PD_t :

$$p_{t(A)} = t - k \quad (3.2)$$

Where $p_{t(A)}$ is the time of arrival for passenger $p_{t(D)}$ and k is a value drawn from a truncated normal distribution which describes the earliness of arrival profile for all passengers. This profile assumed that all passengers arrive at the airport between 30 minutes and 180 minutes prior to flight departure, with the average at 120 minutes. Hence, these values were used for this truncated normal distribution. The resulting continuous data set was rounded off to 5-minute intervals.

The new data set describing when each individual passenger arrived at the airport was then operated on; the arriving passengers per time step was summed to give total passenger arrival per time step, PA_t :

$$PA_t = \sum_t^T p_{t(A)} \quad (3.3)$$

Since not all passengers travel by car to an airport the arriving passenger distribution was multiplied by a passenger parking profile factor to give the number of passengers arriving by car in time step t , with the intention of using parking services.

$$VA_t = PA_t \times PP \quad (3.4)$$

Where PP is the passenger parking profile factor, or the proportion of passengers arriving by car and parking at the airport with respect to all other modes of transport. For this application it was assumed that the parking profile is constant throughout the year at 10.3% [72]. This value excluded all drop-offs, as seen in table 3.4. Furthermore, with the Dutch national EV fleet achieving a 2.04% share of total private automobile ownerships [47, 83], the final EV arrivals were 0.2% of total passenger parking arrivals.

Additionally, it had been considered that often people fly in groups and therefore may travel to the airport in groups. Whilst keeping the occupancy of each flight the same, the passengers were grouped

Table 3.4: Passenger arrival profile

Arrival Mode	2018 Proportion [%]
Public transport	46.3
Drop-off by car	19.8
Parked car	10.3
Taxi	12.7
Other	10.9

together. It was thought that group sizes will likely vary between 1-9, any groups larger than 9 would have a negligible contribution to overall passenger movements. Since no direct data was available detailing occupancy of passenger cars arriving at airports, inspiration was taken from two sources, namely; number of cars per capita in the Netherlands and the average household occupancy. It was found that there were 1.38 passengers per car in the Netherlands [84] and the average household has 2.15 occupants [85]. The weights assigned to each group size was then decided to be as presented in table 3.5. This resulted in an average group size of 2.5. Since passenger cars, and more specifically EVs, rarely seat more than 5 people, only group sizes of 5 or less were considered.

Table 3.5: Passenger grouping profile

1	2	3	4	5	6	7	8	9
0.23	0.28	0.22	0.13	0.07	0.03	0.02	0.01	0.01

Finally, 32% of all arriving vehicles use long term parking. This was estimated with use of the 2018 parking revenue for Schiphol [72] and verified by looking at the data for BLIA where it is thought ratios of short to long-stay parking would be similar. Hence, a function was applied to the 2019 timeseries containing arriving vehicles, randomly selecting 32% of all arrivals for long-stay parking.

BLIA data was used to determine the duration of stay since it was thought long-stay parking durations would not differ significantly between the two airports. For simplicity it was assumed that if two vehicles happened to arrive in the same time step, the second occurrence would be shifted to the subsequent time step. The allowable parking durations are here defined as ranging from 48 hours up to 3 weeks, as per Schiphol airport's policy of 48-hour minimum stay and an assumed upper limit imposed for computational purposes. This upper limit had to be assumed since the BLIA data ended with 14+ days, having been presented in a daily resolution. The resulting distribution is presented in figure 3.2a.

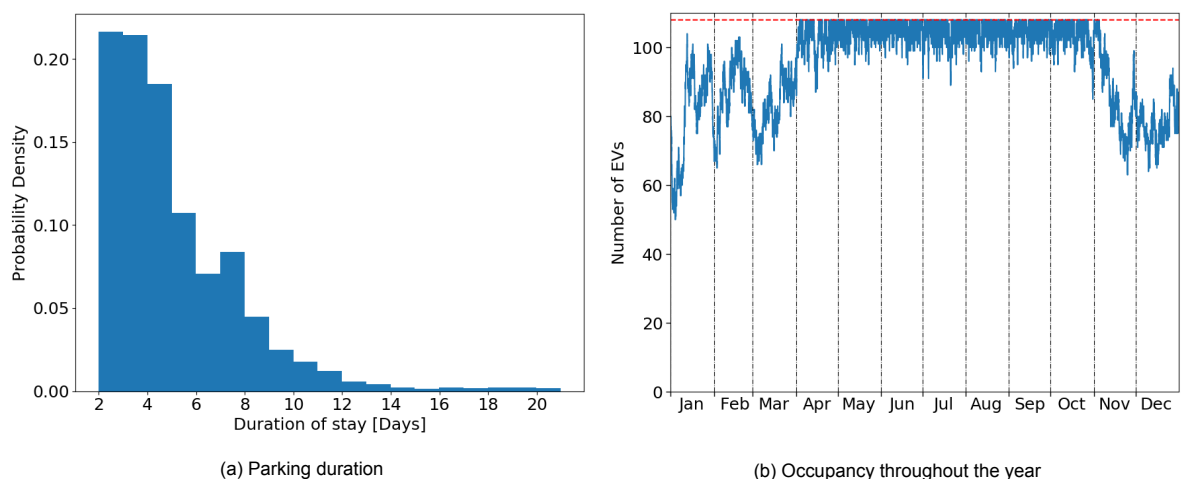


Figure 3.2: Simulated parking patterns of Lelystad Airport

Each occupant of the long stay carpark was assigned a duration of stay value in day integers, drawn

from the distribution presented in figure 3.2a. To then spread the departure of the carpark occupants throughout the day, as would be the case with a real airport carpark, a function was applied that added a random number of minutes to the day value in minutes. There are 1440 minutes in 24 hours, thus 288 5-minute intervals. For each EV, the duration of stay in minutes had a random integer value between 0 and 288, which was then multiplied by 5, added to it. This then gave the total duration of stay in minutes.

$$DS = DS_{min} + x \in [0, 288] \times 5 \quad (3.5)$$

Where DS is the duration of stay after adding some random minutes and DS_{min} is the duration of stay drawn from the distribution in minutes. Finally, the occupancy of the car park at each time step was to be monitored so that the car park would not enter over capacity, and that the power generated from the solar panels could be split between the occupants suitably.

$$N_t = N_{t-1} + VA_t - VD_{t-1} \quad (3.6)$$

N_t is occupancy of the car park in time step t and VD_{t-1} is the number of EVs departing in the previous time step since an EV was considered to be present until the end of the time step in which they were due to depart.

It was assumed that the maximum occupancy of this carpark was 100% since the customer would reserve a space for their required time when booking their flights, hence an optimized schedule for the carpark could be formulated, the result of which is presented in figure 3.2b. Since it was assumed this is the first carpark of its type in this location at Lelystad, there was no extra capacity. Those customers who were unable to enter the carpark must use standard long-stay parking and the charging of their EVs would be done by other means.

3.2.2. EV Model Selection

There is an assortment of variables that define an EV model. Among them, the usable battery capacity and consumption of energy were necessary in order to model the initial SOC at the point of connection to the EVSC for each arriving vehicle. The calculation of the initial SOC is detailed in section 3.2.3.

The top 10 BEVs in the Netherlands as of the end of February 2020 [3] were considered in this model. The EV model assigned to an arrival event was then drawn from a probabilistic set with the probabilities assigned to each EV model being its market share with respect to the total population of those top 10 EVs. It is worth noting that for the Tesla Model 3 performance and battery characteristics of the Long-Range Dual Motor model were considered. The rationale being that since there are a few variants of this EV and further distinction was not possible, the largest capacity model would lend itself to future systems where the average EV battery capacity will be larger [21].

The decision to use only BEVs in this model as opposed to including PHEVs was two-fold. Firstly, in order to have a secure and reliable system it must be able to accommodate the most stressful scenario of 100% occupancy of BEVs. Then any share of another EV type will also be possible since the battery capacity, and therefore energy demand, will be less. Secondly, this system is intended to be 'future proof'. That is, it should not become obsolete due to advancements in technology such as larger battery capacities or shifting societal perceptions and governmental regulations that result in a larger EV penetration. It is likely that the future will bring an ever-increasing penetration of BEVs relative to PHEVs since many nations' end-goal is a zero-emission car fleet.

Having already determined the arrival times of EVs this process simply assigned an EV to each successive arrival event. The next step was to deduce the initial SOC upon entry of each occupant.

3.2.3. Initial State of Charge

Another variable key to developing an accurate system model was the SOC of the EVs upon arrival at the EVSC. A common method of predicting initial SOC is to use a distance travelled dependant calculation with respect to the SOC prior to the journey, usable battery capacity, and the rate of energy consumption [86]. Although the calculation itself is trivial, this method threw up some complications when assuming the prior SOC. Is it fair to assume that all BEVs are 100% fully charged before their journey? How far are they likely to drive? What is the driving style of the driver and what route does he/she take? What is the combined weight of the passengers and luggage? As a result, this model required various assumptions.

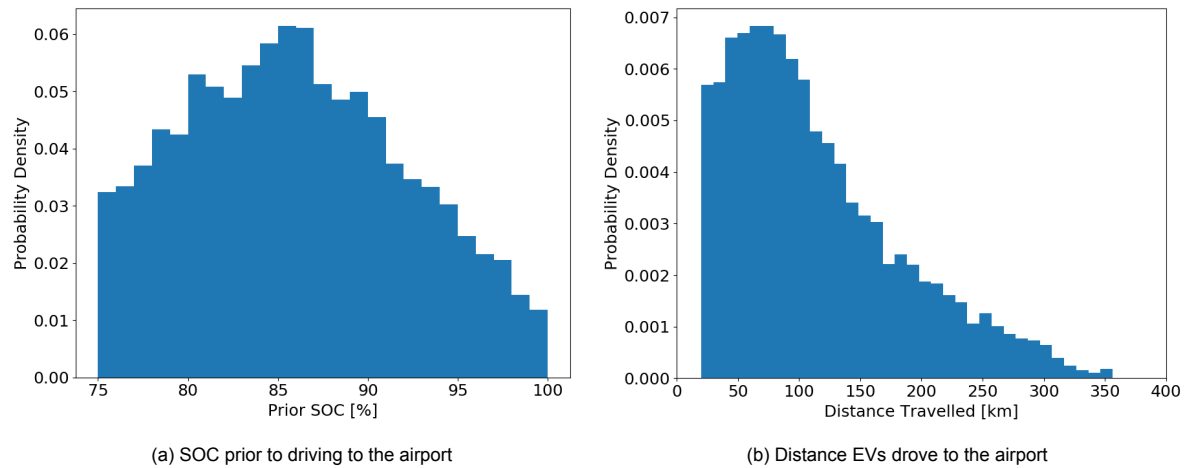


Figure 3.3: Distributions used in calculating the initial SOC upon connection to the EVSC

In this section and henceforth “prior SOC” refers to the SOC of the EV before making the journey to the airport whilst “initial SOC” refers to the SOC of the EV at the time of connection to the EVSC at the airport.

Considering the prior SOC, this is really a question of how a user interacts with their batteries with respect to the EV model they own. For instance, it is fair to assume someone driving a Tesla Model S would generally suffer less range anxiety than someone driving a VW eGolf because the battery capacity and nominal range is much larger. However, this does not account for the particular user’s charging preferences. Some users would charge when they get a chance and as long as possible, some prefer to charge to full, whilst others may charge until they reach a high enough value to complete their next intended journey [67].

Thus, instead of using the unrealistic notion that each EV has a SOC of 100% prior to the journey to the airport, the assumption that this SOC was between 75% and 100% with a mean of 85%, was implemented. A truncated normal distribution was generated as shown in figure 3.3a, from which values were drawn and assigned to an arrival event regardless of EV model or user and represents a general scenario in which the user is aware he/she will embark on an important journey and hence ensures that the vehicle is suitably charged.

Furthermore, it was assumed that no en route charging could take place meaning that the distance driven to the airport had to be possible with any value of SOC prior to embarking. Hence, for each EV model the maximum possible distance driven was equal to 70% of the maximum nominal range of that specific model. For example, a Hyundai Kona with a prior SOC of 75% (the minimum allowable prior SOC) could drive up to 296.25 km without the need to charge en route, whilst the maximum distance allowably driven would be 276.5 km. Of course, this is not taking into account factors that affect the consumption rate, such as; ambient temperature, battery and motor temperatures, urban or motorway use, driving style or traffic flow, all of which could drastically affect the possible range but were outside the scope of this study.

The mean distance travelled regardless of EV model was decided to be 65 km, the distance from Utrecht to Lelystad Airport. It is thought that this mean distance is representative of the distances likely to be driven considering the size of the country and the other airports in the Netherlands, specifically at Groningen, Rotterdam, and Eindhoven. From this, a truncated normal distribution was generated with the upper limit changing for each EV model to extract the distance driven. The combined result of all EVs is presented in figure 3.3b.

For each EV in the data set, the initial SOC upon arrival at the airport was then determined by extracting values from the aforementioned distributions and combining in a simple calculation:

$$SOC_n^i = SOC_n^p - \frac{D \times E_{con,n}}{C_{bat,n}^E} \quad (3.7)$$

Where D is distance driven, $E_{con,n}$ is the nominal consumption of energy for EV_n in question, $C_{bat,n}^E$

is the usable battery capacity of EV_n , SOC_n^p is the prior SOC of EV_n , and SOC_n^i is the initial SOC of EV_n . It must be noted that nominal values of usable battery capacity and energy consumption were used since the added complexity of introducing factors that affect the consumption rate were outside the scope of this study. The resulting distribution of initial SOC upon connection to the EVSC had a mean value of 55.6%, as presented in figure 3.4, and is consistent with the findings of various field studies [67, 87, 88], all of which determined initial SOC upon first connection had a normal distribution with mean value of between 50%-60%.

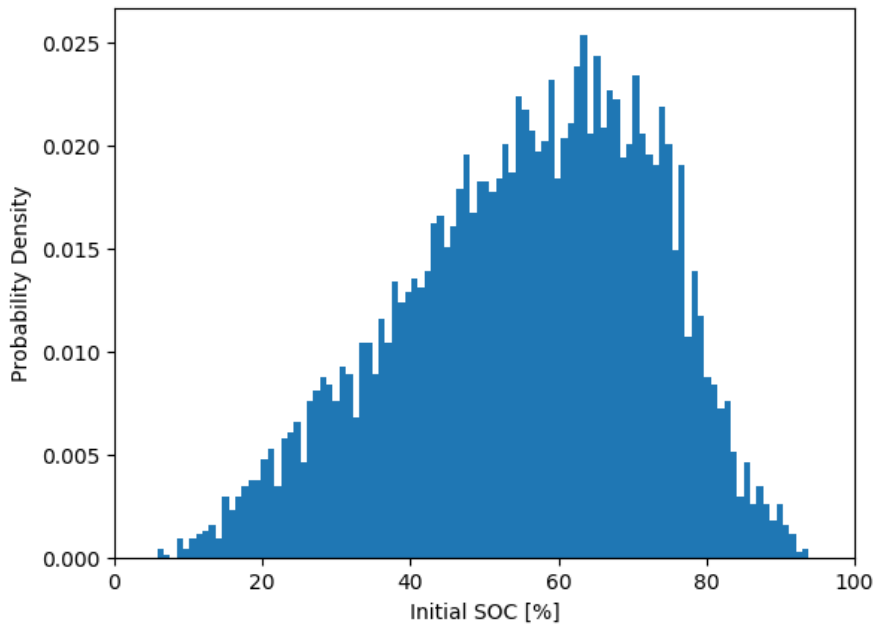


Figure 3.4: Distribution of the initial SOC upon connection to the EVSC

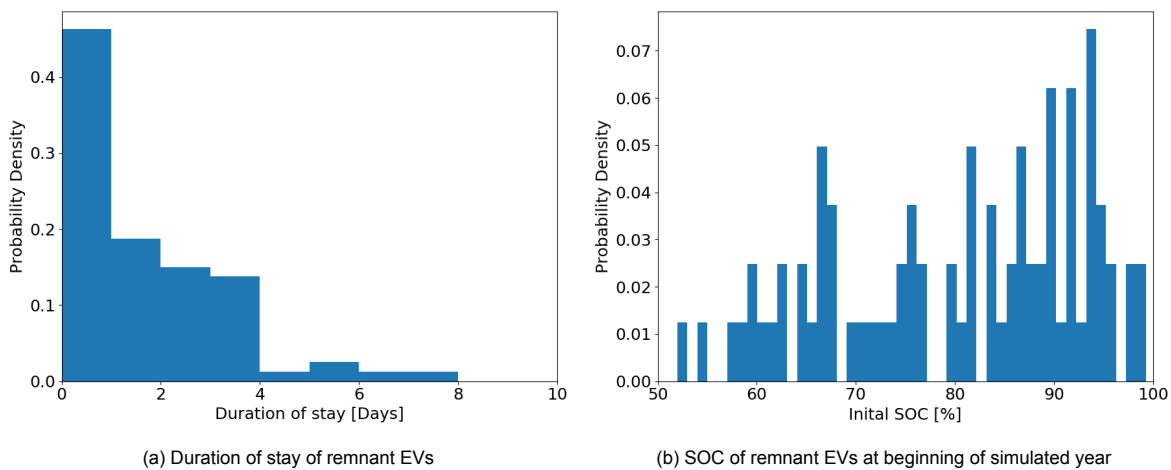


Figure 3.5: Simulated data for EVs occupying the EVSC system from the previous year

In addition to the arrival of EVs throughout the year, it has been considered that a number of remnant EVs would be occupying the EVSC system from the previous year. 80 EVs were decided upon in line with the winter occupation of the year simulated. The method of assigning the duration of stay and model of EV were the same as detailed above but with the probabilities associated to the duration of stay altered, producing the distribution in 3.5a. The initial SOC of these remnant EVs, however,

was simply drawn from a truncated normal distribution with limits 50 and 100 and a mean of 85, as presented in figure 3.5b. The rationale being that these EVs would already have been parked for some duration, meaning their remaining time would be reduced and their SOC raised with respect to newly arriving EVs. The limits and probabilities assigned in this process were arbitrary but thought of as representative.

3.3. Solar PV System Model

Irradiance data was retrieved from the European photovoltaic geographical information system (PVGIS) [89], provided by the Joint Research Centre (JRC) branch of the EU Commission. Using a vast network of sensor stations across Europe myriad data is logged, among which is all that is required for the modelling of PV systems.

A typical meteorological year (TMY) data file for Lelystad (52.456,5.517) was input into SAM, where the system was also modelled. The decision to use SAM was made because it is a verified and accurate modelling program that is intuitive to use and easily accessible. A TMY file contains location specific meteorological data presented as hourly data for: dry bulb (air) temperature, relative humidity, global horizontal irradiance (GHI), direct irradiance (DNI), diffuse horizontal irradiance (DHI), downwards infrared irradiance, windspeed, wind direction, and surface air pressure.

A brief explanation of SAM's modelling process is hereby presented, further information can be found in the documentation [90].

3.3.1. Irradiance Model

Solar irradiance is a measure of the instantaneous power, or intensity, of sunlight incident on a surface, expressed in watts per square meter (W/m^2). It can be split into various components:

Global Horizontal Irradiance (GHI)	The total irradiance incident on a flat surface positioned horizontal to the ground
Direct Normal Irradiance (DNI)	The component of light incident on a surface normal to the sun in a straight beam, considering the solar disk is not a point
Diffuse Horizontal Irradiance (DHI)	The component of light incident on a horizontal surface from all areas of the sky excluding the solar disk. This light has been diffracted by the atmosphere and clouds etc.
Plane-of-Array Irradiance (POA)	The total irradiance incident on a surface in the same plane as the array.

The chosen SAM model used DNI and DHI to calculate POA, this is then simply multiplied by the total array area to yield incident solar power.

For each time step the simulation calculated the solar position, namely the sun's zenith, altitude, and declination angles. SAM's algorithm used the method as described by Michalsky [91] which is based on the Astronomical Almanac's algorithm for period 1950-2050. These angles were then used to calculate the angle of incidence (AOI), that is, the angle between the direct beam irradiance on the PV array, calculated using the extra-terrestrial radiation, and the normal to that surface. From this, the POA beam irradiance was deduced for each time step.

The Perez sky diffuse model was chosen, described in [92, 93], with the added modification that treats radiation for zenith angles $87.5^\circ \leq Z \leq 90^\circ$ as isotropic. The Perez model used empirical data measured in a variety of sky conditions and locations, culminating in the coefficients used rather than mathematical representations. This ultimately produces a more accurate model than other options, namely the Isotropic model and the HDKR model. In brief: the Perez model accounts for the fraction of the sky visible from the array surface, the sky clearness, the optical air mass, and circumsolar and horizon brightness.

POA Ground reflected irradiance is that which arrives at the surface of the array after being reflected off the ground and associated objects and arrives as diffuse irradiation. It is a function of zenith angle, DNI, DHI, and of course the albedo. The albedo value was assumed to be 0.2 year round. This value is consistent with urban areas (0.14 - 0.22), fresh grass (0.26), and asphalt (0.09 - 0.18) [94], the likely

surrounding mediums. Ultimately, however, in this application where the array tilt angle is so low at only 15°, ground reflected irradiance had very little influence on the electricity generated.

The total incident POA irradiance is then the sum of these three components, namely the direct, diffuse, and ground reflected irradiances. Furthermore, no shading effects were considered for this system since the area in question is isolated from large constructions and there is very little in the way of tree coverage. Furthermore, since the effects of shading are very location specific and the general rule of thumb for PV systems is to avoid shade it was thought that by not including these detriments it would better serve to highlight the system potential.

3.3.2. PV Module Model

The module model chosen was the California Energy Commission (CEC) Performance Model which uses the single-diode equivalent circuit model and six parameters as described in De Soto [95]. The model was used in conjunction with the module database provided by the software (in the 2018 release).

The five-parameter single-diode equivalent circuit equation for the current I of the module at a certain voltage V , is:

$$I = I_L - I_o \left[\exp\left(\frac{V + IR_S}{a}\right) - 1 \right] - \frac{V + IR_S}{R_{Sh}} \quad (3.8)$$

Where I_L is the reference light current, I_o is the reference diode saturation current, R_S is series resistance, R_{Sh} is the shunt resistance and a is reference ideality factor. The reference value used here are module specific and are stored in the module database of SAM. Furthermore, the temperature coefficients for I_{SC} and V_{OC} are adjusted from the specified values using the sixth parameter, the adjustment factor as calculated by SAM's coefficient generator.

The only short-coming of this approach was SAM's assumption that the module operated at V_{MP} , which for this application is not the case. As explained in section , the PV array operated at the necessary power level to meet the load. Throughout the winter months this was V_{MP} due to the low irradiance levels. However, during summer large energy curtailments were required. The energy curtailed in these times correlates to the drop in voltage operating point that would be experienced in the real world application.

3.3.3. Cell Temperature Model

Described in Duffie and Beckman [96] and De Soto [95] the Nominal Operating Cell Temperature (NOCT) PV cell temperature model was chosen in conjunction with the CEC Performance Model. It used the wind speed provided in the TMY file adjusted to the specified array height of one story, as well as using an adjusted NOCT for mounting configuration of the modules which was decided to be rack mounted.

The PV cell temperature was then:

$$T_c = T_a + \frac{G}{800} (T_{noct,adj} - 20) \left(1 - \frac{\eta_{ref}}{\alpha\tau}\right) \frac{9.5}{5.7 + 3.8v_{w,adj}} \quad (3.9)$$

Where T_a is the ambient temperature, G is irradiance, $T_{noct,adj}$ is the adjusted NOCT, η_{ref} is the reference module efficiency, $\alpha\tau$ is the effective absorbance-transmittance product, and $v_{w,adj}$ is the adjusted wind speed.

3.3.4. Inverter model

User specified inverter parameters were entered into the SAM software which used a modified Sandia Inverter Model, the equation of which is:

$$P_{ac} = \frac{P_{ac,0}}{P_{dc,0} - P_{s,0}} * (P_{dc} - P_{s,0})^2 \quad (3.10)$$

Where $P_{ac,0}$ is maximum AC power, $P_{dc,0}$ is maximum DC power, and $P_{s,0}$ is night-time power consumption.

The hourly system power generated, as simulated in SAM, had a linear interpolation applied for compatibility with the 5-minute interval series produced in the EV arrival model. This was done using a built-in linear interpolation function for timeseries from the Python data analysis library, pandas, which

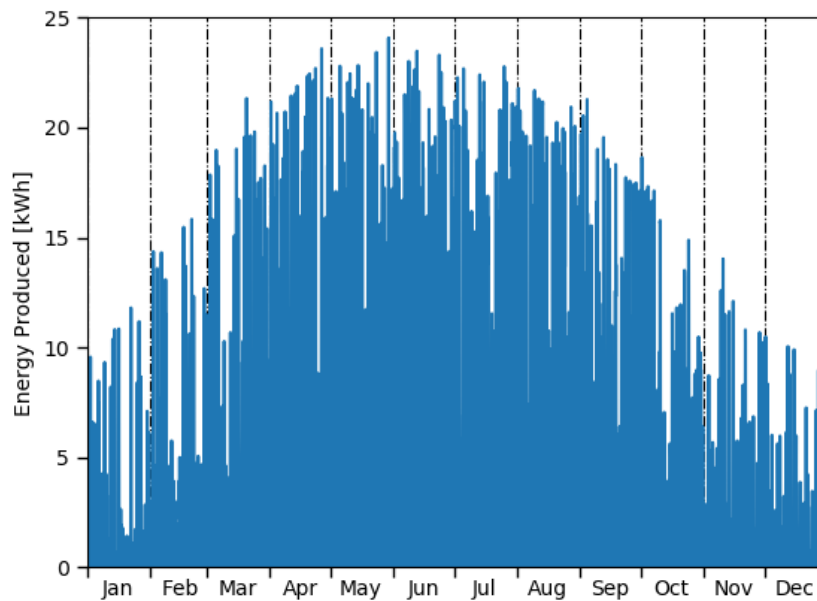


Figure 3.6: Energy produced throughout the year. Simulated power data produced by NREL's SAM software was interpolated and

connected the hourly midpoints. The result of which is displayed in figure 3.6 as the energy produced throughout the year. Of course, a linear interpolation of solar irradiance data cannot account for the characteristic rapid fluctuations in irradiance and could be accused of over-simplifying a complex problem. However, because the time scales considered for charging EVs in this application are typically over multiple days, an average representation of hourly irradiance is suitable since the total energy yield will not differ greatly. There are various other more realistic interpolation methods including: inverse distance weighting, spline (a polynomial function), and kriging (Gaussian process regression) [97]. These should be used in cases where the time scales considered are shorter and a higher resolution of irradiance data is required, for example: an EV charging model in which cars are parked for multiple hours.

3.4. Battery Model

One of the fundamental features of a reliable system model is the battery model itself. To this end, a kinetic battery model, as developed by Manwell and McGowan [98], was used allowing for a detailed characterisation of voltage behaviour within the battery.

For simplicity and ease of simulation, it was assumed all EVs included in this study share the same battery cell, namely, the Panasonic NCR-18650B used in Tesla vehicles [99]. This was because finding specific information on battery cells used by other EV manufacturers proved difficult and in reality most cells have comparable parameter values. With cell V_{nom} equal to 3.6 V and N_s , the number of cells connected in series, equal to 96, the EV battery voltage was 345.6 V, a good approximation for EV batteries. With the useable capacity of all included EVs known, a simple calculation was made to estimate the number of cells in parallel. This was then the fundamental difference between each EV battery.

$$C_{bat}^I = \frac{C_{bat}^E}{V_{bat}^{rated}} \quad (3.11)$$

$$N_p = \frac{C_{bat}^I}{C_{cell}^I} \quad (3.12)$$

Where C_{bat}^I is the rated battery capacity in Ah, C_{cell}^I is the rated cell capacity in Ah, C_{bat}^E is the usable battery capacity in Wh, V_{bat}^{rated} is the rated battery voltage, and N_p is the number of cells connected in parallel.

Table 3.6: EV models and their associated battery parameters. The usable battery capacity in kWh and energy consumption were retrieved from [15]

EV model	C_{bat}^E [kWh]	E_{cons} [kWh/100 km]	N_s	C_{bat}^I [Ah]	N_p
Tesla Model 3	72.5	15.8	96	209.8	66
Tesla Model S	95	18.1	96	274.9	86
Nissan LEAF	36	16.4	96	104.2	33
VW Golf	32	16.8	96	92.6	29
Hyundai Kona	64	16.2	96	185.2	58
BMW i3	37.9	16.1	96	109.7	34
Renault Zoe	52	16.3	96	150.5	47
Tesla Model X	95	20.7	96	274.9	86
Kia Niro	64	17.1	96	185.2	58
Jaguar I-Pace	84.7	22.9	96	245.1	77

The EV batteries had an assumed charging efficiency of 95%, however, this is highly dependant on a number of battery parameters, namely; the SOC, temperature, number of charge cycles, discharge/charge current, and internal electrochemical conditions such as ion mobility [64]. The impact of these variables on system performance were outside the scope of this study.

3.5. Charging Strategy

The amount by which a car battery was charged in a given time step was dependent on a number of variables that can, for the purposes of this model, be simplified to the power produced by the PV array at that instance and the number of other active EVs in the system with which to share that power. An active, as they are described in this paper, is an EV that was still in need of charging, ie. the EV's SOC was less than 100%. An idle EV was one that had completed charging and now occupied the parking space fully charged and idle. Since the simulations completed for this study did not employ any further smart charging methods, the power produced was split evenly between the active EVs. The iterative logic employed in this model is detailed in this section with a flow chart of this logic presented in figure 3.7.

Let the total number of EVs in a carpark in time step t be N_t with $I_{n,t}$ being the charging current to be delivered to EV n in t . Each EV model has different battery properties as detailed in table 3.6. Each active EV had a different state of charge depending on the initial value SOC_n^i upon arrival, the parking duration up until t , the power generated by the solar array at each time step, and the number of active EVs occupying the carpark, N_A , at each t . Note, N_A was counted after the charging cycle in each time step and considered only if an EV was active or not. The first action in the next t was to account for any arrivals in t or departures at the end of $t - 1$, using $N_{A,t-1}$. This can be better understood in equation 3.12 which ensured the correct balance of vehicles in each time step, and as such the energy balance was maintained.

$$N_{A,t} = N_{A,t-1} + VA_t - VD_{A,t-1} \quad (3.13)$$

Where $VD_{A,t-1}$ is the number of active vehicles departing in the previous time step. If an EV that was already idle left no change in $N_{A,t}$ would occur since it was already accounted for in $N_{A,t-1}$.

The decision to charge an EV was based on its SOC in the previous time step. If $SOC_{n,t-1} < 100$, charging can take place. The AC charging current $I_{n,t}$ was limited to $I_{Max,AC} = 16$ A as per the AC charger and cables used. This is the AC current delivered to the chargers and was rectified by the

EV's on-board charger before charging the battery. Since the nominal battery voltage is 345.6 V, I_{Max} becomes:

$$I_{Max,DC} = \frac{16 * V_{LN} * \eta_{OC} * \eta_{Ch}}{V_{Batt}} \quad (3.14)$$

Where V_{LN} is the line-to-neutral voltage, 230 V, η_{OC} is the on-board charger efficiency of 93% [64], η_{Ch} is the AC charger efficiency of 99.5% [64], and V_{Batt} is the nominal battery voltage of 345.6 V. Therefore, $I_{Max,DC} = 9.85$ A.

Below, the decision for $I_{n,t}$ is given.

$$I_{n,t} = \begin{cases} I_{Max} & \text{if } \frac{I_{Gen}}{N_A} \geq I_{Max} \\ \frac{I_{Gen}}{N_A} & \text{if } \frac{I_{Gen}}{N_A} < I_{Max} \end{cases} \quad (3.15)$$

Where I_{Gen} is the total AC current output from the inverter stack. Excess power generation was curtailed as described in equations 3.15 and 3.16. Practically speaking this would be done within the inverter, which shifts the operational voltage point of the PV array.

$$E_{diff,t} = (|\frac{I_{Gen,t}}{N_{A,t}}| - |I_{Max,t}|) * t_s * V_{LN} * N_{A,t} \quad (3.16)$$

$$E_{curt,t} = \begin{cases} E_{diff,t} & \text{if } E_{diff,t} > 0 \\ 0 & \text{if } E_{diff,t} \leq 0 \end{cases} \quad (3.17)$$

Where E_{diff} is the energy difference between that when the charging current is equal to $I_{Max,t}$ and when the charging current is equal to $\frac{I_{Gen,t}}{N_{A,t}}$, t_s is the time step of 0.083 hours (5 minutes), and $E_{curt,t}$ is the curtailed energy in time step t . Absolute values for charging currents are used since the battery model, as described in section 3.4, required a negative voltage for charging.

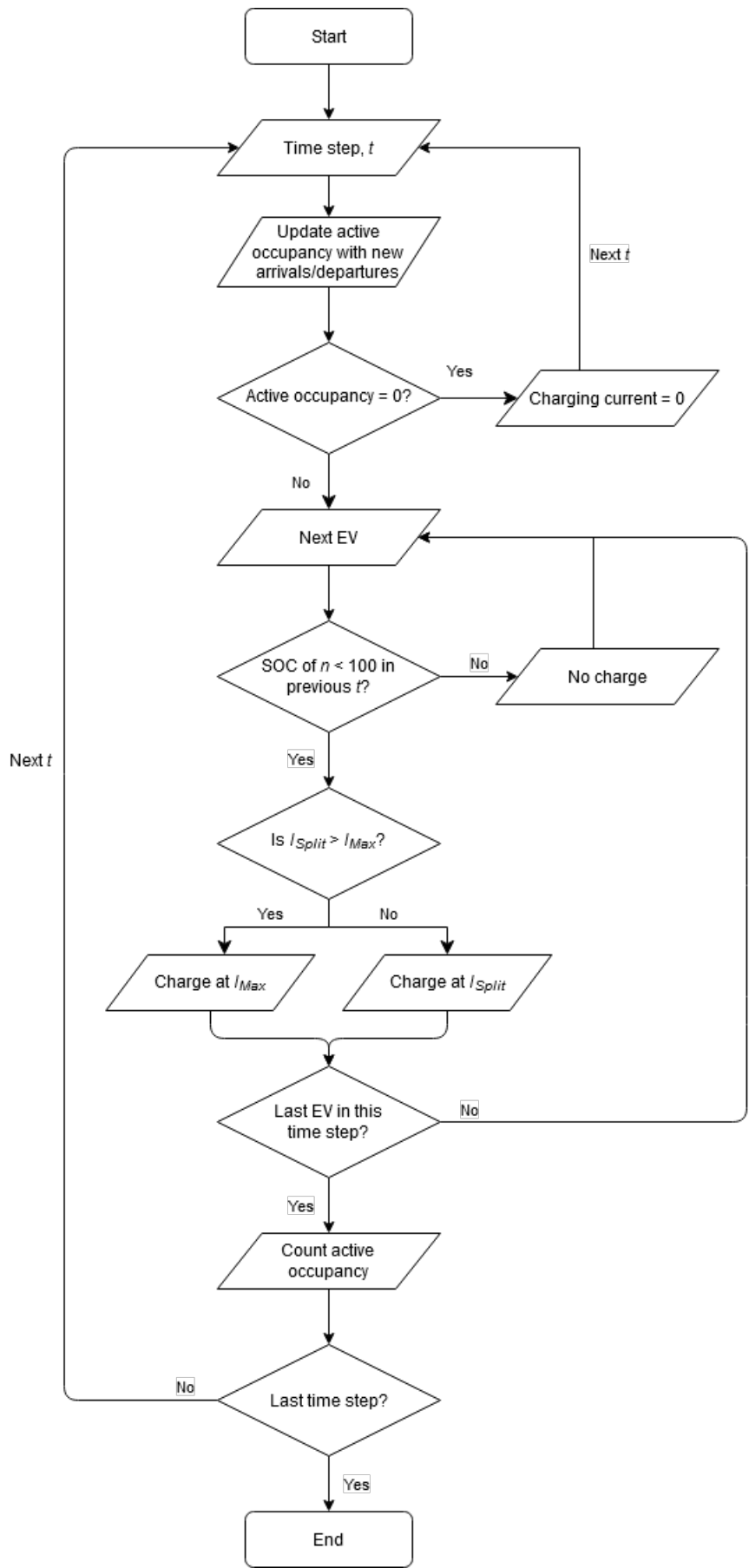


Figure 3.7: Flowchart explaining the iterative logic used through the time series

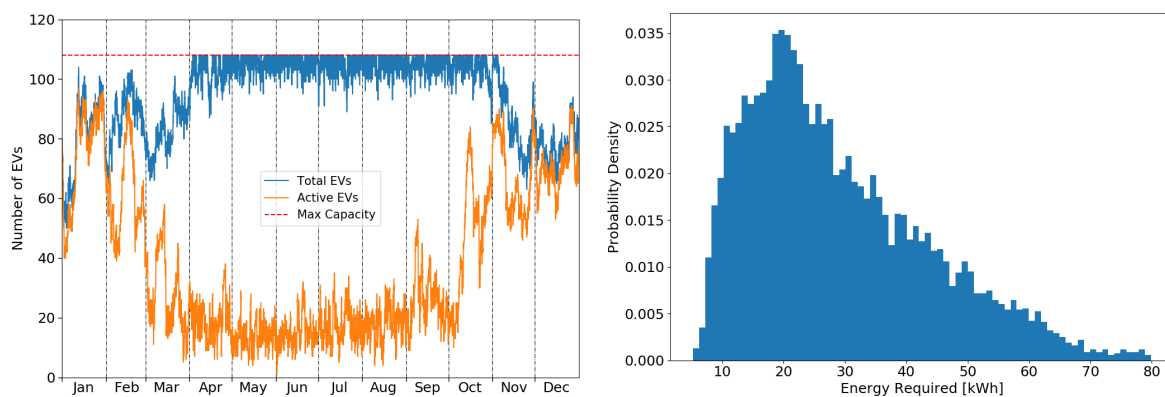
4

Results & Discussion

Using the charging strategy presented in section 3.5 in conjunction with the model developed in section 3.2, the off-grid EVSC system was simulated for a full year. This chapter presents the results of the simulations and analyses the charging efficacy. Firstly, notable figures and results of the initial simulation are presented and discussed. This is then referred to as the base case and serves as a reference against which a sensitivity analysis is compared. Section 4.2 details the methods used to formulate the sensitivity analyses and presents some representative results of that altered input. Section 4.3 then assess the charging efficacy of these scenarios relative to the base case and discusses the implications for off-grid EVSC system design. Finally, section 4.4 further investigates how the worst performing month is affected by the changing inputs.

4.1. Charging Efficacy of an Off-Grid EVSC for Long Stay Carparks

The results of the off-grid EVSC simulation were collated. This section presents and discusses the charging efficacy of this base case simulation and the system design implications. Considering the data presented in table 4.1 and figures 4.1a and 4.1b, the annual energy profile of the system is tabulated in table 4.2. The charging efficacy of the EVSC system can best be visualised in figure 4.2, which divides the final SOC into bands of 25% with fully charged, or 100%, being designated its own count.



(a) Running count of the total number of EVs and number of active EVs within the EVSC system (b) Normalised histogram presenting the energy requirement of the EVs entering the EVSC system

Figure 4.1: Representative data of the EVs using the EVSC

This off-grid EVSC system fully charged almost 75% of the EVs across the whole year with as few as 0.37% of EVs leaving with a SOC lower than 25%. This low final SOC, below 25%, is henceforth referred to as a critically low SOC. As figure 4.3 displays, these all occurred in the winter months of January, February, October, November and December when irradiance levels were at their lowest, as to be expected. Overall, 14.5% of EVs using the system left with a less than adequate SOC, the

Table 4.1: EV usage of the EVSC

Variable	Value
Total EVSC users	6847
Average number of occupants	95.3
Minimum number of occupants	50
Average number of active occupants	37.8
Minimum number of active occupants	1
Average occupancy ratio	52.5%

Table 4.2: Energy values in the EVSC simulation

Variable	Value
Rated electricity generation	2980 MWh
Electricity produced	323.4 MWh
Energy delivered to EV batteries	160.6 MWh
Electricity curtailed	139.7 MWh
Total energy required by EV batteries	197.4 MWh
Capacity factor	5.39%

vast majority did so in the same five months. In other words, 85.5% of the EVSC system users left adequately charged for their return journey. An adequate is hereby defined as one that allows for an EVs return journey to be completed in one leg with no further charging en-route, assuming the driver is returning to the same location they originated from before travelling to the airport. Since the initial SOC model, section 3.2, used a minimum prior SOC value of 75%, an adequate SOC is also defined as 75%.

January and December saw nearly half of the departing EVs leave the EVSC with a less than adequate SOC. Additionally, 1.69% and 2.04% of EVs left with a critical for January and December respectively. Whilst having many EVs leave fully charged is a respectable result, a vital one to ensure system success and installation is to have none leave with a critically low SOC. Hence, this relatively high percentage of critical SOC was used as an indicator of system performance and the sensitivity analysis conducted in section 4.2 sought to decrease this. December was considered for a worst month analysis due to the increased occurrence of EVs with a low final SOC. Figure 4.4 displays the distribution of final SOC during this month.

Whilst the average number of occupants is at its lowest during winter months the occupancy ratio is at its highest, visible in figure 4.1a. The occupancy ratio is defined as the proportion of actively charging EVs relative to the total number of occupant EVs. This is again an indication that the lack of solar energy throughout the winter months has a large impact on operating performance, whereby the EVs within the EVSC struggle to fully charge and remain active for a greater duration of their stay, hindering the chances of other EVs adequately charging. However, by March over 90% of the EVs left with a fully charged battery, consistent with the drop in average number of active occupants to around 25. Whilst the winter months are relatively poor performing, this poor performance is short lived.

Between the months of April - August, where the average occupancy ratio is around 15%, only 3 EVs departed with a SOC below 100%. These months also saw the vast majority of the annual energy curtailment, presented in figure 4.3. As to be expected, the winter months saw no energy curtailment.

In this simulation 43.2% of electricity generation was curtailed due to the large generating capacity available and the lack of actively charging EVs, specifically during summer months. This meant that the capacity factor fell from a potential value of 10.9% through the use of MPPTs, to 5.4% with the PV array operating at a set point dictated by the active load. 140 MWh is a substantial curtailment and it

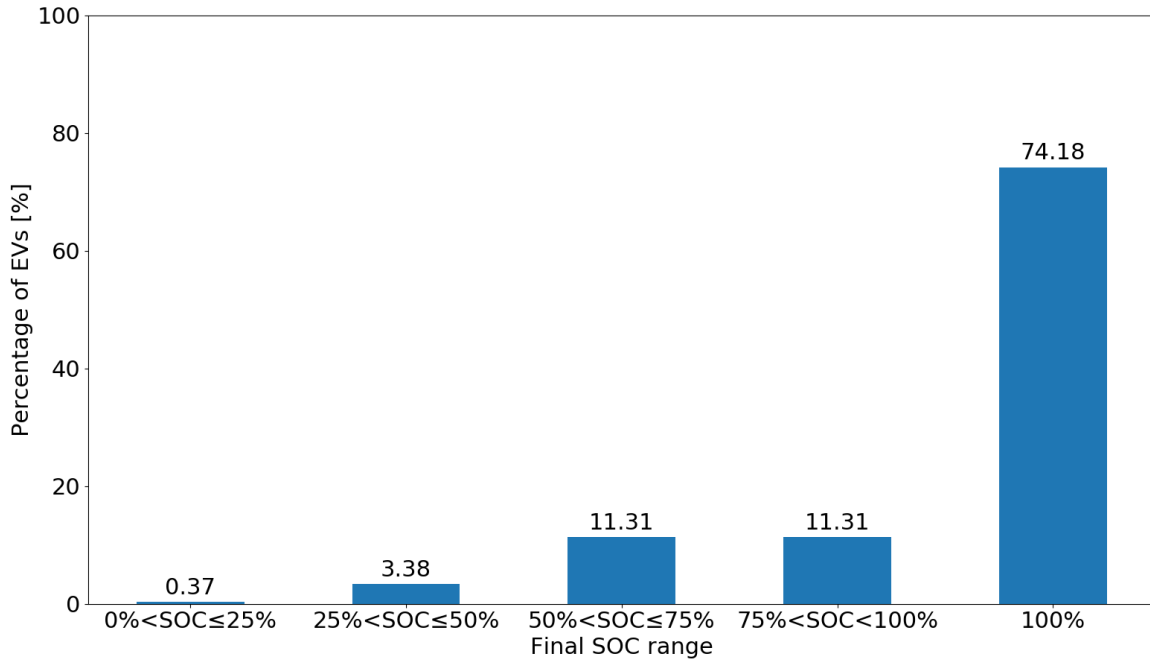


Figure 4.2: Bar chart displaying the charging efficacy of the EVSC system, split into final SOC ranges

is for this reason that an alternative use is suggested for this otherwise lost opportunity for electricity generation, further discussed in section 4.3, where the energy curtailment value is compared against the other simulated cases.

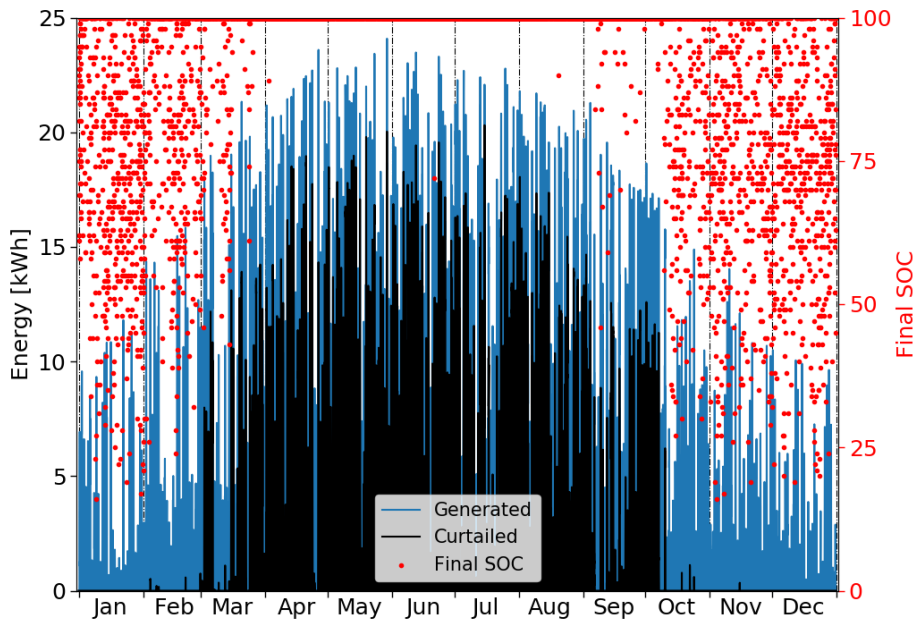


Figure 4.3: Plot showing how final SOC and energy curtailment varies over the year with generation. Each red dot represents a single EV departure event.

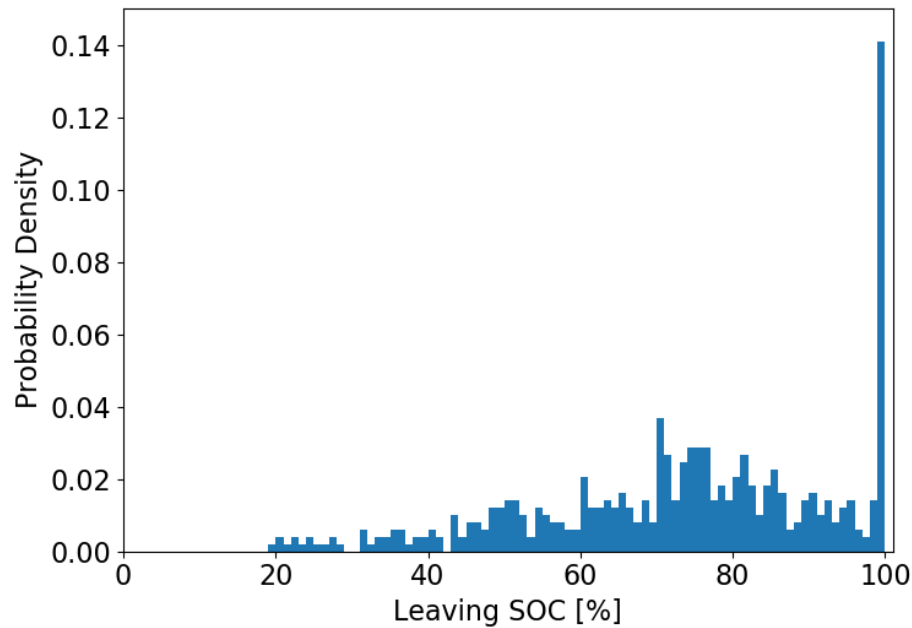


Figure 4.4: Final SOC distribution profile during the worst performing month, December

4.2. Sensitivity Analysis

The results of the base case simulation proved to be very promising with over 75% of EVSC users achieving an adequate SOC before departure. In order to make recommendations for future system design, the controllable variables were systematically altered in a sensitivity analysis which also included some possible uncontrollable scenarios. In order to confine the effects of a specific variable change all other variables within the system must remain constant. This meant seeding all random distributions and choice processes within the model such that identical outcomes were produced when running different iterations of simulation. A further assumption held in these analyses was the initial occupation of remnant EVs occupying the EVSC from the previous year. As in the base case, this number was 80 and the parameters of these EVs remained unchanged.

In line with this study's main research question, the charging efficacy of the off-grid EVSC system is presented for each case studied and the implications discussed. Table 4.3 presents the abbreviations used when referring to each sensitivity analysis case

Table 4.3: Abbreviations used to refer to each sensitivity analysis case, whereby the addition of *X* represents a sub-case

Case	Abreviation
Increased Average Carpark Occupancy	<i>Occ</i>
Altering the Allowable Parking Duration	<i>Dur-X</i>
Lowered Average Initial SOC	<i>SOC</i>
Improved Modules	<i>Mods</i>
Array Tilt Angle	<i>Tilt X</i>

4.2.1. Increased Average Carpark Occupancy - *Occ*

Results of the base case had indicated a promising EVSC system. However, since the arrival of EVs followed the flight departure pattern as per the model described 3.2, a seasonal dependence was introduced leading to the carpark occupancy sharing this pattern. Hence, the relatively low number of occupants during winter months was matched by the relatively low power generation and the number

of EVs leaving with a low final SOC limited.

Young and Wells concluded that a carpark is always between 80-95% occupied [71]. Additionally, future passenger vehicle fleet will include a high share of EVs such that the occupancy of this carpark might not follow seasonal trends, instead remain at a constantly high level of occupancy year-round, as can be expected of a carparking service with high demand. Furthermore, it is assumed this service is provided on a reservation basis, so the scheduling of parking can be made effectively.

To achieve the desired level of occupancy year-round, the EV arrival pattern of May was duplicated for other months with any extra days dropped for the respective months. May was chosen because the occupation remained suitably high throughout the month. No variation or random noise was added at this stage because it was thought of as unnecessary for the purpose intended. The result is displayed in figure 4.5. Although the random selection of EV model assigned to each arrival event was seeded, such that the sequence of EVs arriving remained unchanged relative to the base case, this remained valid only up until the number of arrival events exceeded that of the base case. Since there were now 10,257 arrival events compared to 8505 in the business case, extra EVs were drawn and assigned. This corresponds to all flight departure times after 2019-10-30 13:15.

Since the total number of arrivals in this data set was much larger than the base case, there was an increased occurrence of simultaneous entry attempts. The decision was made to remove many of these to limit computation times whilst achieving the same intended outcome. Therefore, of the 8897 EVs in this data set, 7412 were allowed entry into the carpark. In removing many arrival events from the dataset the sequence of EVs was no longer identical to that of the base case and the EVs chosen to occupy the carpark was not consistent with the base case. However, this is thought to have a negligible effect on the annual, or even monthly, outcome since the EVs are assigned probabilistically meaning the ratio of EV models will be very similar.

By increasing the average number of occupants the annual energy requirement increased by 8.1%. The resulting charging efficacy is visualised in figure 4.6.

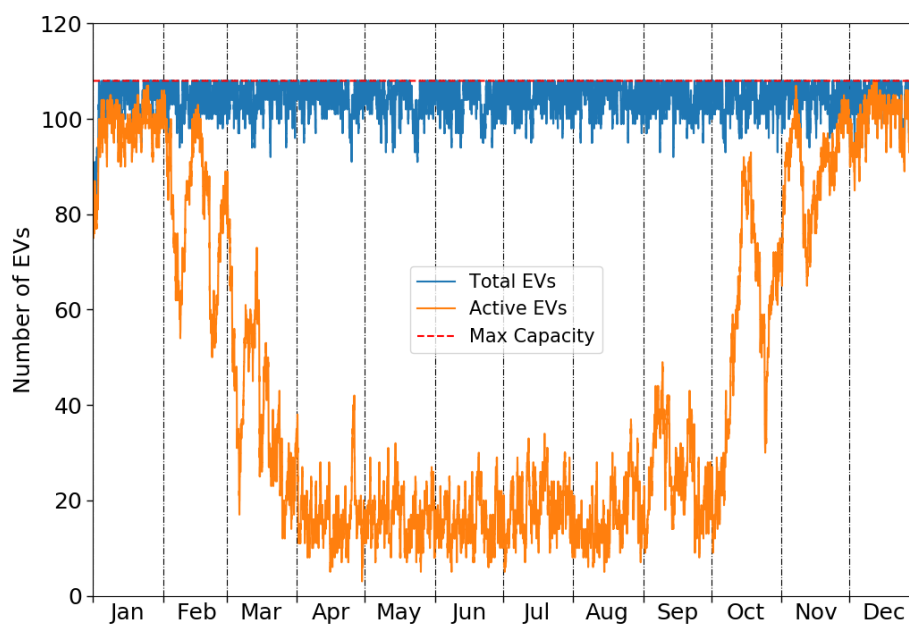


Figure 4.5: Plot showing how the number of active occupant EVs varied relative to the increased average number of occupants

An increased annual average number of occupants was one of the two cases investigated that resulted in a decreased system performance. This presents a very realistic scenario; with the penetration of EVs predicted to increase in coming years it is a fairly safe assumption that such an EVSC would experience a high average occupancy year-round. The increased number of occupants, and thus energy demand, was specifically in months January - March and November and December, the only months in which occupancy fell below 97% throughout the base case. As such, the lowest number of occupants was 75, an increase from 50 in the base case.

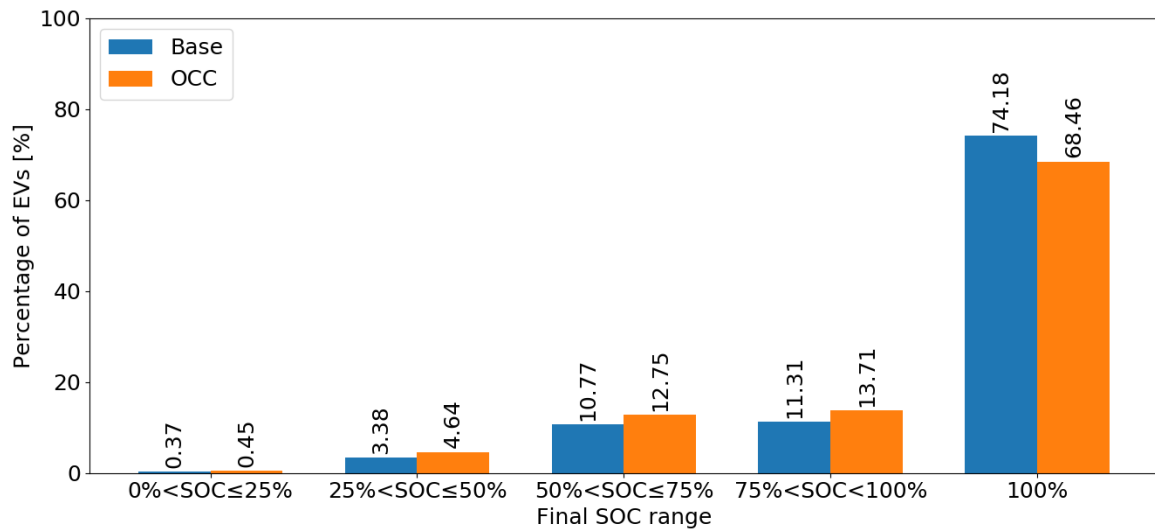


Figure 4.6: Bar chart displaying the charging efficacy in the case of an increased average number of occupants

The drop in fully charged EVs was mostly shifted to the 75%<SOC<100% and 50%<SOC≤75% bands, which saw a 2.4% and 2% increase respectively. The lowest band, the critically low 0%<SOC≤25% band, saw only a 0.08% increase. Of course, any increase is obviously undesirable. The results of this case therefore remain positive, with 82.2% of EVs receiving adequate charge, a little over 3% less than the base case.

This case also saw the second highest occupancy ratio at 45.6%. This is due to the increase in energy requirement resulting from more EVs using the EVSC system. A lower occupancy ratio will result in more effective charging for all active EVs in the EVSC system, hence this is an indication of the reduced performance.

Whilst the base case provided an accurate representation of this specific EVSC system as detailed in in chapter 3, this Occ case describes the potential future situation. These characteristics should be taken into account in order to develop a robust 'future-proof' system. In summary: the summer months performed equally well to the base case since there was no significant change in the system characteristics, whilst the winter months experienced a drop in charging efficacy due to the increased number of occupants and increased energy demand.

4.2.2. Altering the Allowable Parking Duration - *Dur-X*

In designing a long stay carpark one can define the allowable duration of stay interval; for example Schiphol, and hence the base case simulation, allowed parking durations of 48 hours and above. As such, the minimum and maximum allowable duration of stay were altered and analysed.

Firstly, an increase in the minimum allowable duration of stay was performed. Initially 2 days, this was increased in daily increments up to 5. The goal of this was to determine if any significant increase in charging efficacy was achieved and at what point this occurred. The distributions were thus truncated at the respective lower limits, keeping the upper limit at 21 days.

Secondly, the maximum duration of stay allowable in the carpark was lowered from 21 days to 10 and then 7 days separately to better understand the impact of the longest parking durations on system charging efficacy. The distributions were thus truncated at the respective upper limits, keeping the lower limit at 2 days.

Increasing the Minimum Allowable Parking Duration

As made visible in figure 4.7, the greatest improvement in charging efficacy was achieved when the minimum allowable parking duration was increased to 5 days. It resulted in 87% of EVs leaving with a fully charged battery and only 0.06% left with a final SOC below 25%. This trend of improved system performance continued with cases *Dur-4* and *Dur-3*, which saw 0.14% and 0.28% of EVs in that critically low SOC band, compared to 0.37% in the base case.

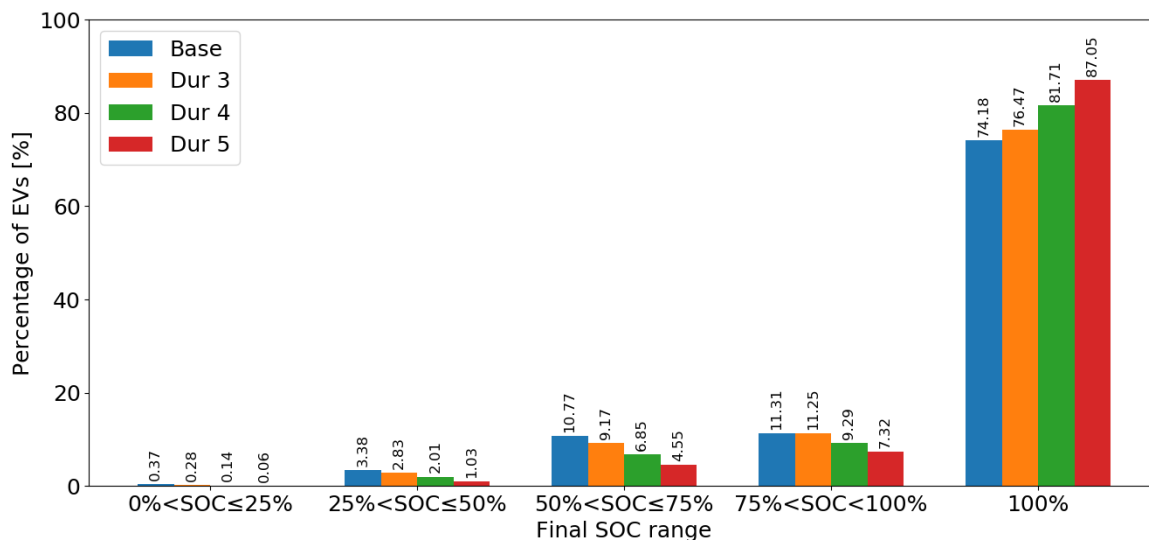


Figure 4.7: Bar chart displaying the charging efficacy in the case of increased minimum allowable parking duration

In total 94.4% of EVs left with an adequate SOC over the year in the *Dur-5* case, with 91.0% and 87.7% in the *Dur-4* case and *Dur-3* case respectively. When compared to the base case, which saw 85.5% adequately charged, this design choice of increasing the minimum allowable parking duration clearly leads to improved charging efficacy.

By increasing the minimum allowable parking duration, the number of EVs using the EVSC per year was reduced and the average occupancy was increased, since those that do use it are staying for a longer time with respect to the base case. This also meant that a greater number were idle and not in need of charging; the average annual occupancy ratio was 24.3%, 28.5% and 34.3% for the cases *Dur-5*, *Dur-4*, and *Dur-3* respectively, with the first two achieving 0 active EVs at times. This resulted in a large increase in energy curtailment of 52.6% for the *Dur-5* case. This large increase meant that in total 65.9% of the power generated by the PV array was curtailed. Considering the research goals of this study and the intentions for this EVSC system to be completely off-grid, this is inevitable.

Deeper analysis of the monthly performances demonstrated the possibility of altering the allowable parking duration depending on the monthly irradiation. Using 3 days as the minimum parking duration in months March and October yielded a percentage of adequately charged EVs of 94.3% and 89.7% respectively, whilst enforcing a 4 day policy in February and November improved the percentage of adequately charged EVs to 84.3% and 84.1% respectively. Of course, there will be repercussions to the revenue stream due to the reduced number of EVSC users. This is in line with Schiphol's sheltered parking tariffs, whereby the first day's stay is €77.50 and then every subsequent 24 hours is €7.50 [100]. This suggests it is more profitable for a carpark to see more cars using the parking service for shorter durations.

Decreasing the Maximum Allowable Parking Duration

Both cases of decreasing the maximum allowable parking duration yielded marginal differences in charging efficacy with respect to the base case, as can be seen in 4.8. The *Dur-10* and *Dur-7* case resulted in 85.6% and 85.9% of EVs receiving adequate charge respectively. This is practically the same as the base case's 85.5%.

With fewer EVs staying for longer durations, a higher throughput of EVs was possible resulting in a 3% and 7% increase in the number of EVSC system users over the year. As discussed, a greater number of EVs using the carpark will produce a higher parking revenue since the first 24 hours incurs a greater tariff than subsequent 24 hours.

Since more EVs were using the EVSC system and stayed for a shorter duration, the average number of actively charging EVs was higher, leading to the increased occupancy ratio for both cases: up to 41.1% and 43.2% for 10 and 7 day maximum durations respectively.

Since the proportion of EVs staying for long durations, specifically over 7 days, was relatively low

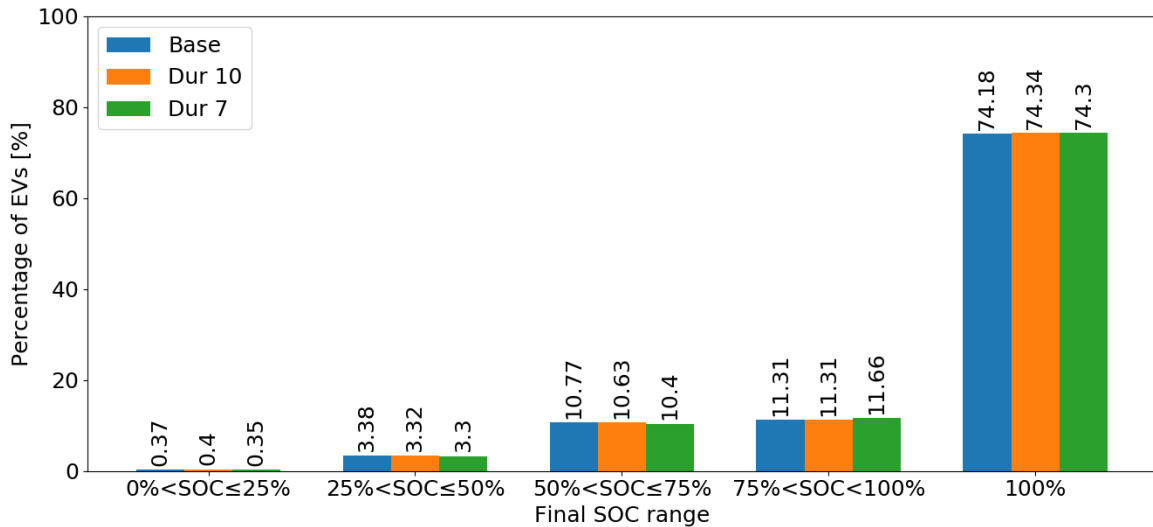


Figure 4.8: Bar chart displaying the charging efficacy in the case of decreased maximum allowable parking duration

there is little change to system performance. However, higher throughput of EVs resulted in a potential for greater parking revenue.

4.2.3. Lowered Average Initial SOC - SOC

The initial SOC upon entry to the carport as shown in 4.9 was originally a normal distribution with a mean value at approximately 60%. This mean was shifted to around 40%. The intention was to further investigate the dependency of charging efficacy on the EVs' initial SOC, an uncontrollable parameter; lower initial SOC presented the system with a larger energy requirement. To generate this new distribution, the mean distance driven to the airport was increased to 120 km and both the lower limit of SOC prior to the journey and the mean value of that distribution were decreased to 60% and 65% respectively. Although these values are less realistic for the case of Lelystad, due to the short journeys necessary to reach an airport in the Netherlands and the high density of charging infrastructure available, the desired outcome is the initial SOC distribution for analytical purposes and the reasoning to reach the values not significant.

It is clear that having a lower average initial SOC, and hence a larger energy requirement, produces the greatest decrease in system performance, as displayed in figure 4.10. Whilst for the case of Lelystad Airport the initial SOC may not actually decrease much, since the charging infrastructure in the Netherlands will only become more extensive, for other airports in similar climates which will likely see an increased average driving distance, such as those in Germany, the average initial SOC may resemble this distribution.

During winter months it was inevitable that many EVs would suffer from a lack of charging. As a result, the annual charging efficacy profile displayed just over 1% of EVSC users leaving with a critically low SOC, over double that of the base case. The next SOC band up, 25% < SOC ≤ 50% also experienced a two-fold increase in occurrences. So, whilst both the *Occ* case and *SOC* case saw a similar ratio of fully charged EVs, this *SOC* case had far more occurrences of low final SOC. Even still, the months of April - August averaged over 98% of the EVs being fully charged.

This case therefore resulted in the lowest number of adequately charged EVs at 76.8%, almost 10% fewer than the base case.

This case also saw the highest occupancy ratio at 48.3%. This is indicative of the constant shortage of energy in the system required to charge the EVs due to the increased energy demand. However, due to the significant increase in energy required by the EV batteries to reach a full SOC, the annual percentage of energy curtailment was the lowest of all cases studied, at 32.4%.

This was certainly the worst performing case, as to be expected, and is uncontrollable for a system designer. As such, consideration must be given in order to mitigate the effect of such a case. Moreover, if this case were to occur with the *Occ* case simultaneously then the EVSC system's charging efficacy

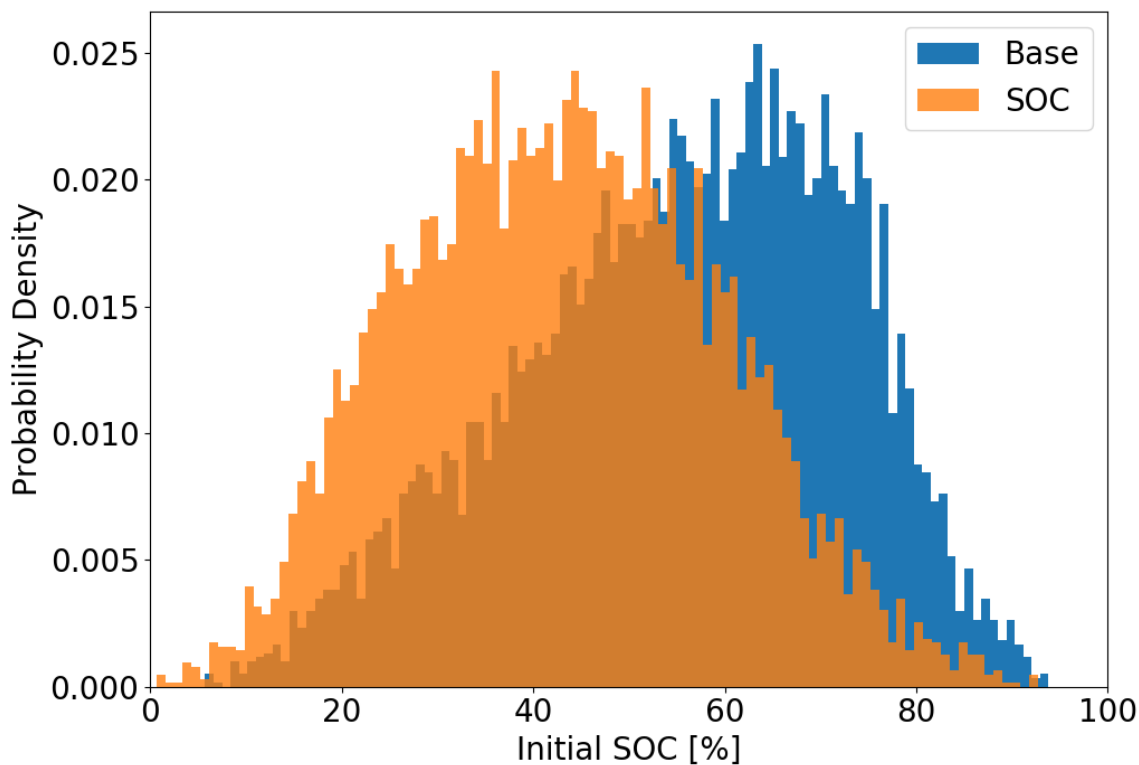


Figure 4.9: Shifted distribution of the initial SOC upon connection to the EVSC

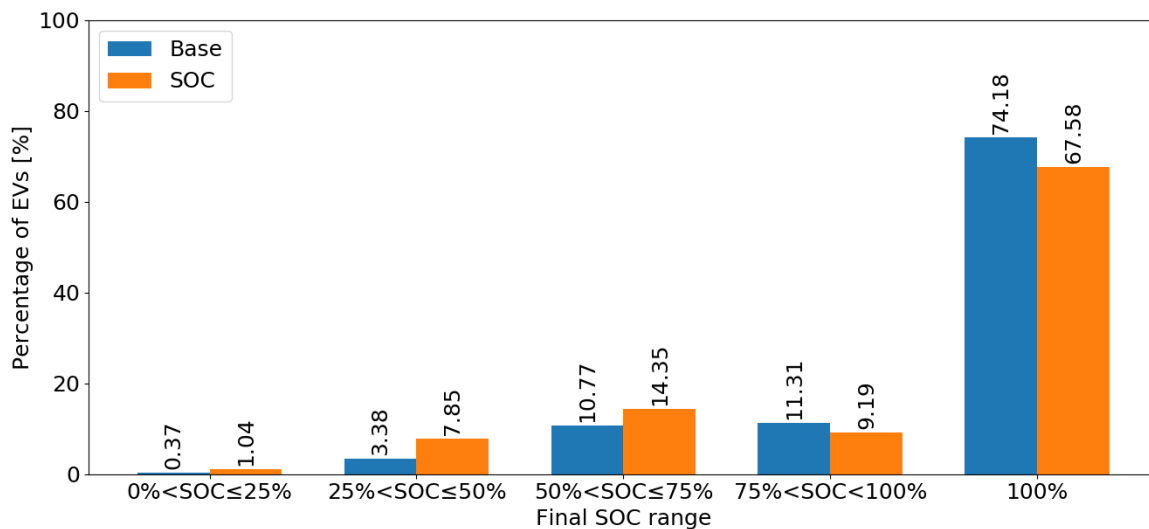


Figure 4.10: Bar chart displaying the charging efficacy in the case of decreased average initial SOC

would suffer greatly during the winter months.

4.2.4. Improved Modules - Mods

The choice of PV modules used are representative of mc-Si modules currently installed in the field. However, in the past year (2019-2020) average power has increased with 350 W - 370 W 60-cell modules being very common. Jinko recently announced the Tiger Pro series, in which their 60 cell module achieves 430W [101] with JA Solar also having announced a 500 W 72 cell module with similarly

high-powered 60 cell modules [102]. Risen has also announced 440 W 60 cell modules [103]. However, no datasheets were available at the time of writing. So a method of extrapolating Jinko's Cheetah module to the Tiger module was employed, from which it was possible to approximate the parameters of this new 430 W module, the parameters of which are defined in table 4.4. Temperature coefficients and module dimensions were assumed to be the same as both the Cheetah and Tiger modules and conversion efficiency was stated in the press release.

Table 4.4: Theoretical module used

Parameter	Value
P_{\max}	430 W
V_{OC}	47.69 V
I_{SC}	11.42 A
V_{MP}	40.07 V
I_{MP}	10.73 A
η	21.6%

The third largest improvement was produced by the installation of 430 W modules which is also a very realistic scenario when considering the trend of increasing module rated power and falling module prices. Higher efficiency modules can generate more electricity than the those used in the base case in the same lighting conditions and can charge the EV batteries quicker resulting in a lower annual average occupancy ratio, here found to be 34.0%. It should go without saying that the improvement to charging efficacy with respect to higher efficiency modules is entirely dependent on the rated power of the modules, with higher rated powers producing a greater improvement. As such, this sensitivity analysis case is illustrative of the current top of the range modules.

As presented in figure 4.11, the number of EVs departing with a critically low SOC fell to 0.25%, whilst the number of fully charged EVs rose to 80.0%. The number of adequately charged EVs reached 90.6%, compared to the 85.5% of the base case.

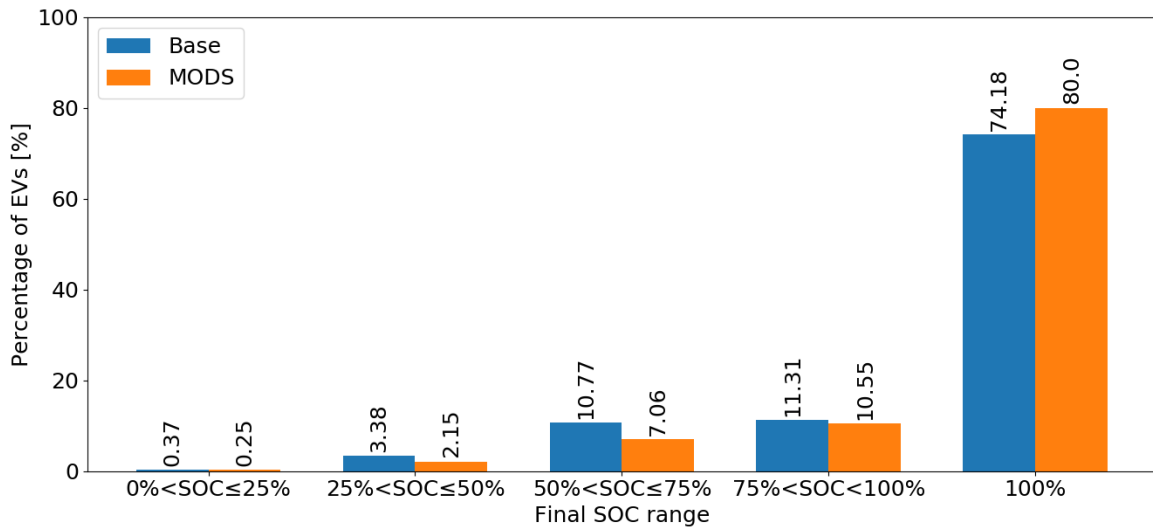


Figure 4.11: Bar chart displaying the charging efficacy in the case of increased PV module efficiency

Figure 4.14 shows that the annual increase in energy production associated with higher efficiency modules is 36.2%; spread throughout the year this increase is more prominent during summer months but winter months also experience an increased generation. The energy curtailment increased to 55.4% of total generation which further reduced the capacity factor of this system.

An important finding was that the increase in electricity generation attained with higher efficiency modules has the potential to offset the decreased system charging efficacy that would result from an

increased average occupancy. The 8.1% increase in energy demand associated with an increased average occupancy is focused in the winter months. This point is further discussed in section 4.4.

4.2.5. Array Tilt Angle - Tilt X

The tilt of the modules can have a drastic effect on system performance due to the solar cells' dependence on direct irradiance. As such, an investigation into the effect tilt angle had on charging efficacy was performed. The base case used a module tilt angle of 15° whilst the sensitivity analysis considered an approximate winter optimal tilt of 69.5° the Dutch annual optimum of 37° and module tilt angles in increments of 5° from the initial 15° up to 35°. The aim of this sensitivity analysis was to determine at what tilt angle a reasonable improvement to charging efficacy could be expected and to illustrate the relative improvement with respect to annual and winter optimums. The annual and winter optimum tilt angles were not intended to be installed but included for completion. This would aid future system design decisions regarding the pay-off between charging efficacy and potential cost of installation due to wind load.

The winter optimal angle is based on the average maximum sun altitude during winter months and therefore direct irradiance, whilst the annual average is a known for the Netherlands and can be found stated in various sources, such as [8, 104]. As can be observed in figure 4.12, December 21st has a maximum sun altitude of approximately 14.5° and June 21st has a maximum sun altitude of approximately 62°. Winter months, here considered November – February, have an average max sun altitude of 20.5°. This value was used to approximate the winter optimal tilt, verified in SAM using a trial and error approach to be approximately 69.5°.

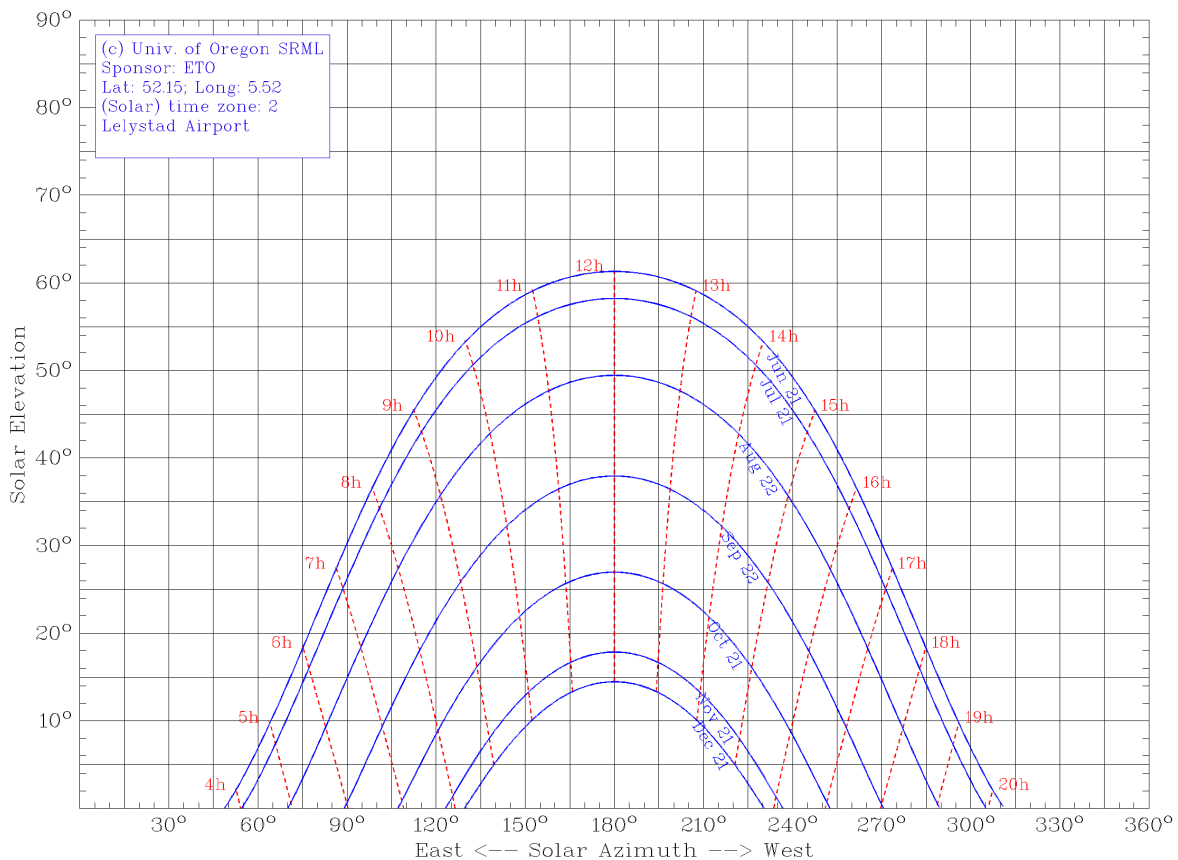


Figure 4.12: Sun chart showing the sun's position throughout the year

It should be noted that cloud coverage, and hence a greater ratio of diffuse irradiance relative to direct, can alter the optimal winter tilt drastically for certain locations that suffer from high cloud coverage, such as the Netherlands. So, whilst the tilt angle may be as high as 70° in winter months for locations at high latitudes, the amount of direct irradiance incident on a PV module in winter months

across northern Europe is relatively low. Rather, diffuse irradiance accounts for a much larger share of the incident light [105] due to the typically cloudy climate.

Increasing the module tilt angle has a direct impact on the annual generation, with tilt angles up to the annual optimum resulting in greater annual energy yield. However, this also resulted in an increasing energy curtailment with module tilt angle, since the annual generation profile increased greater during summer months at angles up to the annual optimum.

By increasing the tilt angle the intention was to determine if any meaningful improvement to charging efficacy was attained. Of course, an improvement was observed, as can be seen in figure 4.13, yet the increased performance is marginal at lower tilt angle increases.

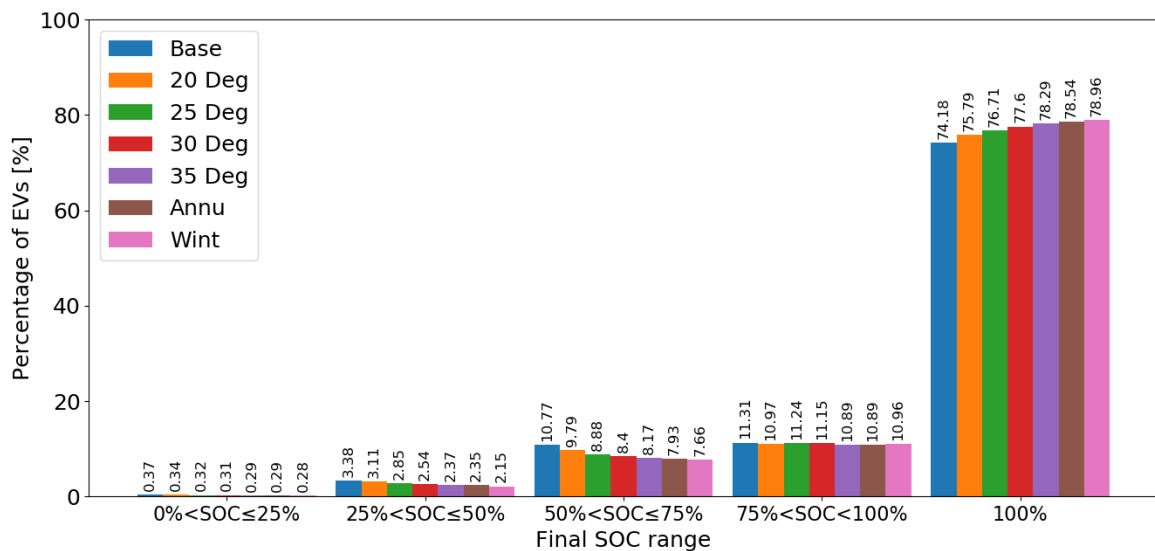


Figure 4.13: Bar chart displaying the charging efficacy in the case of increased module tilt angles

With the goal of reducing the number of occurrences of low final SOC departures in mind, only the larger increases to module tilt angle offer meaningful improvements to charging efficacy. Increasing the tilt angle to 20° yielded a 0.03% decrease in the critically low final SOC, whilst the number of EVs departing with a SOC of 25% < SOC ≤ 50% was reduced by 0.26%. At 30° these reductions reached 0.06% and 0.83% respectively. This correlated to a 1.3% and 3.3% increase in the number of adequately charged EVs for 20° and 30° respectively.

The best performing case of this sensitivity analysis was the winter optimum tilt angle, which offered a 0.09% and 1.23% reduction in the below 25% and 25% < SOC ≤ 50% final SOC ranges respectively, and a 4.4% increase in the number of adequately charged EVs. This should come as no surprise since the majority of poorly charged EVs occurred in the winter months, as depicted earlier in figure 4.3, so a tilt angle better suited to increase energy yield in winter would best charge these EVs.

Practically speaking, the additional costs associated with more extensive foundation works required for higher tilt angles would likely limit the increase in angle to the lowest few iterations. As shown, these lowest tilt angle increases do not prove to have much of an impact relative to other sensitivity analysis cases.

4.3. Conclusive Remarks

The sensitivity analysis conducted has shown that various design alterations result in an increased annual charging efficacy. However, there are also scenarios which result in a decreased charging efficacy, namely the decrease in average initial SOC and increase in annual average occupancy.

Provided here in figures 4.14 - 4.16 is a summary of the changes in annual energy yield, including that which was delivered to EV batteries, curtailed energy, and total energy requirement of the EVSC users to reach a full SOC.

Increasing the minimum allowable parking duration produced the greatest increase in charging efficacy, the amount by which performance improved depended on the defined minimum parking duration.

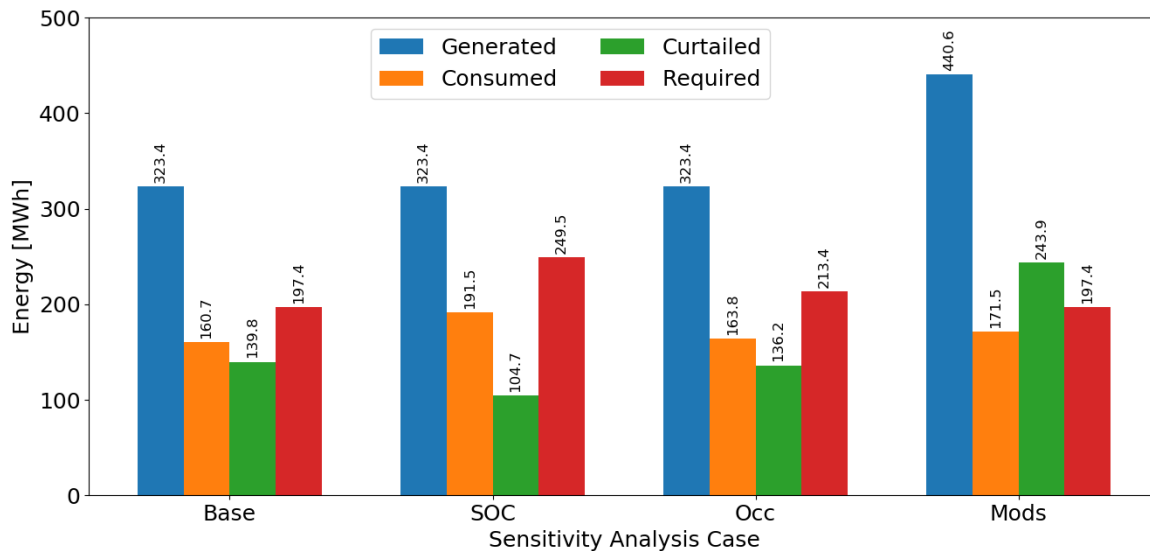


Figure 4.14: Bar chart displaying the annual energy profiles of the SOC, Occ, and Mods cases. “Consumed” represents the energy delivered to EV batteries.

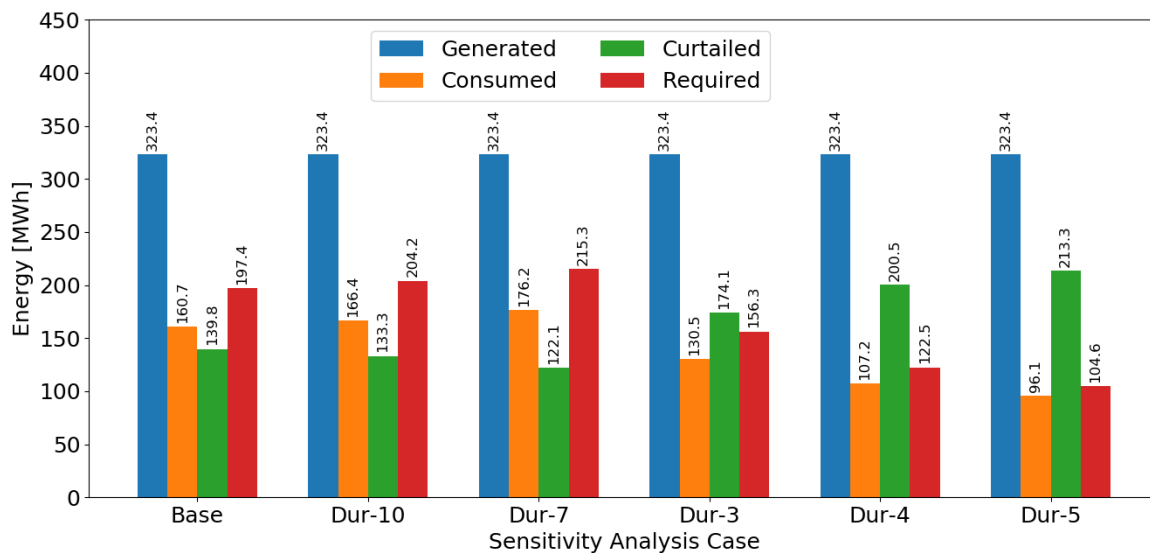


Figure 4.15: Bar chart displaying the annual energy profiles of altered allowable parking durations. “Consumed” represents the energy delivered to EV batteries.

Installing higher efficiency modules resulted in the 3rd largest improvement to charging efficacy, however, this too has its dependency. The case used in this sensitivity analysis considered the very best 60 cell modules (soon to be) available; the amount by which a system’s charging efficacy can be improved therefore depends on the rated power of the modules chosen. Increasing the module tilt angle only produced significant improvements at the very highest angle increases. This will most likely be impractical for EVSC systems due to the raised costs of foundation works.

Decreasing the mean initial SOC had highly detrimental effects on the charging efficacy. Whilst it was deemed unlikely for the case of Lelystad Airport, other EVSC systems might not be situated in a region with an extensive EV charging infrastructure. As such, the potential for this case should be considered when designing EVSC systems and resilience should be embedded. Alternatively, decreasing the maximum allowable parking duration had little effect on the charging efficacy due to the relatively few vehicles parking for such durations. Hence, no worthwhile conclusions were drawn from this sensitivity analysis case and the maximum allowable parking duration can be defined at the operator’s

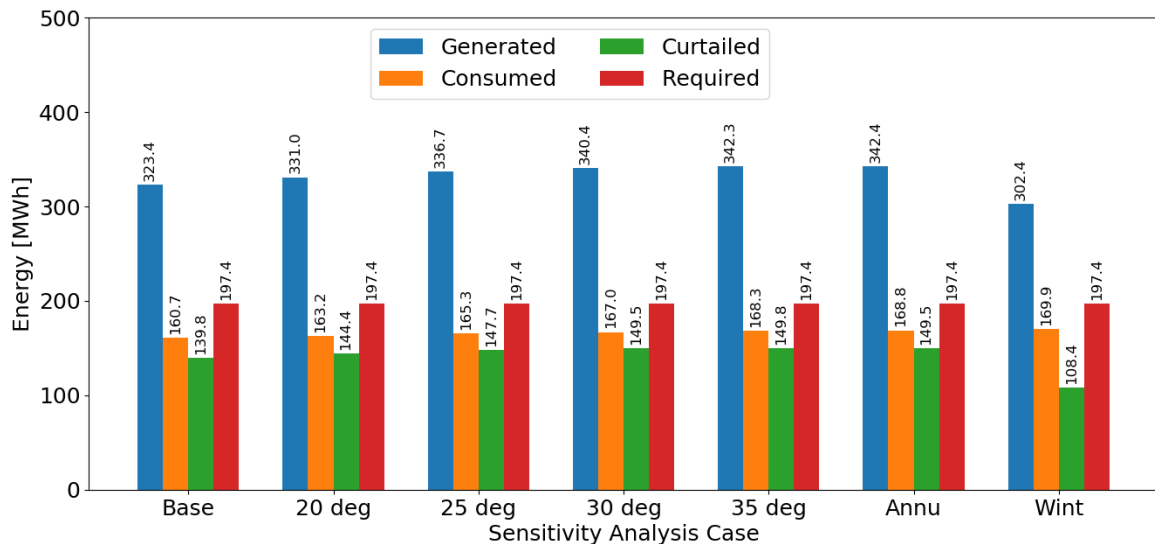


Figure 4.16: Bar chart displaying the annual energy profiles of various module tilt angles. “Consumed” represents the energy delivered to EV batteries.

discretion.

Considering that the market share of EVs is expected to increase, it is highly likely that in the coming years the carpark will remain at near maximum parking capacity throughout the year. This is especially of concern for the months November - March, which in this model were the only months to see average occupancy fall below 97%. Since this increase in occupancy coincides with a decrease in operational performance due to the lower irradiance levels, improvements must be made so as to ensure charging efficacy remains adequate during these low irradiance months.

Actively decreasing the energy curtailment itself is not a meaningful ambition, since only the capacity factor is decreasing. Yet given the large underutilisation of generating capacity achieved throughout these simulations, suggestions on how to better use this lost potential generation is presented. It was found that 140 MWh was curtailed throughout the year in the base case, with the vast majority occurring in months April - August. The obvious recommendation is the installation of a battery energy storage system; if sized and managed appropriately this could store energy for use in winter months. Alternatively, the installation of an electrolyser could prove profitable if hydrogen fuel cell cars become popular. This would of course require a larger investment and extensive study should be performed to gauge the suitability. One other option is to provide charge for airport ground support equipment and terminal building vehicles, many of which are electrically powered. Examples include: shuttle buses, various equipment and luggage transporters, aeroplane loaders and more. This final scenario would require further cabling and a designated area separated from the carpark to allow the charging of such vehicles, but would reduce the grid dependence of an airport during summer months by offering an alternative source of electricity for these vehicles.

In conclusion, a mixture of design decisions can be utilised to not only improve on the base case, but offer assurance to withstand increased energy demands with lower initial SOC and increased winter occupancy. The key parameter that is to be considered is the alteration of the minimum allowable parking duration. The number of days this is changed to is optional but discussed more in the next section since it best improves winter months. Changing the module tilt angle had little meaningful effect at the tilt angles most likely to be employed, i.e. 20° - 30°, and as such this should not be a variable that is altered. Of course, installing better PV modules is a given and depends on the technology available at the time of system design and the respective price of an array using those modules.

4.4. Worst Month Analysis - December

As to be expected for a PV array at a latitude of 52°, the winter months do not offer ideal solar conditions. The effects of this low winter irradiance is best depicted in figures 4.17 and 4.18 for the base case. This clear decrease in performance must be addressed so suitable measures can be taken to better equip

the system to cope during this period. Thus, an analysis of the worst performing month is hereby conducted with the intention to better inform future system design. January and December both had a very similar ratio of fully charged EVs, at around 13%, however, December had produced more EVs with a SOC below 25% and more EVs in the 25%<SOC≤50% range. Hence, December is considered for the worst month analysis.

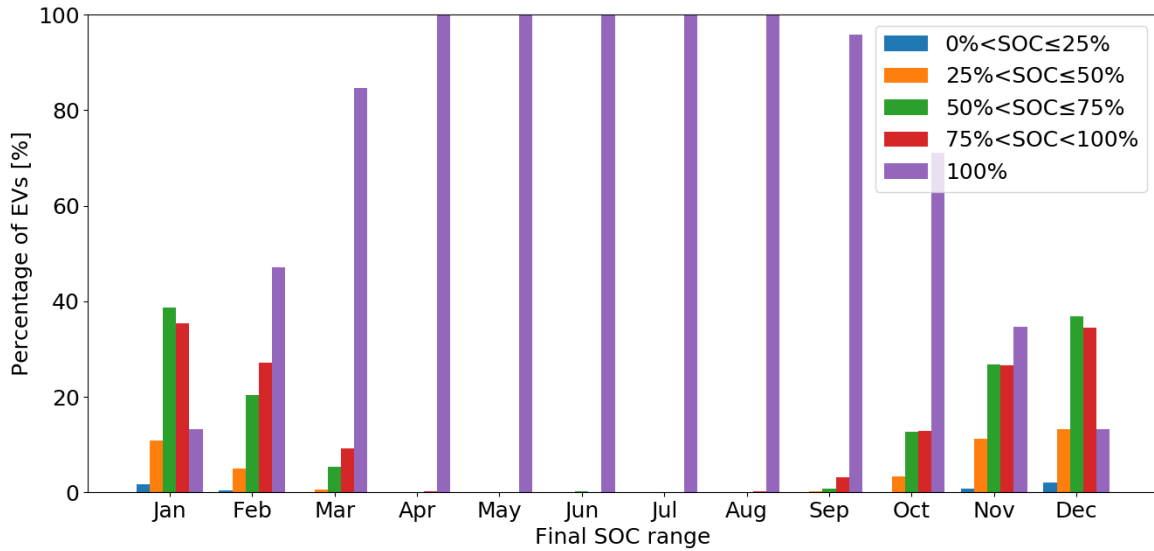


Figure 4.17: Bar chart displaying the monthly variance in charging efficacy for the base case

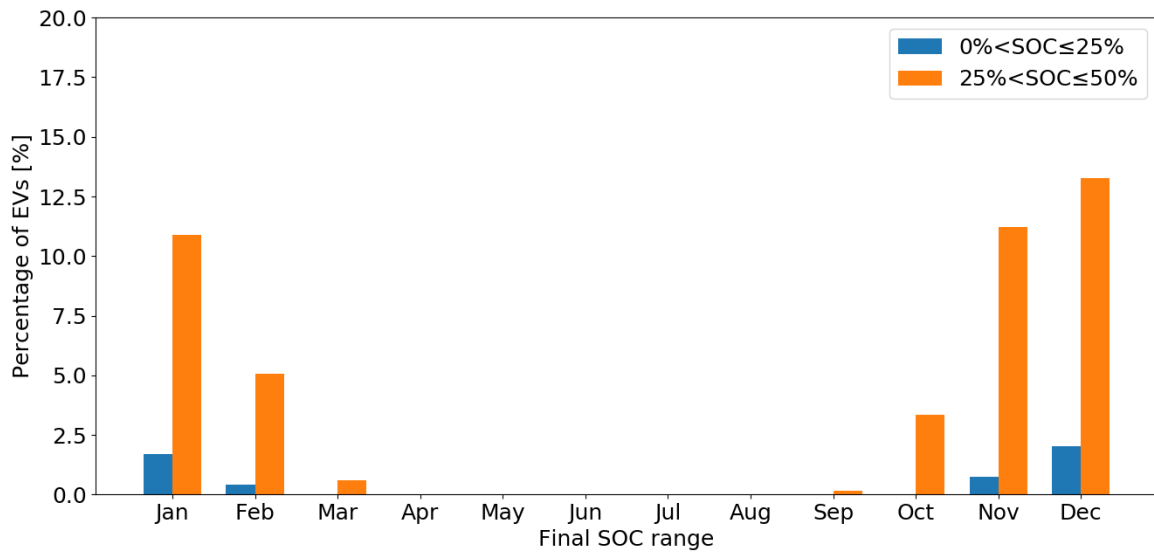


Figure 4.18: Bar chart displaying the monthly variance in charging efficacy, clipped for the lower final SOC

In the base case half of the EVSC users left with a less than adequate SOC in December, regardless of the fact it had the lowest monthly average number of occupants at 78 EVs. Even though the monthly energy requirement of the EV batteries was the lowest in the simulated year, the lack of electricity generation resulted in an occupancy ratio of 90.5%. The 5.7 MWh generated in December was over 40 MWh less than that of May, an indication of the seasonal imbalance. Therefore only 13.3% of EVs left fully charged during December compared to the outstanding fully charged rate of 100% in May, as displayed in figure 4.17. Moreover, 2.0% left with a final SOC less than 25%, a critically low SOC considering the journey home the driver must then embark upon.

So comparing this month with the Occ case, observed in figure 4.19, one can immediately see the

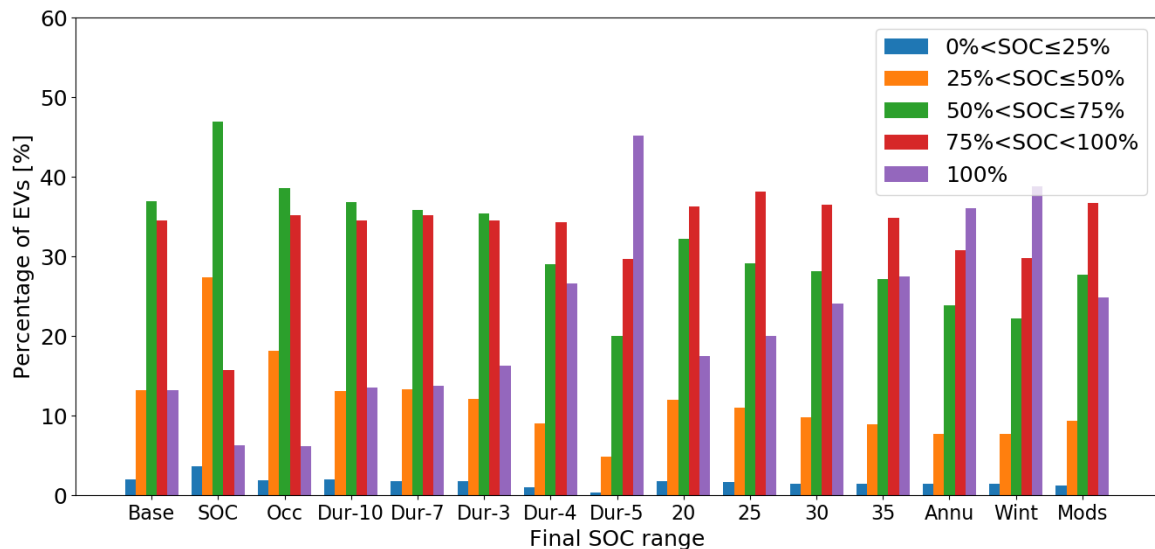


Figure 4.19: Bar chart displaying the changes in December charging efficacy with sensitivity analysis cases

drop in performance. The average number of occupants increased to 104, equivalent to that experienced in summer months of the base case, however the average number of active occupants was 100, unlike those summer months. So, with the occupancy ratio at 96.1%, demand was constantly near its maximum whilst the generation remained its lowest. The share of adequately charged EVs fell to 41.3% in line with an increase to the lower portion of the final SOC distribution, with a 5% increase in the 25% < SOC ≤ 50% range. Interestingly, the share of critically low final SOC fell to 1.9%. Whilst the base case saw 16 occurrences of EVs entering with a SOC below 25%, the *Occ* case saw 38. However, the mean duration of stay was 76.3 hours and 94.0 hours respectively. It is thought that the additional 17.7 hours stay can go some way to explain this abnormal behaviour, however, the true cause is undetermined. Concluding this case, if no other design changes are implemented to counteract this case, winter performance will only get worse with the inevitable increase in average occupancy.

The *Dur-10* and *Dur-7* cases both saw little change. Despite the reduced average number of occupants, the occupancy ratio increased for both cases with *Dur-7* reaching 93.3%. This was to be expected since the average duration of stay was now shorter than the base case.

Of course, cases *Dur-3*, *Dur-4*, and *Dur-5* resulted in progressively better performances. The average number of occupants increased for each case, with 100.1 in the *Dur-3* case whilst *Dur-5* saw an average of 105.9 EVs. The active number of occupants, each higher than the base case, fell with increasing minimum parking duration resulting in the occupancy ratio successively falling. *Dur-5* saw the lowest occupancy ratio in this analysis of 75.6%. Between the longer average parking duration and lowest occupancy ratio, the number of fully charged EVs rose to its highest December value of 45.2%, with 74.8% being adequately charged, for a minimum of 5 days parking duration. An important conclusion drawn from this result is that the increase in occupancy during winter months arising in this case would negate the detrimental effects of the *Occ* case. This is because it is primarily the increase in shorter parking durations coupled with higher energy demand that reduces charging efficacy. By increasing the minimum allowable parking duration these short durations are excluded. This controllable EVSC variable, regardless of the extent to which minimum parking duration is increased, must be considered when designing such an EVSC system.

The *SOC* case produced the worst December performance of all the cases. The larger energy requirement per EV, indicative of this case, combined with the high occupancy ratio of 96.2% meant 3.7% of departing EVs left with a critically low SOC. Furthermore, only 22.0% were adequately charged. This variable is out of the control of EVSC designers and is dependent on factors such as average driving distance to the airport, charging infrastructure in the region, and EV user habits.

The *Mods* case is a direct solution to the lack of generated power throughout the winter months because in using modules with a higher conversion efficiency, and hence higher rated power, the same amount of irradiance incident on the modules results in larger power output. In this case using 430

W modules in place of the initial 315 W modules generated a 34.6% energy yield increase during December. Therefore, for the same parking data as the base case a lower average number of active occupants is achieved and the occupancy ratio became 83.4%. Here, 1.2% left with a critically low SOC, 0.8% lower than the base case, and 9.4% of EVs left with a SOC between $25% < \text{SOC} \leq 50%$, a 3.9% improvement on the base case. Furthermore, 61.6% of EVs left adequately charged. This design decision would certainly not be the single solution to poor winter performance but should certainly be considered as a part of the system improvement. The amount by which the modules are improved depends on the EVSC system budget and available module options at the time of system development.

Finally, the various tilt angles are analysed. Since all simulations made use of identical parking data the number of occupants is constant across all cases, however the successive increase in energy delivered with increasing tilt angle resulted in the occupancy ratio falling. The modular tilt angle of 20° led to a 88.0% average occupancy ratio and the winter optimal tilt resulted in an average occupancy ratio of 76.1%, a drop of almost 15% relative to the base case, driven by the 68.1% increase in electricity generated. Therefore, with 68.6% of EVs leaving with an adequate SOC and 1.4% leaving with a critically low SOC, the 69.5° module tilt angle used as the winter optimum did indeed prove to be the best tilt angle for December, unsurprisingly. The added benefit over the annual tilt angle, however, is marginal at the low end of the scale, both saw 1.4% of EVs leave with a final SOC lower than 25% and only 1% less EVs left in the $25% < \text{SOC} \leq 50%$ final SOC range for the winter optimal tilt. In fact, the goal of improving winter performance is to reduce the number of occurrences of low final SOC. Figure 4.19 displays the charging efficacy profile, and is also tabulated in table 4.5 for the tilt angle sensitivity analysis.

Table 4.5: Charging efficacy of the tilt angle sensitivity analysis case during December

Case	$0\% \leq \text{SOC} < 25\%$	$25\% \leq \text{SOC} < 50\%$	$50\% \leq \text{SOC} < 75\%$	$75\% \leq \text{SOC} < 100\%$	100%
Base	2.0%	13.3%	36.9%	34.5%	13.3%
20°	1.8%	12.0%	32.2%	36.3%	17.6%
25°	1.6%	11.0%	29.2%	38.2%	20.0%
30°	1.4%	9.8%	28.2%	36.5%	24.1%
35°	1.4%	9.0%	27.1%	34.9%	27.6%
Annual Opt.	1.4%	8.8%	26.7%	33.8%	29.2%
Winter Opt.	1.4%	7.8%	22.2%	29.8%	38.8%

Here we see diminishing returns on charging efficacy improvement on the low end. Therefore, not only does it become more expensive to install a steeper tilt angle, but the benefits grow less with increasing angle. As such, it is not recommended to alter the tilt angle from the 15° used in the base case.

To ensure the annual system performance is as high as possible, that is the charging efficacy profile tends towards the EVs being fully charged, it is the performance during the winter months that must be improved. For the base case, and even the *Occ* case, the summer months cannot be improved further; monthly average final SOC is 100% between April - September.

Thus, the recommended design improvements for the month of December are to increase the minimum parking duration to 5 days which by itself would raise the percentage of adequately charged EVs to 74.8% and reduce the share of critically low charged EVs to 0.3%. This design decision would also result in a near full carpark, preventing any negative effects from an increase in the number of occupants as seen in the *Occ* case. Of course, the use of higher efficiency modules is a must and is expected for any modern PV system design. Again, the tilt angle must be increased drastically to result in any meaningful performance increase and is not advised, due to the aforementioned installation cost increase.

5

Business Case Analysis

It has been shown that an off-grid EVSC system will produce positive results in long stay car parks with various design alterations yielding improved winter performance, but what of the business case? Does such a system encourage investment and what are the likely electricity savings that are to be expected? In this chapter an approximate economic assessment is made using values found in literature and industry benchmarks, presenting the levelised cost of electricity (LCOE), net present value (NPV), and discounted payback period (DPBP).

5.1. Component Costs

5.1.1. AC Charger

The Netherlands Knowledge Platform (NKL) published a 2018 benchmark for public EV charger costs in [10], in which the cost of a 3-phase, 25 A AC charger with 2 sockets is around €1300. Including the layout costs and placement costs this results in an approximate cost of €2100 per charge point, which is corroborated by an NREL review [106]. This value is excluding the location determination costs and grid connection costs used in their benchmark assessment. In total, around €113,000 can be expected for this system's charger installation costs. This and other system breakdown costs are presented in table 5.1.

5.1.2. Carport Structure

The carport structure itself has been quoted at approximately €2200 for a 2 car structure with a tilt angle of 15°, to maintain anonymity the carport provider will remain nameless. Assuming the structures capable of housing 4 parking spaces used in this system cost €4400, a total installation cost of approximately €119,000 is expected for the entire 27 structures. It must be considered that the location of the site is a large factor in carport structure costs, with ground conditions and site accessibility being crucial. This figure was deemed acceptable for this approximate business case assessment since the quotation was for a realised project in the Netherlands, however, it is likely to see some variation.

5.1.3. PV System

Assuming a price of €0.3 per Wp [107], this system would incur a module purchase cost of approximately €102,000. The SMA inverters have been found at €6000 each [108], totalling €18,000. Of course, for both the PV modules and inverters these costs are only component prices and do not include the cost for installation, administration, cables, and planning. The 2020 benchmark for a non-tracking large scale system, provided by the Joint Research Centre (JRC) [56], sets capital expenditure (CAPEX) at approximately €700 per kWp installed, operational expenditure (OPEX) at €9.50 per kWp and the system lifetime at 20 years. This is further confirmed in the Fraunhofer ISE (FISE) 2018 review of renewable energy technologies' levelized costs of electricity [109], which gives CAPEX to be between €800 - €1000 per kWp and is subject to a reduction in costs in line with 2020 technology.

Using the JRC benchmark value means a PV system CAPEX of €238,000. However, this includes extra BOS components and a grid connection not included in this base case simulation. Using the breakdown provided in the study from European Photovoltaic Technology Platform (EPTP) [110], we

see that BOS and module costs each account for roughly half of the CAPEX and that the BOS costs would be reduced by roughly 35% without the grid connection, mounting hardware, and transformer. Hence, the figure used in these calculations is €196,000.

5.1.4. Total System

This business case assessment will consider three cases and compare them with the indicators previously mentioned. Table 5.1 presents a summation of costs in these systems.

Base EVSC System

The total EVSC system as presented in this study is expected to cost around €428,000 installed. Of course, there will be large discounts that can be applied in developing a large system: bulk equipment orders, reduced planning and administration costs with scaling, etc. Without a quotation from a contractor, however, the inclusion of such savings would be entirely speculative and hence have not been included in this illustrative analysis.

Purely Grid-Dependent System

The base EVSC system will be compared to a purely grid-dependent EV charging system. For better comparison this case is considered to be sheltered with the same carport structure, the only difference being that no PV system is included and that the EV chargers are connected to the utility grid. Of course, this system would ensure all EVs are charged at the maximum charging power for the duration of their stay and would result in all EVs leaving fully charged. For the same number of chargers this upfront cost would be around €296,000.

Grid-Included EVSC System

A third case is also presented in which a grid connection is included in the initial EVSC design. This would allow for the auxiliary supply of power from the utility grid to meet EV load demand and ensure each EV is fully charged. The total CAPEX for this case would be around €492,000. A further consideration of this case is the possibility of net metering whereby excess generation is sold to the grid. Current Dutch net metering regulations ensure a tariff equal to the consumer electricity tariff (including taxes) [111]. However, from 2023 payments for sales to the grid will fall 9% per year until 2031 when all such tariffs will cease [112]. This has been included in the calculations for revenue.

OPEX

The NKL benchmark leads to an annual OPEX of €17,280 for the off-grid EVSC system [10], however, the learning curve that follows EV charger installations will surely have produced OPEX reductions through manufacturing of higher quality products, more efficient practises, a more competitive market, and so on. So, whilst this figure presented in the 2018 benchmark is used in this study, modern 2020 systems would likely benefit from reduced OPEX. For a grid connected case, this AC charger OPEX rises to €27,540 [10]. The PV system incurs an annual OPEX of €3230 as taken from the JRC benchmark value [56].

Table 5.1: Summary of the all costs, first components and then for the entire system

Component	CAPEX	OPEX
AC chargers, no grid connection	€113,000	€17,280
AC chargers with grid connection	€177,000	€27,540
Carport structure	€119,000	-
PV system	€196,000	€3232
System	CAPEX	OPEX
Base	€428,000	€20,512
Grid-dependent	€296,000	€27,540
Grid-included	€492,000	€30,772

5.2. Revenue and Savings

The annual energy delivered to the EV batteries in the base case simulation was 161 MWh since 43% of the potential electricity generation was curtailed. Assuming Schiphol would pay the industrial electricity price of €0.0941 per kWh [113] drawn from the grid with an additional electricity tax rate of €0.05083 for electricity supplying EV charging installations [114], the savings on annual electricity grid-purchase was €23,300 for the year simulated. For each EV to leave with a full SOC the energy requirement was 197 MWh which would cost €28,600 if only purchased from the grid as in the grid-dependent system. The grid-included system would only need to purchase the difference, 36.8 MWh, at a cost of €5300.

Schiphol Airport offers 12 EV charging points in the P3 garage with a fee of €0.36 per kWh [100] and a connection cost of €1.21. Assuming this rate is used in this EVSC system, a revenue of €66,100 can be expected from the sale of electricity in the base case. In the grid-dependent system, which sees all EVs leave fully charged, the revenue from electricity sales would be €79,300. Accounting for grid purchase the net cash flow for electricity is €50,700. For the case where only the shortage in energy demand is purchased from the grid, net cash flow of €87,200 could be expected. This is until 2023 when revenue from electricity sale to the grid would fall 9% per year as previously mentioned. These cash flows are only for the purchase and sale of electricity and do not account for O&M expenditure or parking revenue. Furthermore, it was assumed that charging tariffs did not change throughout the system's lifetime. In reality this would likely change to some extent.

Using figures on the Schiphol Airport website for drive-in sheltered long stay parking at the P3 garage [100], the first 24 hours of parking costs €77.50, with €7.50 for every subsequent 24 hours. The number of EVSC users in the simulated base case was 6844 for the year, with the mean duration of stay being 122 hours. On average, an EVSC user pays €107.50 for the use of the parking space and the annual parking revenue would then be over €735,000. This revenue stream would be the same for each system case studied.

As an additional financial support the Dutch subsidy for the sustainable energy transition, the SDE++ (Stimulerend Duurzame Energietransitie) [115], offers partial remuneration for systems and technologies that generate renewable energy or provide CO₂ reduction abilities. There are various conditions that must be met besides the competitive nature of the scheme. Projects and developments must bid against each other to gain a part of the €5 billion made available from the government. The potential contribution of this subsidy has not been considered in this assessment, but if this EVSC system were to be awarded some subsidisation the profitability would only increase.

For the calculations of the LCOE, NPV and the DPBP only the revenue from electricity sales is considered where required, alongside OPEX for both the PV system and EV chargers. It is thought that a long stay carpark at an airport would be in place regardless and that the added value of this system is the EVSC. If the revenue from the sheltered parking were considered as well, the payback period would be less than a year for all systems.

Table 5.2: Summary of the all revenue streams

Source	Value
Grid-purchase tariff	€0.0941/kWh
Electricity tax	€0.05083/kWh
Sheltered parking tariff	€77.50 + €7.50/24hrs
Charging tariff	€1.21 + €0.36/kWh
Electricity grid-sale (2020)	€0.14493/kWh
<hr/>	
System	Net Revenue
Base	€45,600
Grid-dependent	€19,900
Grid-included (2020 - 2031 onwards)	€63,500 - €43,300

5.3. Net Present Value

An NPV of €326,000 was found for the base system using equation 5.1. A positive NPV signifies a good investment, one that sees profit over the investment's lifetime, and this value of NPV indicates a theoretical 76% profit on the initial investment.

$$NPV = \sum_{y=1}^Y \frac{R_y}{(1+r)^y} \quad (5.1)$$

Where R_y is the net cash flow in year y up to the system lifetime Y . r is the discount rate and accounts for the time value of money.

Of course, this NPV calculation is highly dependent on the value of r for which FISE [109] found that the average interest rate in Germany over the past 20 years was around 2.6%. The average interest rate in the Netherlands over the past 10 years was about 1.9 and has been falling constantly throughout that time. However, an increase could be expected in the future, hence 2% is also used in this study. The accurate prediction of future cash flows also has a large influence on the NPV. The cash flows used were those stated earlier with no inclusion of subsidisation. Other assumptions made in this calculation were that in the 20 year system lifetime the parking pattern did not fluctuate from the simulated base case, the sale price of electricity to the EVSC users remained constant, and that the annual array power degradation was 0.25%.

The NPV of the purely grid-dependent system is €116,000, with the same assumptions used. Although there is a reduced initial investment in this scenario, the profit margin is relatively low meaning the final system value is far lower. For the grid-included case the NPV comes to €403,000, a value 24% greater than the base case.

5.4. Levelised Cost of Electricity

The LCOE, which determines the price electricity must be sold at to break even on investment over the system lifetime, was calculated to be €0.275/kWh using equation 5.2. This is considerably higher than the LCOEs estimated by FISE [109], the JRC [56], and EPTP [110] to be approximately €0.05/kWh - €0.08/kWh, approximately €0.04/kWh - €0.05/kWh, and approximately €0.07/kWh - €0.09/kWh, respectively, for a PV system of comparable size. However, one must take into consideration that an increased initial investment was required for the EV chargers and EVSC structures relative to a standard PV system and this in turn incurs higher O&M costs. Furthermore, a large amount of energy was curtailed resulting in underutilisation of generating capacity.

With the same assumptions holding true, the LCOE of the grid-dependent and grid-included systems are €0.228/kWh and €0.289/kWh respectively. Since the LCOE calculation does not depend on cash flows it makes sense that the grid-dependent system would have the lowest LCOE, since this system

had the lowest initial investment. As for the grid-included case, the highest initial investment and OPEX results in the highest LCOE. It should be noted that for all three of these systems the LCOE is less than the current electricity tariff charged to EV charger users at Schiphol. This confirms other indicator results that show this system to be profitable over the lifetime.

$$LCOE = \frac{CAPEX + \sum_{y=1}^Y \frac{OPEX(y)}{(1+WACC_{Nom})^y}}{\sum_{y=1}^Y \frac{(Utilisation_0(1-Degradation))^y}{(1+WACC_{Real})^y}} \quad (5.2)$$

Where $CAPEX$ is the total investment in year y (€/kWp), $OPEX$ is the operational and maintenance expenditures in year y (€/kWp), $Utilisation_0$ is the initial annual utilisation in the first year without degradation (kWh/kWp), $Degradation$ is the annual degradation the PV array is subject to, here assumed to be 0.25% [109], Y is the system lifetime of 20 years, $WACC_{Nom}$ is the nominal weighted average cost of capital, here assumed to be 4.1% [109], and $WACC_{Real}$ is the real weighted average cost of capital. Assuming a 2% discount rate, $WACC_{Real}$ becomes 2.1% as per equation 5.3:

$$WACC_{Real} = \frac{(1 + WACC_{Nom})}{(1 + r)} - 1 \quad (5.3)$$

5.5. Discounted Payback Period

The third and final analytical indicator included in this study is the discounted payback period (DPBP) which deduces the period required to recover the initial investment. Using the values for EV charging revenue calculated earlier and equation 5.4, the DPBP was found to be 10.2 years.

$$DCF = \frac{ACF}{(1 + r)^y} \quad (5.4)$$

Where DCF is the discounted cash flow in a given year and ACF is the actual cash flow, or annual profit. This was calculated for each year in the system lifetime and the values added to the initial investment.

The purely grid-dependent system, however, would have a DPBP of 14.9 years with the same assumptions used and the grid -included case would have a DPBP of 9.2 years.

5.6. Results

A summary of the values is presented in table 5.3. It is clear that both the base case system and grid-included system are similar from a financial perspective: both require a similar, albeit relatively high LCOE, and both result in a profit of over 75% on the initial investment. The grid-dependent system is far less profitable over the system lifetime and is clearly a worse choice of investment for this application based on the assessment here performed.

Of course, such a system does not come without its risks all of which would potentially diminish the system's profitability. As mentioned earlier, the monetary values used in this economic analysis were deduced through industry benchmarks and approximations based on previous work or data, meaning all are subject to change. For instance, a different installation cost for the EVSC structures could arise at the chosen location based on a lower quality of ground requiring more extensive foundations, a different contractor could give a more expensive quote due to regional differences, and perhaps the site is less accessible than it appears. Alternatively, the interest rate could experience a large increase in coming years which, however unlikely it now seems, would have a large and detrimental effect on all the indicators used. Perhaps the hardware chosen in the application are of a low quality and require more maintenance than the average system, or an unforeseen complication arises during their installation.

As for the revenue stream, the electricity tariff imposed on EVSC users could change, a decision made by the system operator and influenced by the need to be both profitable yet fairly competitive with other charging options. The need to be only fairly competitive comes from the lack of direct competition for this application, yet consideration of standard charging or fast charging services should be maintained. Additionally, the parking habits of airport users could drastically change in coming years with improved public transport infrastructure, rapidly developing car-sharing platforms, or autonomous taxi services. So, although this system is intended to be fairly future proof and the simulation accurate, there are risks to the profitability as with any investment.

Table 5.3: Summary of the economic assessment, the subscript *Grid* indicates the purely grid-dependent alternative

Indicator	Value
$LCOE_{PV}$	€0.275/kWh
NPV_{PV}	€326,000
$DPBP_{PV}$	10.2 years
$LCOE_{Grid}$	€0.228/kWh
NPV_{Grid}	€116,000
$DPBP_{Grid}$	14.9 years
$LCOE_{PV+Grid}$	€0.289/kWh
$NPV_{PV+Grid}$	€403,000
$DPBP_{PV+Grid}$	9.2 years

The base case system has the potential to mitigate growth in airports' grid electricity demand, shifting from a fossil fuel based power dependency to the use of clean, self-generated electricity. The use of clean electricity reduces EV lifetime emissions and adds further incentive for consumers to own EVs if there is suitable charging infrastructure in every-day life. This grid independence would also alleviate the risk of grid congestion during peak load hours due to the charging demand of EVs. As an application yet to see realisation, this system generate interest and bring with it publicity. Moreover, governmental and regional incentives that have not been included in this study could further improve profitability. However, the two systems with a grid connection can ensure fully charged EVs. The real decision variable, therefore, is what are the intentions of installing such an EV charging system? Is the main goal to reduce emissions whilst adequately charging the majority of EVs. Or is it to ensure all customers are completely satisfied, no matter the cost.

The economic assessment performed in this study does not claim to be all encompassing, nor was it intended to be absolute. The limitations, such as the use of benchmark values and the various assumptions, are acknowledged. However, these are in the very nature of such economic assessments; assumptions and estimations. This analysis does give a good idea of likely profitability and the relationship between the three system cases studied. It has shown that the off-grid and grid-included systems are far more profitable than the grid-dependent system.

6

Conclusions & Recommendations

The research presented in this study investigated the charging efficacy of an off-grid, solar powered electric vehicle charging system for long stay parking, notably at airports. The so-called electric vehicle solar carport (EVSC) system was modelled using historical data and well justified assumptions and simulated with the intention to answer the following research question:

What is the charging efficacy of an off-grid, solar powered electric vehicle charging system in long stay parking applications?

With the sub questions:

1. To what extent do the defining system variables alter the charging efficacy of the system?
2. How does the business case of such a system compare to a conventional grid-dependent system?

This section provides a conclusive summary of all that has been discussed with the key take-aways highlighted in section 6.1. Section 6.2 then goes on to provide the recommendations for future system design based on the findings of this study, as well as recommendations for future research. Finally a review from the author on the research conducted is provided in section 6.3, which offers reflections and further insights post-research.

6.1. Conclusion

With various climate directives in place nations, regions, and businesses are looking to become more sustainable in their operational practises. This, as well as stiff competition, is leading to more EV models becoming available to the market and a rise in the percentage of newly registered vehicles that are electric. In the coming decade the penetration of EVs will grow leading to an increased demand for EV charging services at airports. Simultaneously, airports are wanting to reduce their energy footprint.

An off-grid charging service for EVs parking at an airport for long durations of time is therefore a logical option. The high grid connection and maintenance costs associated with EV chargers and the limited airport grid capacity are further motivations for an airport to have this system off-grid. But from the grid operator's perspective, the detrimental grid effects resulting from large EV load connections are to be avoided where possible, so an off-grid solution to a problem that would otherwise require a grid-connection has many benefits. There are, of course, some down sides to this design, such as the potential for undercharging EVs due to the intermittent nature of solar PV as well as the large underutilisation of generating capacity present in the summer months.

For a theoretical system of 108 parking spaces at Lelystad Airport, the Netherlands (52.456°N, 5.521°E), a PV array sized at 340.2 kWp was installed on carport rooves over the parking spaces themselves, with 10 modules per parking space. 54 AC chargers were installed, each capable of feeding two EVs simultaneously, rated at 3.7 kW, 16 A. They were split across the three phases evenly with the phase imbalance effects outside the scope of this study. The charging strategy was then to simply split the generated power among the active EVs present in the carpark at that time.

The initial simulation, or base case, used the model as described in chapter 3. Here the parking patterns of the EVSC users was modelled with the use of flight departure data retrieved from Schiphol Airport, since a clear correlation between flight departure time and arrival time at an airport can be drawn. The initial SOC of arriving EVs was modelled using a distance dependent calculation and an approximated distribution of EV SOC prior to travel. The resulting initial SOC distribution was corroborated by various field studies, namely a distribution with a mean value around 50% - 60%. As for the meteorological data retrieved from EU PVGIS, this was put into NREL's SAM software where the PV system had been modelled. The output of this was used in the EV charging model from which the final results were produced.

This was then compared to various other simulations that formed a sensitivity analysis, performed to better understand the variables that affect the system's charging efficacy. Included in this sensitivity analysis was the module tilt angle, lowered average initial SOC distribution, increased average occupancy, improved choice of modules used, and altered allowable parking durations.

As presented and discussed in chapter 4, this system performed exceptionally well overall, with only the harshest of winter months bringing down the average final SOC of EVSC users. This can best be observed in figures 6.1a and 6.1b.

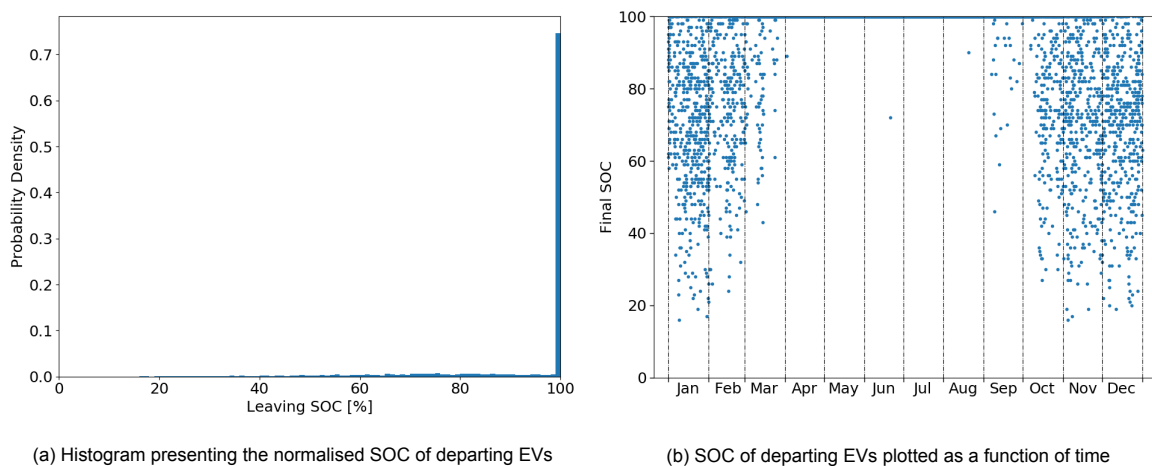


Figure 6.1: The performance of the EVSC system in the base case

6.1.1. Off-grid EVSC System

As figures 6.1a and 6.1b show, this EVSC system proved to have a high charging efficacy; the months April - September achieved an average final SOC of EVs departing the EVSC of 100%. Throughout the winter months the charging efficacy dropped, to be expected for a location at a latitude of 52°. With the initial SOC model developed such that the minimum SOC prior to the EV's journey to the airport was 75%, this too was used to define the adequate level of final SOC. This EVSC system produced adequate charge for 85.5% of users, with only 0.4% departing with a critically low final SOC, below 25%.

Both January and December showed particularly poor relative performance, with December being chosen for a worst month analysis. In the base case it was shown that 47.8% of EVs left with an adequate SOC and 2.0% of EVs left with a SOC below 25%. Regardless, 13.3% of the December EVSC users left with a fully charged battery.

A further finding was the large amount of energy that had been curtailed in the base case. This was found to be 140 MWh throughout the year, with the vast majority occurring in months April - August. It is thought that rather than have underutilised generating capacity this large amount of energy could be better used. The installation of a battery energy storage system is an obvious recommendation and if sized and managed appropriately could offer reserve energy into the winter months and improve charging efficacy in the worst performing period. Alternatively, the installation of an electrolyser could prove profitable if hydrogen fuel cell cars become popular, of course this would introduce far more costs and requires extensive study.

Another option is to provide charge for the variety of airport vehicles and ground support equipment,

since many are electric vehicles. Examples include: shuttle buses, various equipment and luggage transporters, aeroplane loaders and more. This final scenario would require further cabling and a designated area separated from the carpark to allow the charging of such vehicles.

6.1.2. Profitability of the System

An economic analysis was conducted to determine the suitability for investment in this system design, in which only the base case simulation was considered and compared against a purely grid-dependent and a grid-included alternative. The grid-dependent case purchased all the electricity required for charging from the grid, whereas the grid-included case prioritised the PV array and purchased only the difference required to fulfil demand, as well as selling excess generation back to the grid. Both these cases would end with all EVs fully charged.

Considering the estimated CAPEX of €428,000 for the proposed EVSC system, a combined OPEX for the PV array and EV chargers of €20,500 and only the revenue from electricity sales, found to be €0.36/kWh, the levelised cost of electricity, net present value, and discounted payback period are presented in table 6.1. For the grid-dependent case a CAPEX of €296,000 and OPEX of €27,500 can be expected, whilst the grid-included case sees CAPEX and OPEX at €492,000 and €30,800 respectively.

Table 6.1: Summary of the economic assessment, the subscript *Grid* indicates the purely grid-dependent alternative, whilst the subscript *PV+Grid* refers to the grid inclusive case.

Indicator	Value
$LCOE_{PV}$	€0.275/kWh
NPV_{PV}	€326,000
$DPBP_{PV}$	10.2 years
$LCOE_{Grid}$	€0.228/kWh
NPV_{Grid}	€116,000
$DPBP_{Grid}$	14.9 years
$LCOE_{PV+Grid}$	€0.289/kWh
$NPV_{PV+Grid}$	€403,000
$DPBP_{PV+Grid}$	9.2 years

It was shown that the proposed EVSC system and grid-included system are the best options for investment, with similar final system value and a similar LCOE. An approximate profit of 76% on the original investment can be expected for the base case EVSC system, and 82% for the grid-included system. Of course, this is highly dependent on the assumptions made in the analysis, such as a discount rate of 2% based on a 10 year average interest rate in the Netherlands, constant electricity tariff of €0.36/kWh, constant parking pattern, and constant annual PV array degradation of 0.25%.

6.1.3. Potential for Improvement

Whilst the system performed exceptionally well there is still room for improvement, especially considering that the coming years will see a larger penetration of EVs. The sensitivity analysis showed that with the number of winter occupants increased such that the annual average occupancy rose above 99%, a worse winter performance ensued. December saw only 41.3% being adequately charged for the case of increased average number of occupants. This being one of the more realistic scenarios for the location studied meant that this was the performance on which to improve if the EVSC system is to be resilient to future advances in technology, car fleet mix, and user behavior.

Shifting the initial SOC distribution such that the mean was 40% led to the largest drop in charging efficacy. This was most noticeable in December where a 25.7% drop in the number of adequately charged EVs was experienced with 3.7% of departing EVs attaining a SOC below 25%. Additionally, it was shown that for this EVSC system the summer months retained a strong charging efficacy, with the months April - September averaging a final SOC of 100%. Whilst this scenario was thought of as

unlikely for the location studied, conscious design should be performed to limit the effects should it occur. Ultimately, however, it is an uncontrollable parameter.

Through the use of higher efficiency modules it was shown that a substantial increase in winter performance was possible. In December the adequate charge rate rose by 13.9% relative to the base case. With this, a decrease of 0.8% was achieved for the number of EVs below 25%. This alone would provide some ability to negate the effects from an increased winter occupancy. However, the increase in electricity generation was greater in summer months than winter months, resulting in an annual curtailment of 55.4%.

For December, an increased module tilt angle performed better. Obviously the winter optimum tilt angle performed best, yet the improvement in charging efficacy saw diminishing returns with each 5° increment. Therefore, only the 20° and 25° tilt angles should be considered for installation, after which no further decrease in the critically low final SOC was achieved. However, when considering the annual charging efficacy neither of these two tilt angles yielded a significant improvement. Increasing the tilt angle will improve winter performance but also increase installation costs; the cost-benefit decision of each tilt would be unique to the location in question, since EVSC installation costs cannot easily be predicted without site specific knowledge.

Reducing the maximum allowable parking duration had little effect at any level, mostly due to the relatively few EVs parking for extreme durations. Rather, the interesting variable being increasing the minimum allowable parking duration. This showed great potential in the month of December, whereby increasing the minimum duration of stay to 4 days resulted in a 1.0% decrease in the share of critically undercharged EVs and a 13.2% increase in the number of EVs leaving with an adequate SOC. Taking this up to 5 days results in a 1.7% decrease in critically undercharged and a 27.1% increase of adequately charged EVs.

In this simulation the months January - March and October - December were the only periods that did not return near perfect results and as such these are the periods that require improvement. Through this sensitivity analysis and investigation of worst month performance it was shown that there are a number of design decisions that have the potential to greatly improve charging efficacy during the worst performing period. Whilst the best combination of choices are site specific, the recommendations section of this chapter provides the suggested improvements.

6.2. Future System Designs and Research: Recommendations

This study has shown the feasibility of an off-grid EVSC system and investigated some potential design improvements. But what are the recommended system parameters? A single brush cannot be used to paint all pictures since obvious PV array dependence on location presides, but some generalisations are hereby provided.

For a location at such a northerly latitude as the Netherlands, it is the winter months that upsets the annual charging efficacy profile. As such, design changes that target these months are strongly recommended. The simplest and most effective is increasing the minimum allowable parking duration during these months; in January and December this should be 5 days, for February and November this should be 4 days, and during March and October this should be 3 days. Whilst this will reduce winter revenue, since a higher tariff as charged for the first 24 hours of usage, the users that do use the EVSC system are more likely to be adequately charged. Additionally, any negative effects arising from an increased EV penetration would be mitigated since the carpark would already be operating at near maximum capacity. Summer months should retain the initial 48 hour minimum parking duration.

The installation of modern modules should be paramount. Modules produced 2 years ago, such as those used in this model, are already outdated. The development of cell technology is progressing rapidly with innovations such as half-cut cells, the use of 9 bus bars per cell, and tiled/shingled cells becoming the norm. This has led to higher conversion efficiencies and higher module rated power output per square meter. Moreover, as module prices fall these better performing modules are becoming cheaper than their predecessors.

The initial SOC of EVs entering the EVSC system is uncontrollable. Regardless, suitable measures should be taken to provide resilience to the possibility of a lower distribution. The design alterations already discussed should provide a good measure of security. Furthermore, it is not recommended to increase the module tilt angle. No significant improvement will result unless the tilt angle is increased dramatically and any tilt increase would only further raise installation costs.

Regarding future research, there are a few topics that should be investigated further. Firstly, smarter charging can be adopted that would likely increase the charging efficacy profusely. This EVSC system relies on reservations and as such the necessary information can be attained to potentially provide adequate charging for all. With the knowledge of: EV model, arrival and departure dates, and home address, one could develop a charging algorithm that would seek to only provide the necessary charge to allow each EV to make the return journey plus a safety margin for detours etc. For example, an EV that drives 100km and uses 16.4 kWh (Nissan LEAF) would only need 16.4 kWh to make the return journey assuming they have the same origin and destination, i.e. their home address, unless stated otherwise. Therefore, the defined level of adequate charge would vary for each EV and the charging efficacy of the EVSC system could improve drastically, since EVs are not being unnecessarily overcharged for their return journey.

A further sensitivity analysis that would prove useful is the variation in charging efficacy that comes with azimuth angle. This case considered only a south facing PV array; in reality the orientation may be less than ideal since many carparks are pre-existing. This means the orientation of a PV array on an EVSC canopy roof is somewhat limited to the orientation of the parking spaces that such a system would be retrofitted to.

Additionally, an exhaustive and well-founded economic analysis should be conducted. Using various sources in the industry, quotations for products and services should be assembled culminating in an all-encompassing assessment of the financial viability of this proposed system.

As for the solution to the curtailed energy: the inclusion of a battery energy storage system should be studied to determine if such an addition can improve charging efficacy in winter months, and at what battery capacity this becomes an option. Moreover, a regular battery management system would likely not preserve adequate battery charge over the long time period spanning summer to winter. Hence, an intelligent battery management strategy would have to be developed that prioritises future times of poor performance over the need to maximise charging power capacity.

Alternatively, an investigation into the benefit of including an electrolyser should be conducted. Such an addition to the system would result in a large increase to initial investment but the added revenue from hydrogen sales might be enough to recover this cost. Moreover, hydrogen fuel-cell vehicles are also likely to become more abundant and the refuelling infrastructure must be in place for when they do gain traction.

Studying the potential for this EVSC system in other applications besides airports would also be valuable research. These could include ports where off-shore workers are based. These types of workers are often working in long shifts in cycles of 2-4 weeks on/off, meaning their cars would be laying idle for some time between journeys. Other potential applications include car/van rental services which see vehicles sit idle for some time between rentals, camping/caravanning parks, larger music festivals that are spread over multiple days such as Glastonbury Festival, and perhaps future autonomous taxi services, depending on the operation model these could see a central hub of operation for charging, cleaning and maintenance. The advantage with camping and music festivals is the time of year; summer months were found to fully charge all EVs using the system for more than 48 hours. An easily installable, temporary EVSC system would be well suited for such applications.

6.3. Limitations of the System and Approach Used: Reflections

This study was not without its challenges and limitations. This was first encountered in the lack of parking data from Schiphol Airport. Due to the connections with Schiphol Nederland B.V. through the PowerParking project it was thought parking data could be acquired, however this was unsuccessful. Whilst a solution was found and the results were consistent with values found in literature for passenger movement and use of parking for Schiphol and use of parking for BLIA, historical data is always preferred for such studies due to the added validity it provides. The model used in its stead was developed between October - December of 2019 and delayed progress by well over a month. On the other hand, it did allow for plenty of experience with Python, a skill which was learned in the process of this study.

The model developed to produce a distribution for the initial SOC was also based on assumptions. As with the parking pattern model, the results were corroborated by values found in literature. In this case 3 field studies had been identified to contain data regarding initial SOC at the point of connection, these allowed for the parameters that defined both the prior SOC and distance driven distributions to be altered so that the initial SOC distribution developed was reliable. The assumptions made on prior

SOC were logical yet ungrounded, as with the distance driven argumentation. Hence, the acquisition of verifiable data would further add to the validity of this study.

A third shortcoming in this model is in the use of SAM. One of the PV module model assumptions is that all modules operate at the MPP. Of course, in this system that would not be the case; modules operate at the setpoint determined by the load. During most of the winter months this was MPP, however, much of the spring and summer months resulted in high energy curtailment. This curtailment is equivalent to the shift in operating voltage, since the power generated is higher than the demanded power. This in turn would lead to added losses within the inverter relative to its efficiency curve and allowable voltage limits.

SAM is designed to model grid-connected PV systems only. As such, it assumes the choice of inverter is grid-tied and not a stand-alone inverter. Since SAM was used only to get a power output series of data, it is thought this had little effect as PV array operation would not change.

The final flaw in this approach was in the use of SAM's Sandia Inverter Model with user specified parameters. This implementation of inverter model disables the power consumption losses if a weighted efficiency is specified. The use of the weighted efficiency accounts for operating losses in its calculation. However, this is not an accurate representation of this specific inverter's operation, only an estimation. Additionally, the inverter's efficiency varies with the percentage of rated power output, known as the efficiency curve. The weighted efficiency only estimates this behaviour. Having an accurate efficiency curve will of course lead to a more accurate inverter output power.

Glossary

AC

Alternating current.

Active EV

An electric vehicle that was actively charging and had not reached full charge, at which point it became *idle*.

Adequate SOC

The adequate SOC is defined by the minimum SOC prior to driving to the airport, hence is 75%. If an EV reaches this SOC it can certainly make the return journey, assuming there are no detours and the destination is the same as its origin.

BESS

Battery energy storage system.

BEV

Battery electric vehicle.

BLIA

Boston Logan International Airport.

BOS

Balance of systems.

CAPEX

Capital expenditure.

Charging efficacy

The charging performance of the EVSC system in a given simulation or time period. It is a loose term that has no quantifiable metric but considers the percentage of fully charged EVs, adequately charged EVs, and EVs with a critically low SOC. The more EVs leaving adequately charged and the fewer leaving with a critically low SOC, the higher the charging efficacy.

Critical SOC

Anything below 25% and indicates a need for further charging of the EV as soon as possible.

DC

Direct current.

DPBP

Discounted payback period.

Energy requirement

The total energy required by all EVs in a given time period, such that all EVs leave fully charged.

EV

Electric vehicle.

EVSC

Electric Vehicle Solar Carport.

FCEV

Fuel cell electric vehicle.

GHG

Greenhouse gases.

HVAC

Heating, ventilation and air conditioning.

ICE

Internal combustion engine.

Initial soc

The SOC of an EV upon connection to the EVSC at the airport.

LCOE

Levelised cost of electricity.

MPPT

Maximum power point tracking.

NKL

Nationaal Kennisplatform Laadinfrastructuur (Netherlands Knowledge Platform).

NPV

Net present value.

NREL

National Renewable Energy Laboratory.

Occupancy

The number of EVs occupying the EVSC system in a given instance, presented as a percentage of maximum capacity.

Occupancy ratio

The percentage of active EVs occupying the EVSC relative to the total number of EVSC occupants in a given time period, whether that be the full year, a specific month, or precise time step.

OPEX

Operating expenditure.

PBL

Planbureau voor de Leefomgeving (Netherlands Environment Agency).

PCC

Point of common coupling.

PERC

Passivated emitter and rear contact.

PHEV

Plug-in hybrid electric vehicle.

Prior SOC

The SOC of an EV before departing on its journey to the airport.

PV

Photovoltaic.

SAM

System Advisor Model.

SOC

State of charge.

V2G

Vehicle-to-grid.

WACC

Weighted average cost of capital.

Bibliography

- [1] Solarsense. Ev charging and solar carports for business. <https://www.solarsense-uk.com/commercials/commercial-ev-charging-and-solar-carports/>, 2020. retrieved 13/07/2020.
- [2] Anastasios Tsakalidis and Christian Thiel. Electric vehicles in Europe from 2010 to 2017: is full-scale commercialisation beginning. *Publications Office of the European Union: Luxembourg*, 2018.
- [3] Netherlands Enterprise Agency. Statistics electric vehicles in the netherlands, up to and including may 2020. Technical report, Ministry of Infrastructure and Water Management, 2020.
- [4] RetailNews. Toch winkels mogelijk bij snellaadstations fastned. <https://retailtrends.nl/news/55315/toch-winkels-mogelijk-bij-snellaadstations-fastned>, 2019. retrieved 07/06/2020.
- [5] IEA. Data and Statistics. <https://www.iea.org/data-and-statistics>, 2019.
- [6] InfraMarks. Solar carport met zonnepanelen. <https://inframarks.nl/solar-carport/>, 2020. retrieved 08/05/2020.
- [7] C. Jackson Hartnell and G. Solar car parks, a guide for owners and developers. Technical report, BRE National Solar Centre, 2016.
- [8] Klaus-Dieter Jäger, Olindo Isabella, Arno HM Smets, René ACMM van Swaaij, and Miro Zeman. *Solar energy: fundamentals, technology and systems*. UIT Cambridge, 2016.
- [9] Gautham Ram Chandra Mouli, Prasanth Venugopal, and Pavol Bauer. Future of electric vehicle charging. *19th International Symposium on Power Electronics, Ee 2017*, 2017-Decem:1–7, 2017.
- [10] R.F.P Blok. Verslag Benchmark Publiek Laden 2017. (december):1–42, 2017.
- [11] Photovoltaics Report. Technical report, Fraunhofer ISE, 2020.
- [12] LONGi. *LR6-60PB 295-315M, Datasheet*.
- [13] SMA. *Sunny Highpower PEAK3*.
- [14] Traffic Review 2018. Technical report, Schiphol Group, 2019.
- [15] Electric Vehicle Database. Usable battery capacity of full electric vehicles. <https://ev-database.org/cheatsheet/useable-battery-capacity-electric-car>. retrieved 28/01/2020.
- [16] UN Unfccc et al. Kyoto protocol reference manual on accounting of emissions and assigned amount. Technical report, eSocialSciences, 2009.
- [17] Paris Agreement. Paris agreement. In *Report of the Conference of the Parties to the United Nations Framework Convention on Climate Change (21st Session, 2015: Paris)*. Retrived December, volume 4, page 2017. HeinOnline, 2015.
- [18] IRENA. Future of Solar Photovoltaic - Deployment, investment, technology, grid integration and socio-economic aspects. Technical report, International Renewable Energy Agency, 2019.
- [19] European Environment Agency. Greenhouse gas emissions from transport in europe. Technical report, EEA, 2019.

- [20] Michael Cembalest. Eye on the Market - Electric vehicles: a 2% or 20% solution? Technical report, J.P. Morgan, 2018.
- [21] IEA. Global EV Outlook 2020 to electric mobility. 2020.
- [22] Laura Novoa and Jack Brouwer. Dynamics of an integrated solar photovoltaic and battery storage nanogrid for electric vehicle charging. *Journal of Power Sources*, 399:166–178, 2018.
- [23] G. R. Chandra Mouli, P. Bauer, and M. Zeman. System design for a solar powered electric vehicle charging station for workplaces. *Applied Energy*, 168(2016):434–443, 2016.
- [24] Shi Jie Tong, Adam Same, Mark A. Kootstra, and Jae Wan Park. Off-grid photovoltaic vehicle charge using second life lithium batteries: An experimental and numerical investigation. *Applied Energy*, 104:740–750, 2013.
- [25] Hassan Fathabadi. Novel grid-connected solar/wind powered electric vehicle charging station with vehicle-to-grid technology. *Energy*, 132:1–11, 2017.
- [26] Mart van der Kam and Wilfried van Sark. Smart charging of electric vehicles with photovoltaic power and vehicle-to-grid technology in a microgrid; a case study. *Applied Energy*, 152:20–30, 2015.
- [27] Azhar Ul-Haq, Carlo Cecati, and Essam A Al-Ammar. Modeling of a photovoltaic-powered electric vehicle charging station with vehicle-to-grid implementation. *Energies*, 10(1):4, 2017.
- [28] Hasan Mehrjerdi. Off-grid solar powered charging station for electric and hydrogen vehicles including fuel cell and hydrogen storage. *International journal of hydrogen Energy*, 44(23):11574–11583, 2019.
- [29] Yun Wang, Milad Kazemi, Sayyad Nojavan, and Kittisak Jermsittiparsert. Robust design of off-grid solar-powered charging station for hydrogen and electric vehicles via robust optimization approach. *International Journal of Hydrogen Energy*, 2020.
- [30] Pedro Nunes, Raquel Figueiredo, and Miguel C. Brito. The use of parking lots to solar-charge electric vehicles. *Renewable and Sustainable Energy Reviews*, 66:679–693, 2016.
- [31] Abdulsalam S Alghamdi, AbuBakr S Bahaj, and Yue Wu. Assessment of large scale photovoltaic power generation from carport canopies. *Energies*, 10(5):686, 2017.
- [32] Jan Rotmans, René Kemp, and Marjolein Van Asselt. More evolution than revolution: transition management in public policy. *Foresight-The journal of future studies, strategic thinking and policy*, 3(1):15–31, 2001.
- [33] William Todts and Lucien Mathieu. Recharge EU: how many charge points will Europe and its Member States need in the 2020s. Technical report, European Federation for Transport and Environment AISBL, 2020.
- [34] Vehicles and fleet. <https://www.eafo.eu/vehicles-and-fleet/m1>, 2020. retrieved 27/07/2020.
- [35] M Niestadt and A Bjørnåvold. Electric Road Vehicles in the European Union: Trends, Impacts and Policies, 2019.
- [36] IEA. Global EV Outlook 2019 to electric mobility. 2019.
- [37] Andreas Poullikkas. Sustainable options for electric vehicle technologies. *Renewable and Sustainable Energy Reviews*, 41:1277–1287, 2015.
- [38] US Department of Energy. All-Electric Vehicles. <https://www.fueleconomy.gov/feg/evtech.shtml>. retrieved 18/08/2020.

- [39] L Ellingsen and C Hung. Research for tran committee-battery-powered electric vehicles: market development and lifecycle emissions. *STUDY, European Parliament, Directorate General for Internal Policies, Policy Department for Structural and Cohesion Policies, Transport and Tourism*, 10:944056, 2018.
- [40] Maarten Messagie. Life cycle analysis of the climate impact of electric vehicles. *Journal of Life Cycle Assessment*, 2014:14, 2014.
- [41] Richard Schmuch, Ralf Wagner, Gerhard Hörpel, Tobias Placke, and Martin Winter. Performance and cost of materials for lithium-based rechargeable automotive batteries. *Nature Energy*, 3(4):267–278, 2018.
- [42] Yu Miao, Patrick Hynan, Annette Von Jouanne, and Alexandre Yokochi. Current li-ion battery technologies in electric vehicles and opportunities for advancements. *Energies*, 12(6):1–20, 2019.
- [43] Abdul Rauf Bhatti, Zainal Salam, Mohd Junaidi Bin Abdul Aziz, and Kong Pui Yee. A critical review of electric vehicle charging using solar photovoltaic. *International Journal of Energy Research*, 40(4):439–461, 2016.
- [44] Thomas Bowen, Ilya Chernyakhovskiy, and Paul L Denholm. Grid-Scale Battery Storage: Frequently Asked Questions. Technical report, National Renewable Energy Lab.(NREL), Golden, CO (United States), 2019.
- [45] allego. The World of Electric Charging Costs. <https://www.allego.eu/blog/2019/november/the-world-of-electric-charging-costs>, 2019. retrieved 21/05/2020.
- [46] Gereon Meyer, Richard Bucknall, and Dominique Breuil. Electrification of the Transport System. Technical report, Directorate-General for Research and Innovation, European Commission, 2017.
- [47] European Alternative Fuels Observatory, Netherlands. <https://www.eafo.eu/countries/netherlands/1746/summary>, 2020. retrieved 05/07/2020.
- [48] Erik Johnson. Introduction to Electric Vehicle Battery Systems. <https://www.allaboutcircuits.com/technical-articles/introduction-to-electric-vehicle-battery-systems/>, 2019. retrieved 27/07/2020.
- [49] EC (European Commission) et al. A European Strategy for Low-Emission Mobility. *Communication from the commission to the European parliament, the council, the European economic and social committee and the committee of the regions*, 2016.
- [50] Guzay Pasaoglu, Michel Honselaar, and Christian Thiel. Potential vehicle fleet CO2 reductions and cost implications for various vehicle technology deployment scenarios in Europe. *Energy Policy*, 40:404–421, 2012.
- [51] Christian Thiel, Wouter Nijs, Sofia Simoes, Johannes Schmidt, Arnold van Zyl, and Erwin Schmid. The impact of the EU car CO2 regulation on the energy system and the role of electro-mobility to achieve transport decarbonisation. *Energy Policy*, 96:153–166, 2016.
- [52] Pantelis Capros, A De Vita, N Tasios, P Siskos, M Kannavou, A Petropoulos, S Evangelopoulou, M Zampara, D Papadopoulos, Ch Nakos, et al. EU Reference Scenario 2016-Energy, transport and GHG emissions Trends to 2050. 2016.
- [53] ERTRAC, EPoSS, and ETIP SNET. European roadmap electrification of road transport. Technical report, ERTRAC, 2017.
- [54] Official Journal of the European Union. REGULATION (EU) 2019/631 OF THE EUROPEAN PARLIAMENT AND OF THE COUNCIL of 17 April 2019 setting CO2 emission performance standards for new passenger cars and for new light commercial vehicles, and repealing Regulations (EC) No 443/2009 and (EU) No 510/2011. Technical report, European Parliament and Council, 2019.

- [55] Vision on the charging infrastructure for electric transport, policy agenda looking ahead to 2020. Technical report, Ministry of Economic Affairs, 2017.
- [56] A Jaeger-Waldau. PV Status Report 2019. *JRC Science for Policy Report*, 2019.
- [57] Emilliano Bellini. Netherlands to reach 27 gw of solar by 2030. <https://www.pv-magazine.com/2019/11/04/netherlands-to-reach-27-gw-of-solar-by-2030/>, 2019. retrieved 24/05/2020.
- [58] Ministry of Economic Affairs of the Netherlands. Energy report transition to sustainable energy. Technical report, Ministry of Economic Affairs of the Netherlands, 2016.
- [59] ORNL's Electric Vehicle Charging Station. <https://www.ornl.gov/sustainable-ornl/ornl-s-electric-vehicle-charging-station>, 2020. retrieved 01/07/2020.
- [60] M Tesfaye and Charles C Castello. Minimization of impact from electric vehicle supply equipment to the electric grid using a dynamically controlled battery bank for peak load shaving. In *2013 IEEE PES Innovative Smart Grid Technologies Conference (ISGT)*, pages 1–6. IEEE, 2013.
- [61] EVEXPERT. <https://www.evexpert.eu/>. retrieved 12/07/2020.
- [62] RN van Gijlswijk, Emiel van Eijk, Elisah van Kempen, Norbert Ligterink, Evie Cox, and Sponsor Planbureau voor de Leefomgeving. Inputs and considerations for estimating large scale uptake of electric vehicles in the dutch passenger car fleet up to 2030. Technical report, 2018.
- [63] Vervangt Nen. *Nen* 2443. 2443:132, 2013.
- [64] Elpiniki Apostolaki-Iosifidou, Paul Codani, and Willett Kempton. Measurement of power loss during electric vehicle charging and discharging. *Energy*, 127:730–742, 2017.
- [65] Andreas Kieldsen, Andreas Thingvad, Sergejus Martinenas, and Thomas Meier Sørensen. Efficiency test method for electric vehicle chargers. In *International Battery, Hybrid and Fuel Cell Electric Vehicle Symposium*, 2016.
- [66] Province Flevoland. PowerParking. <https://www.flevoland.nl/dossiers/lelystad-airport/duurzame-luchthaven/powerparking>. retrieved 15/11/2019.
- [67] Thomas Franke and Josef F. Krems. Understanding charging behaviour of electric vehicle users. *Transportation Research Part F: Traffic Psychology and Behaviour*, 21:75–89, 2013.
- [68] Anamika Dubey and Surya Santoso. Electric Vehicle Charging on Residential Distribution Systems: Impacts and Mitigations. *IEEE Access*, 3:1871–1893, 2015.
- [69] Qiuwei Wu, Lin Cheng, Ulysse Pineau, Arne Hejde Nielsen, and Jacob Ostergaard. Impact and cost evaluation of electric vehicle integration on medium voltage distribution networks. *Asia-Pacific Power and Energy Engineering Conference, APPEEC*, 2013.
- [70] Anamika Dubey, Surya Santoso, and Matthew P. Cloud. A practical approach to evaluate voltage quality effects of electric vehicle charging. *2013 International Conference on Connected Vehicles and Expo, ICCVE 2013 - Proceedings*, pages 188–194, 2013.
- [71] Alexander T. Wells and Seth B. Young. *Airport planning & management*. McGraw-Hill, 6th edition, 1992.
- [72] Schiphol Group. Royal Schiphol Group - 2018 Annual Report. 2018.
- [73] Sergio Ortega Alba and Mario Manana. Energy research in airports: A review. *Energies*, 9(5):349, 2016.
- [74] Rishabh Ghotge and Ad van Wijk. Long Term Electric Vehicle Parking Spaces for Behind-the-Meter Storage of Solar Energy - A Simulation Study. 2019.
- [75] Johan Enslin. Grid impacts and solutions of renewables at high penetration levels. *Quanta Technology*, 2009.

- [76] MS ElNozahy and MMA Salama. Technical impacts of grid-connected photovoltaic systems on electrical networks—a review. *Journal of Renewable and Sustainable Energy*, 5(3):032702, 2013.
- [77] Farid Katiraei, Konrad Mauch, and Lisa Dignard-Bailey. Integration of photovoltaic power systems in high-penetration clusters for distribution networks and mini-grids. *International Journal of Distributed Energy Resources*, 3(3):207–223, 2007.
- [78] Giuseppe Pretticco, Flavia Gangale, Anna Mengolini, Alexandre Lucas, and Gianluca Fulli. Distribution system operators observatory. *European Commission. Joint Research Centre*, 2016.
- [79] Longi Solar LR4-60HPH-360M 360Wp. <https://www.blijmetzonnepanelen.nl/product/longi-solar-lr4-60hph-360m-360wp/>, 2019. retrieved 29/05/2020.
- [80] LR6-60PB 295-315M. <https://www.enfsolar.com/pv/panel-datasheet/crystalline/34694>, 2019. retrieved 29/05/2020.
- [81] Jiajun Li. *Quantitative Analysis of Automobile Parking at Airports by Jiajun Li A THESIS SUBMITTED TO THE FACULTY OF GRADUATE STUDIES IN PARTIAL FULFILMENT OF THE REQUIREMENTS FOR THE DEGREE OF MASTER OF SCIENCE DEPARTMENT OF CIVIL ENGINEERING CALGARY, ALBERTA* Nove. Number November. 2009.
- [82] Expert from Lelystad Airport. Personal communication.
- [83] Number of all-electric cars has doubled. <https://www.cbs.nl/en-gb/news/2019/19/number-of-all-electric-cars-has-doubled>, 2019. retrieved 05/07/2020.
- [84] European Environment Agency. Car Occupancy Rates. <https://www.eea.europa.eu/data-and-maps/figures/term29-occupancy-rates-in-passenger-transport-1>, 2010. retrieved 24/01/2020.
- [85] statista. Average household size in the Netherlands from 1950 to 2019, by number of residents. <https://www.statista.com/statistics/521777/netherlands-average-household-size-by-number-of-residents/>. retrieved 24/01/2020.
- [86] Jayakrishnan Harikumaran, György Vereczki, Csaba Farkas, and Pavol Bauer. Comparison of quick charge technologies for electric vehicle introduction in netherlands. In *IECON 2012-38th Annual Conference on IEEE Industrial Electronics Society*, pages 2907–2913. IEEE, 2012.
- [87] Luis Ochoa and Jairo Quiros. EV Charging Impacts on Residential LV Networks. Technical report, The University of Manchester, 2015.
- [88] P I James Francfort. 2014 DOE Vehicle Technologies Office Review - EV Project Data & Analytic Results. 2014.
- [89] European Commission. Photovoltaic Geographical Information System. https://re.jrc.ec.europa.eu/pvg_tools/en/tools.html#TMY, 2020.
- [90] Paul Gilman, Aron Dobos, Nichola DiOrio, Janine Freeman, Steven Janzou, and David Ryberg. SAM Photovoltaic Model Technical Reference Update. Technical report, NREL, 2018.
- [91] Joseph J Michalsky. The astronomical almanac’s algorithm for approximate solar position (1950–2050). *Solar energy*, 40(3):227–235, 1988.
- [92] Richard Perez, Ronald Stewart, Robert Seals, and Ted Guertin. The development and verification of the Perez diffuse radiation model. Technical report, Sandia National Labs., Albuquerque, NM (USA); State Univ. of New York ..., 1988.
- [93] Richard Perez, Pierre Ineichen, Robert Seals, Joseph Michalsky, and Ronald Stewart. Modeling daylight availability and irradiance components from direct and global irradiance. *Solar energy*, 44(5):271–289, 1990.

- [94] PVSyst. Albedo coefficient. <https://www.pvsyst.com/help/albedo.htm>, 2020.
- [95] Widalys De Soto, Sanford A Klein, and William A Beckman. Improvement and validation of a model for photovoltaic array performance. *Solar energy*, 80(1):78–88, 2006.
- [96] John A Duffie and William A Beckman. Solar engineering of thermal processes, fourth editio, 2013.
- [97] Diane Palmer, Ian Cole, Tom Betts, and Ralph Gottschalg. Interpolating and estimating horizontal diffuse solar irradiation to provide uk-wide coverage: Selection of the best performing models. *Energies*, 10(2):181, 2017.
- [98] Jon G. Manwell, F James. McGowan. Extension of the kinetic battery model for wind/hybrid power systems. *Proceedings of the 5th European Wind Energy Association Conference (EWEC '94)*, (January 1994):284–289, 1994.
- [99] Panasonic. *NCR-18650B Datasheet*.
- [100] Schiphol Airport. Why choose p3 long-term parking. <https://www.schiphol.nl/en/parking/product/p3-long-term-parking/>. retrieved 14/07/2020.
- [101] Emiliano Bellini. Jinko launches pv module with record output of 580 W. <https://www.pv-magazine.com/2020/05/15/jinko-launches-pv-module-with-record-output-of-580-w/>, 2020. retrieved 20/06/2020.
- [102] Emiliano Bellini and Marian Willuhn. 500 W plus panel race intensifies with JA Solars new module and Risens first shipment. <https://www.pv-magazine.com/2020/05/11/500-w-plus-panel-race-intensifies-with-ja-solars-new-module-and-risens-first-shipment/>, 2020. retrieved 20/06/2020.
- [103] Vincent Shaw. Risen energy unveils 500 Wp half-cut mono-PERC modules. <https://www.pv-magazine.com/2019/12/12/risen-energy-unveils-500-wp-half-cut-mono-perc-modules/>, 2019. retrieved 20/06/2020.
- [104] Wilfried van Sark, Lex Bosselaar, Pierre Gerrissen, KBD Esmeijer, Panagiotis Moraitis, Menno van den Donker, and Gerjan Emsbroek. Update of the Dutch PV specific yield for determination of PV contribution to renewable energy production: 25% more energy! *Proceedings of the 29th EUR-PSEC*, pages 4095–4097, 2014.
- [105] Mark Z Jacobson and Vijaysinh Jadhav. World estimates of pv optimal tilt angles and ratios of sunlight incident upon tilted and tracked pv panels relative to horizontal panels. *Solar Energy*, 169:55–66, 2018.
- [106] Margaret Smith and Johnathan Castellano. Costs associated with non-residential electric vehicle supply equipment: Factors to consider in the implementation of electric vehicle charging stations. Technical report, 2015.
- [107] ENF. Solar Panel Directory. <https://www.enfsolar.com/pv/panel>. retrieved 15/07/2020.
- [108] 0Bills. SMA Sunny Highpower Peak3 SHP 150-20 150kW Solar Inverter. <https://zerohomebills.com/product/sma-sunny-highpower-peak3-shp-150-20-150kw-solar-inverter/>. retrieved 17/07/2020.
- [109] Levelized Cost of Electricity Renewable Energy Technologies. Technical report, 2018.
- [110] Eero Vartiainen, Gaetan Masson, and Christian Breyer. PV LCOE in Europe 2014-2030. Technical report, European Photovoltaic Technology Platform, 2015.

- [111] Marc Londo, Robin Matton, Omar Usmani, Marieke van Klaveren, Casper Tigchelaar, and Suzanne Brunsting. Alternatives for current net metering policy for solar PV in the Netherlands: A comparison of impacts on business case and purchasing behaviour of private homeowners, and on governmental costs. *Renewable Energy*, 147:903–915, 2020.
- [112] Emilliano Bellini. Netherlands to support residential PV through net metering for the entire decade. <https://www.pv-magazine.com/2020/04/01/netherlands-to-support-residential-pv-through-net-metering-for-the-entire-decade/>. retrieved 11/08/2020.
- [113] Statista. Prices of electricity for industry in the Netherlands from 2008 to 2019 (in euro cents). <https://www.statista.com/statistics/596254/electricity-industry-price-netherlands/>. retrieved 14/07/2020.
- [114] Belastingdienst. Tabellen tarieven milieubelastingen. https://www.belastingdienst.nl/wps/wcm/connect/bldcontentnl/belastingdienst/zakelijk/overige_belastingen/belastingen_op_milieugrondslag/tarieven_milieubelastingen/tabellen_tarieven_milieubelastingen. retrieved 11/08/2020.
- [115] RVO. Stimulation of Sustainable Energy Transition (SDE++). <https://english.rvo.nl/subsidies-programmes/sde>. retrieved 14/08/2020.